THE DEPENDENCE OF CONTRACTILE PROPERTIES OF THE CANINE GASTROCNEMIUS MUSCLE UPON THE LEVEL OF REFLEX RECRUITMENT

by

Dwain J. Reed

A THESIS

Presented to the Department of Physiology
and the Graduate Division
of the University of Oregon Health Sciences Center
in partial fulfillment of
the requirements for the degree of

Doctor of Philosophy
June 1976

APPROVED: [redacted]

. . . . . (Professor in Charge of Thesis) . . . . . .

[redacted]

. . . . . (Chairman, Graduate Council) . . . . . .

ACKNOWLEDGEMENTS

I wish to thank Dr. Clarissa Beatty and Dr. Rose Mary Bocek of the Department of Biochemistry and the Primate Center for their assistance in making preliminary cytochemical assays which indicated that the canine gastrocnemius muscle was cytochemically heterogeneous.

I am grateful to the staff and faculty of the Department of Physiology for their help and encouragement. I was particularly fortunate to have the assistance of Don Morrow and Fred Arfman during the surgical preparations. It is a credit to their good natures that our friendship has survived these ordeals. I am indebted to Dr. Job Faber for advice and constructive criticism, particularly in the area of muscle mechanics.

To my advisor, Dr. John Brookhart, I wish to express my gratitude for his continuous encouragement and support. He never sought to impose his own ideas, but forced me to clarify my own thoughts and to express them in words. This process was only temporarily painful; I will remember our association with fond regard.

TABLE OF CONTENTS

DISCUSSION

LIST OF TABLES

LIST OF ILLUSTRATIONS

INTRODUCTION

Formulation of the Problem

The contractile response of a muscle during a reflex is the net response of many individual muscle fibers and is dependent upon two components: a neural response which determines the degree of activity in the individual motor units and a muscular response which depends upon the contractile properties of the active population, rather than the net properties of the total population. In mammalian skeletal muscle (twitch muscle) an action potential in the motoneuron results in an "all or none" response in all of the muscle fibers of the motor unit, that is, those fibers innervated by the motoneuron. Thus the neural organization underlying the reflex response can control the muscle response by the frequency of action potentials and the number of motor units recruited, or active, in order to provide grading of magnitude of the muscle contraction. If there are two or more populations of motor units which differ in their contractile properties, then the contractile properties expressed in the response could also be controlled neurally by the selective activation of motor units from one specific population.

A direct test of this latter possibility would be the determination of the contractile properties of muscle during different levels of reflex activity. The variation in contractile properties expressed in the reflex response will be limited not only by the degree of heterogeneity but by the specificity of the neural mechanism of recruitment for a particular fiber type. Thus, if motor units exhibiting different types

of contractile properties are activated simultaneously, the full range of heterogenity may not be expressed. Reflex activation of the motorneuron pool has the advantage that it makes possible a direct test of the specificity of recruitment for a particular fiber type.

While some contractile properties have been determined directly for individual motor units in a muscle, the force-velocity relation has not, for technical reasons, been examined. To the degree that reflex activation is found to be specific for motor units of a particular contractile type it will be possible to determine this property for the different fiber types composing the muscle. The determination of different force-velocity relations at different levels of reflex recruitment would reinforce the inference that differences in intrinsic rates of shortening are related to differences in cytochemical properties.

The background for this thesis will treat the topics of recruitment of motor units, the heterogeniety of contractile properties, and muscle mechanics in separate discussions.

Recruitment of Motor Units

Sherrington's Scheme of Recruitment.

The central issue addressed in this study is whether the mechanical properties of muscle are different at different levels of activation of the motorneuron pool. Changes in level of activation are manifest by changes in the proportion of neurons of a pool which are brought to discharge by the presynaptic input. Sherrington used the descriptive word

"recruitment" to express the notion that increasing levels of activation brought more neurons in the pool to their firing levels.

In the preface to Reflex Activity of the Spinal Cord, Sherrington and his co-authors declare their objective to be "the interpretation of reflex response in terms of the motor-unit itself" (1). In the text, they formulated a mechanism of recruitment the essential features of which are still valid today. This is particularly remarkable because it depended upon indirect evidence; the patterns of single unit activity in motoneurons had not yet been described.

The motor unit was defined as a single motoneuron and the muscle fibers within a muscle which it innervated. The motor pool was defined as the collection of motoneurons common to a given muscle. The muscle fibers of a motor unit act as slaves to the motoneuron, that is, the motor unit acts as a functional unit. During a given level of reflex activation, the motor pool is "fractionated" into parts by different levels of excitation. In their scheme (Figure 1), motor units receiving no excitation were referred to as zeros. Subliminals represented that part belonging to the subliminal fringe, that is, below the threshold level for firing but revealing an enhanced excitability when tested with a reflex augmentation. The subtetanics were those above the threshold for firing, but firing below the frequency for "fusion" or tetanus of the motor unit. Finally, the maximals were those motor units which no longer increased their tension with increased firing rate, already firing above the rate for maximal tetanic tension (1). In light of subsequent arguments as to the importance of "recruitment" vs. "firing rate"

Figure 1. Scheme of recruitment after Sherrington. P is the motor pool of cell bodies with a distribution of excitement during a reflex. Grades of excitement are plotted against numbers of motoneurones (a to a') and numbers of motor units (b to b'). As excitement increases, firing frequency increases. From Creed et al. (1), p. 122, Figure 61.

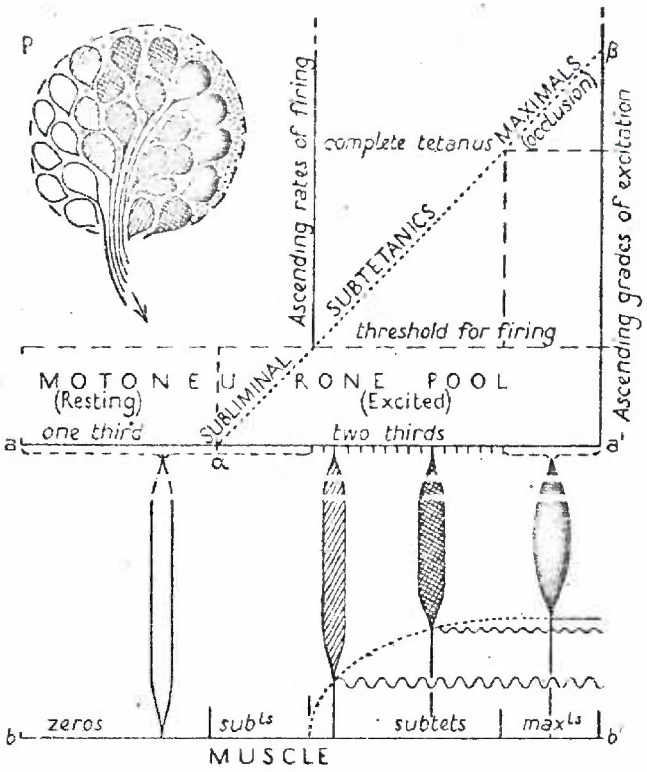
P
Ascending rates of firing
complete tetanus
MAXIMALS (occlusion)
B
SUBTETANICS
threshold for firing
Ascending grades of excitation
MOTONEURONE POOL
(Resting)
(Excited)
SUBLIMINAL
one third
two thirds
a
a'
b
b'
zeros
subtets
maxtets
MUSCLE

in the grading of muscle tension, it should be noted that increased firing rate was an integral part of this suggested explanation of motor recruitment.

Sherrington et al. recalled Bronk's (2) recognition that for whole muscles an incomplete tetanus requires more energy expenditure than a complete tetanus developing the same tension. On this basis they emphasized the economy achieved by recruiting new units into the tetanized fraction of the pool. This feature would be especially important in tonic reflexes and they felt that recruitment was more important here.

In their view, the pattern of fractionation of the motor pool was not constant; different reflexes utilizing different afferent pathways to the motor pool would result in different patterns of fractionation. The pattern of fractionation was thought to be determined by the distribution of afferent connections in the motor pool, rather than by the properties of the motor unit themselves.

The Size Principle of Henneman.

The above scheme of recruitment has been modified by Henneman by making the motor unit itself a determinant of the pattern of activation of the motor pool. Some attribute associated with size of the motor unit appears to be responsible for determining how the motor pool is fractionated. He has suggested that the motoneuron input resistance, which is inversely related to cell size, would influence the size of summated EPSP's (excitatory post synaptic potentials) produced from synaptic currents (3). Thus relative excitability to synaptic activa-

tion of a motor unit would be inversely related to size. This is in contrast to relative excitability of axons to electrical current which is directly related to axonal diameter (4).

Henneman considered it reasonable to assume that all parts of the motor unit would be of proportionate size, that is, cell body, axon, and the number of muscle fibers innervated, simply on the basis of metabolic or trophic demands. Thus, size itself would provide the principle relating the tension produced by a motor unit, and its relative excitability, determining its place in the order of recruitment. Henneman has provided experimental evidence for the size principle as the mechanism guiding the order of recruitment by establishing the following points:

1) The order of recruitment of motoneurons in a motor pool is inversely related to the size of the motor unit. Using the size of the extracellularly recorded axonal action potential as an indication of the size of the motor unit, the small motor units were found to be recruited first as the reflex activation increased, and dropped out last as activation diminished (3).

2) The order of recruitment progresses from small to large units regardless of the source of afferent input. The order was found to be preserved for mixed excitatory and inhibitory spinal reflexes (5) and also during midbrain, cerebellar and cerebral cortex stimulation resulting in tension development (6).

3) A given spindle-activated muscle afferent fiber distributes its terminals throughout the entire motor pool. By using post tetanic potentiation to facilitate EPSP's produced by stimulating single homonymous Ia afferents, it was found that a given afferent innervated at least 94% of the motor pool (7). Thus, for any given distribution of synaptic efficacies within a motoneuron pool, the manner in which the pool is fractionated is conditioned by the properties of the motor units of the pool.

4) The motor unit tension is directly related to the size of the motoneuron. Measuring the tetanic tension produced by stimulating single isolated ventral root filaments and measuring the conduction velocity of the efferent impulse, a direct relation was observed between motor unit tetanic tension and axon conduction velocity. Since conduction velocity is known to be directly related to axon diameter, it was inferred that the larger axons innervated motor units producing larger twitch tensions (8,9).

A relation was also noted between motor unit tensions and twitch contraction times, with large motor units having shorter rise times to peak twitch tensions. The distribution of contractile properties will be considered in more detail in a later section.

To account for the exceptions to the size principle which were encountered in his experiments (12-15% at most), Henneman distinguished

between true exceptions and exceptions occurring as the result of injury to nerve fibers occurring during the separation of fine ventral root filaments. It was felt that the adherence to the size principle was even closer than shown in the experiments, but the possibility was considered that true exceptions could occur due to local influences on motoneuron excitability. As a statistical property the size principle would still be valid (3).

The recruitment of motor units according to their size would appear to have some functional advantage. At low levels of activation recruitment of small motor units would allow fine grading of tension, while at high levels of activation the increment upon recruiting a large motor unit would be proportionately larger. Thus a larger dynamic range in the grading of tension is produced for a given number of motor units (10).

Criticism has been made of Henneman's studies because pairs of motor units in a ventral rootlet may not share the same motor pool (they may innervate different muscles). Wyman et al. (11) found a significant number of reversals of order of recruitment when comparing motor unit potentials in the EMG (electromyograph) during reflexes elicited by "natural" stimulation in decerebrate cats. Other authors (12) have found reversals of the order of recruitment of motor units recorded in the EMG of humans during voluntary and reflex movements. Factors which tend to increase the incidence of reversals are a "phasic" onset of the reflex and proximity of the pair in the order of recruitment.

The important question is not whether the order of recruitment between two particular motor units can be changed, but whether a given motor unit is always recruited at the same level of activation of the motor pool. When the percentage of discharge of the motoneuron pool is used as a measure of threshold it has been shown to be invariant during excitatory and inhibitory inputs from various sources (13).

There remains the possibility that certain specific afferent inputs to the motoneuron pool might activate a different fraction of the pool preferentially, as Sherrington thought. Burke (14), while agreeing that the small motoneurons are generally more excitable than the large motoneurons, found that rubrospinal synaptic input to triceps surae motoneurons produced predominantly EPSP's in those innervating large motor units, and IPSP's in those innervating small motor units. This suggested that cell size alone was not always the determining factor in the order of recruitment. What is lacking is a functional advantage for activating only the large motor units, to the exclusion of the small motor units. It is argued that the large, fast motor units are used in phasic movements, and the small, slow units are tonic units. But the simultaneous activation of the small motor units in accordance with the size principle would not slow the muscle response, and would not appreciably affect the expenditure of energy (13).

The present status seems to be that while there is some disagreement as to the generality of the size principle, there is general agreement that the smallest members of the motor pool are more easily excited by presynaptic input.

Heterogeneity of Contractile Properties within a Muscle

It has been known for many years that different muscles have different twitch contraction times. More recently, it has been demonstrated that most mammalian skeletal muscles are composed of a mixture of fiber types, having differing cytochemical properties. It has also been shown that the motor units of a single muscle may have a range of differing twitch contraction times. In order for this heterogeneity of contractile properties to be expressed during reflex activation of the muscle, two conditions must exist:

1) Individual motor units must be homogeneous, that is, consist of muscle fibers of a single contractile type.
2) There must be a relation between the contractile properties of the motor unit and its order of recruitment.

The details of the structural, chemical, and behavioral properties of different kinds of muscle fibers which are emerging at the present time suggest that these conditions are met; that there is an ordered relation between recruitment, contractile properties, and their cytochemical properties. This section will discuss the heterogeneities of muscle behavior and their possible relation to recruitment.

Early Suggestions of Heterogeneity of Contractile Properties.

As early as 1884 Grutzner (15) provided evidence that twitch contraction times of motor units within a muscle differed. He used a stimulus frequency which at a submaximal intensity caused an unfused

tetanus, but resulted in a fused tetanus when the stimulus intensity was maximal. The results could be explained if the motor units added last by the more intense stimuli had longer twitch contraction times.

Inflections (or their absence) in the relaxation curves of twitch or tetanic isometric contractions have been used as evidence for or against heterogeneity within a muscle. Denny-Brown (16) showed that if a small portion of soleus (cat) was included with gastrocnemius, such an inflection was readily apparent. When all of soleus was excluded, however, the inflection was not present and the interpretation was made that gastrocnemius was homogeneous. Gordon and Phillips (17) found that tibialis anterior (cat) gave such "impure" twitches; after dissecting the superficial portion the remaining deep portion gave a "pure" twitch approximately 50% longer than that of the whole muscle. It should be noted that a wide distribution of twitch contraction times could result in a "smooth" twitch relaxation curve; therefore, the lack of an "inflection" in the twitch curve is not evidence against heterogeneity within a muscle.

Measurement of Motor Unit Contractile Properties.

Isolated motor unit contractions in soleus and gastrocnemius (cat) were obtained by Wuerker, McPhedran, and Henneman (8,9) by stimulating ventral root filaments which had been finely divided. They obtained histograms of the frequency of distribution of axon conduction velocities, twitch contraction times, and motor unit tetanic tensions. Twitch contraction times (time to peak twitch tension) for gastrocnemius ranged

from 18 to 129 milliseconds (a six-fold range). The range of twitch contraction times for soleus was more than three-fold, from 58 to 193 milliseconds. The motor units were grouped according to their axonal conduction velocities (in increments of 5 meters/second); the units with the slowest conducting axons had the smallest tensions (tetanic) and the longest contraction times. Between 55 and 90 meters/second axonal conduction velocity, the mean tension of the units in each group increased from .5 to 47.8 grams, while the mean contraction time of the group decreased from 129 to 39.1 milliseconds. Between 90 and 110 meters/second the mean tension remained approximately constant, while the mean twitch contraction continued to decline to 25.5 milliseconds (gastrocnemius, cat). The measurement of axonal conduction velocities allows the contractile properties to be related to their order of recruitment (see page 8) on the basis of the size principle. The faster conducting axons have larger diameters, and presumably larger cell bodies and higher thresholds for excitation. Thus the small units with longer twitch times would be recruited earlier than the large units with shorter twitch times.

Burke (18) also studied isolated motor units of gastrocnemius and soleus (cat), using intracellular stimulation of motoneurones in the ventral horn to activate the motor unit. He found a group of large motor units with short twitch contractions (approximately 18 msec) and a group of small motor units with a range of longer contraction times (40-90 msec). The relation between size and contraction time was similar to that found previously; however, a clearly bimodal distribution suggested

to him the presence of two functional groups of motor units. The differences in results might reflect differences in sampling of motor units inherent in the two different techniques, and one cannot be sure that either technique gives a representative sample.

More recently, Burke (19) has used the relative sensitivity to fatigue during a prolonged sequence of recurrent tetani as an index of motor unit behavior. Units which were fatigue sensitive he termed FF; these also were the largest motor units (highest tetanic tension) and had short twitch times (25-45 msec). Fatigue resistant units (FR) had intermediate tetanic tensions and twitch contraction times (38-55 msec). The units which were insensitive to fatigue were his S units, where were small and had long twitch durations (55-100 msec). The median axonal conduction velocity for type FF and FR units was 100 meter/second for both, and was 85 meters/second for type S units. The fatigue was assumed to be that of the muscle fibers since the tetani were interrupted periodically to allow recovery of the neuromuscular junction.

Direct measurement of intrinsic speed of the contractile mechanism of single motor units has not been made, therefore, there is no direct evidence that the contractile mechanisms of these fibers are different.

Relation between Cytochemical and Contractile Properties.

The existence of muscles which are homogeneous in their cytochemical properties provided one basis for associating a particular contractile behavior with certain cytochemical properties. Soleus, a 'slow' muscle, and semitendinosus, a 'fast' muscle, are both homogeneous

with respect to their cytochemical properties in the rat, although they differ from each other. On the assumption that the muscles are homogeneous with respect to their contractile properties also, the contractile properties of the whole muscle have been associated with their fibers, and their cytochemical properties. These associations of cytochemical and contractile characteristics do not necessarily imply a causal relationship. It cannot be assumed, without proof, that fibers in heterogeneous muscles with the same cytochemical properties as particular homogeneous muscles also have the same contractile properties. Considerable effort continues to be expended on the problem of relating the cytochemical characteristics of fibers of heterogeneous muscles to the contractile properties of these fibers. These studies have taken two general directions: one has involved the premise that the relative utilization of glycolitic vs. oxidative metabolic pathways is related to contractile behavior differences; the other is based on the premise that variations in specific myofibrillar ATPase activities determine contractile behavior.

Cytochemical Classification of Muscle Fibers.

The differences in glycolytic and oxidative enzymes, and in the myofibrillar ATPase activites, have been used in a scheme of cytochemical classification of fibers which recognizes three fiber types:

1) A white fiber, characterized by high glycolytic versus low oxidative activity, and high myofibrillar ATPase activity at pH 9.4.

2) A red fiber, characterized by low glycolytic versus high oxidative activity, and high myofibrillar ATPase activity at pH 9.4.

3) An intermediate fiber also characterized by low glycolytic versus high oxidative activities but differing from the red fiber by having low myofibrillar ATP activity at pH 9.4.

(This classification is from a recent review by Close (20) using the nomenclature originally suggested by Padykula and Gauthier (21); other nomenclature used to describe the equivalent fibers is cross-listed in the review, Table 1).

Red and intermediate fibers, both having high oxidative activities, also have numerous mitochondria, consistent with the localization of the coupled oxidative phosphorylation and respiratory systems to the mitochondria. They also both contain a high content of myoglobin, which maintains the local PO_2 during short periods of reduced perfusion which occur during muscle contraction (22). The white fibers have fewer mitochondria and lack myoglobin, which results in its pale, clear appearance.

Glycolytic vs. Oxidative Metabolism.

Burke (19) has recently used the method of glycogen depletion previously used by Edström and Kugleberg (23) to identify the fiber type of his FF or fatigue sensitive units. The method uses repetitive tetanic stimulation of a motor unit for a prolonged period (15-60 min.) to deplete the fiber of glycogen; then alternate thin sections are stained for glycogen (periodic acid-Schiff stain) and for oxidative, glycolytic

and myofibrillar ATPase activities. Thus, he has determined that his fatigue sensitive units (FF) correspond the the white fibers as determined by histochemical properties. The FR units, which were fatigue resistant but had short twitch contraction durations, were separable from the S units (which had a large range of longer twitch durations) on the basis of myofibrillar ATPase. The FR units corresponded to the red fibers while S units were identified as intermediate fibers.

The functional differentiation between white and red fibers may be due to the pattern of activity which the motor unit experiences. Barnard, Edgerton and Peter (24) looked at the effects of chronic "low intensity" exercise on guinea pig gastrocnemius muscle. Their results suggested that white fibers were converted to red fibers, based upon the relative proportion of white and red fibers respectively in controls and the exercised animals. There were no significant alterations in the proportions of fibers with low and high levels of histochemical myosin ATPase activities, that is, the proportion of intermediate fibers remained constant.

Thus the relative oxidative and glycolytic activities may reflect a functional adaptation to the animals' needs, depending upon whether these needs are for short periods of intense activity or long periods of maintained activity.

Myofibrillar ATPase Activity.

The relation between myofibrillar ATPase activity and the intrinsic speed of shortening (V_{max}) is of particular interest since V_{max} has not

been measured directly for different motor units within a muscle. The first suggestion of such a relation was the discovery by Englehardt and Ljubimova (35) in 1939 that isolated threads of actomyosin catalyzed the hydrolysis of ATP. Experimental confirmation of the role played by ATP in the contraction of muscle was finally achieved in 1962 by Cain and Davies (26), who showed that there was a net reduction in ATP during a muscle twitch when reconstitution of ATP was blocked. If the hydrolysis of ATP by the myofilaments is the rate limiting process during maximal muscle shortening the specific myosin ATPase activity should be directly proportional to the intrinsic rate of shortening (the maximum rate of shortening the unloaded muscle or fiber is capable of).

Barany (27) has examined the relation between the ATPase activity of myosin isolated from muscle and intrinsic rate of shortening of the muscle. In 14 different muscles from several different species, he found a direct correlation between the specific ATPase activity and values of intrinsic rate of shortening which had been previously determined (19,28,29,30). Both the intrinsic rate of shortening and myosin specific ATPase activity were also found to change in the same direction following cross-innervation of fast (extensor digitorium longus) and slow (soleus) muscles of the rat (19,31,32). This relation has also been shown to hold during the ontogenetic changes in enzyme activity and V_{max} which occur in developing rat fetal muscle (28). In all these studies the ATPase activity was determined with myosin extracted from whole muscles, with the assay performed in vitro under controlled conditions of substrate concentration, ionic composition and pH, which

allows comparison of enzyme activities to be made. In a heterogeneous muscle, however, the result would reflect a mixture of myosin ATPase activities.

The usual cytochemical method used to stain for myofibrillar ATPase is to preincubate the tissue in an alkali medium (pH 9.4), then stain for inorganic phosphate evolved in the presence of excess ATP (substrate) by the Gomori method (33). The myosin ATPase's differ in their stability under acid conditions, however (34), with the ATPase extracted from fast muscles (white or red fibers) being acid labile and alkali stable. The ATPase from slow muscles (intermediate fibers) shows the opposite sensitivity to pH. Thus the assay performed with alkali preincubation accentuates what would be a darker staining of white and red fibers. In fact the pH sensitivity is the determining factor in the relative staining. This is shown by the fact that fetal rat muscle, which has a low intrinsic rate of shortening and low specific myosin ATPase activity in a biochemical determination, stains as intense as adult fast muscle, due to the fact that they have the same pH sensitivity (35). It has also been reported that extraocular and intrafusal muscle fibers are both acid stable and alkali stable (36). Therefore, the pH sensitivity of the myofibrillar ATPase does not appear to have a unique relation to its rate of ATP hydrolysis (as determined in a biochemical assay) and therefore by inference to the intrinsic rate of shortening.

The difference in pH sensitivity strongly implies a difference in the myosin protein structure, but it is not clear that these are the same differences underlying the variation in ATPase activity and intrin-

sic rate of shortening. This is emphasized by the variation in intrinsic rate of shortening of homologous muscles as a function of size. Generally there is an inverse relation between size and intrinsic speed of contraction such that the overall muscle shortening of homologous muscles in different sized animals is similar. Thus the intrinsic rate of shortening, that is, per sarcomere, of cat soleus is less than one half that of mouse soleus, although both are composed almost entirely of intermediate fibers (19). Yet each specie shows the same pattern of staining for myofibrillar ATPase, that is, the differences in myofibrillar ATPase activity between the two species which can be demonstrated in a biochemical assay, are not detected by the present cytochemical method.

Implications of Cytochemical Differences to Present Thesis.

As was stated earlier, the heterogeneity of contractile properties must meet three requirements to satisfy the hypothesis put forward: 1) the motor unit must be homogeneous, 2) the muscle must be heterogeneous with respect to the contractile properties of its motor units, and 3) the contractile property of the motor unit must be related to its order of recruitment in the muscle.

The glycogen depletion method was used by Burke (37) to definitively demonstrate that the motor unit is composed of a single fiber type on the basis of cytochemical properties, although the fibers composing a single motor unit were found to be widely distributed in the muscle. It was shown that the territory of a single motor unit occupied as much as 20% of the cross-sectional area in gastrocnemius (cat), with 400-800

muscle fibers composing the motor unit. The implication of this observation is that significant mechanical interaction between an active motor unit and adjacent motor units, active or inactive, should occur. It also suggests that all fibers of a motor unit have the same contractile properties, a proposition which is nearly impossible to test directly.

Taking into account the reservations about the cytochemical method for myofibrillar ATPase noted above, the relative proportions of white and red, and intermediate fibers respectively, give an idea of the possible heterogeneity of V_{max} among motor units composing various muscles. Henneman (38) found only 21% of the fibers of medial gastrocnemius were intermediate in the cat, while they represented 100% of soleus. The intrinsic rate of shortening of soleus (cat) was found to be 13 μ/sec compared to 31 μ/sec for a cat fast muscle (quadriceps) (19,30). If the relative rates of shortening (V_{max}) of intermediate, white, and red fibers are similar in medial gastrocnemius to the rates in the cytochemically homogeneous muscles, and motor units composed of intermediate fibers are recruited preferentially, the intrinsic rate of shortening of the muscle could more than double between low reflex and maximal reflexes. The proportion of intermediate fibers might be even higher in the dog, considering it lacks a soleus muscle, with a resulting larger effect on the contractile properties of the whole muscle.

If the differences in myofibrillar ATPase staining actually reflect a difference in intrinsic rate of shortening of the fibers, the relations noted by Burke between twitch times and fatiguability of motor

units, and their cytochemical properties, can also be extended to include the intrinsic rate of shortening. On this basis his FF and FR fiber types would have a high intrinsic rate of shortening (relative to that of the S units) and would be recruited at higher thresholds than the S units. The correlation of contractile properties with recruitment threshold is indirect, depending upon identification of the motor unit by the glycogen depletion method, identification of fiber type by cytochemical methods, and finally depending upon the presumed relation of intrinsic rate of shortening to the myofibrillar ATPase stain.

Muscle Mechanics

The Development of the Classical Model.

The classical model of muscle contraction developed out of a series of unsuccessful attempts to account for the contractile properties of muscle with simple physical elements. In the middle of the nineteenth century Weber (39) is reported to have proposed that tension in an active muscle was the result of a change in elastance; that the active muscle behaved like a stretched spring. He believed that the tension depended only on muscle length, not on the rate of change of length. In 1892 Blix (40) showed this assumption to be in error; using a device he called a myographion which recorded muscle tension vs. muscle length directly, he showed that a curve determined while stretching the muscle during contraction was higher (greater tension) than one determined when the muscle was allowed to shorten. Fick (41) confirmed these results in the

same year. He suggested that stretching the muscle produced a greater physiological response; to test this possibility he measured the total energy expended (heat plus work) in muscle contractions when the muscle was stretched and when it was allowed to shorten. Contrary to expectation he found that the total energy expenditure was smaller during stretch than when the muscle was allowed to shorten. He concluded that it was the process of performing mechanical work that was responsible for the expenditure of chemical energy. This was opposed to the prevalent notion that the chemical energy in a contraction was converted to stored elastic potential energy at the beginning of the contraction, and any energy left after doing work during the contraction was dissipated as heat during relaxation. Fick's results were criticized on technical grounds, and were disregarded until Fenn (42) confirmed them 30 years later. Improvements in the measurement of heat during shortening put to rest previous criticisms, and the extra energy released in a contraction during shortening is now known as the Fenn effect.

At approximately the same time A.V. Hill (43) suggested the addition of viscosity to the contractile "elastance". In studies on human muscles he had found that as the speed of shortening of a muscle increased, the work performed fell linearly, which could be accounted for by assuming the elastance was 'damped'. This version of the model is shown in Figure 2b. The model also predicted a linear relation between force and velocity.

In 1927 Levin and Wyman (39) introduced their ergometer, which allowed the study of contractions at constant velocities of shortening

Figure 2. Development of the classical model of muscle.

CE = Contractile element

SEC = Series elastic component

PEC = Parallel elastic component

Based upon references 39,43,44,47,48.

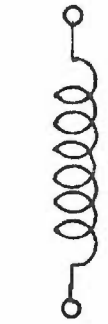

WEBER 1850~
a)

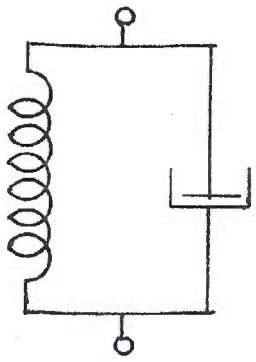

HILL 1924
b)

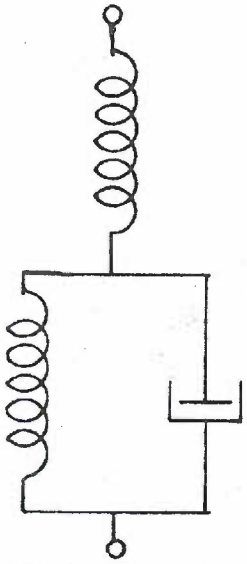

LEVIN & WYMAN
1927
c)

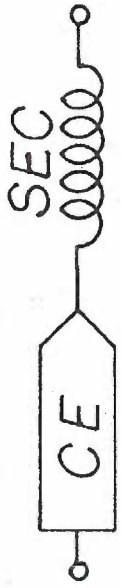

FENN & MARSH
1935
d)

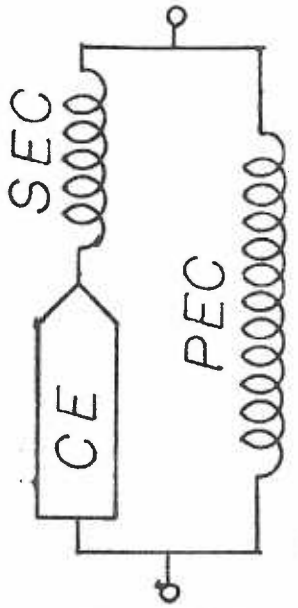

HILL 1951
e)

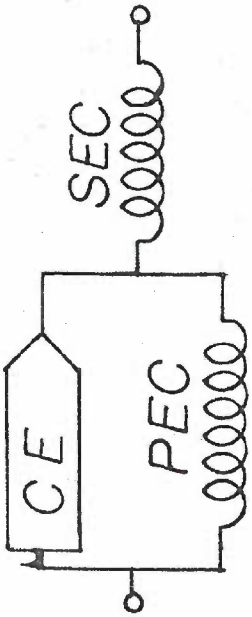

AUBERT 1956
f)

or lengthening. They did not find a linear relation between force and velocity as expected, and they concluded that muscle could be represented by a system of two components, an undamped elastance in series with the visco-elastic model of Hill. This model, shown in Figure 2c, was used generally at the time, and still survives as a simple analog mechanical model in some textbooks.

The Force-Velocity Relation.

Fenn and Marsh (44) in 1935 introduced a method to measure the rate of change in length with time of the 'visco-elastic' element in isolation from the series 'undamped' elastance. They reasoned that if the muscle shortened at constant tension (an isotonic contraction), the length of the series 'undamped' elastance would be constant, and the velocity of shortening of the muscle would be identical to the rate of change of the 'visco-elastic' element length with time. The experiments were performed with the muscle shortening from a constant rest length under different loads supplied by different weights hung on the isotonic muscle lever. The velocity of shortening was measured just after shortening began. The plot of force vs. velocity which was obtained is shown in Figure 3. This same method is the one usually used to determine the force-velocity relation. Fenn and Marsh fitted their data with the empirical exponential relation given in the figure. They suggested that the observed force-velocity relation probably had a chemical rather than a mechanical basis. Therefore, the visco-elastic model was no longer of theoretical interest, and the empirical relation between force and velocity replaced

Figure 3. Original force-velocity relation of Fenn and Marsh. Force (W) is calculated per cm^2 cross-section of muscle and velocity of shortening in cm per sec per cm length of muscle. Solid line through data is relation given in Figure. Log (W + 1.8V) is plotted vs. velocity, and fits a straight line. From reference 44.

Figure 4. Length-tension relation after A.V. Hill. (1) At rest passively stretched; (2) Extra force developed during maximal tetanus; (3) Dotted line, total force in maximal tetanus, sum of (1) and (2). Length is given in fraction of L_o, tension in fraction of P_o. Frog sartorius muscle. (Hill, Proc. Roy. Soc. B 141, p. 113.)

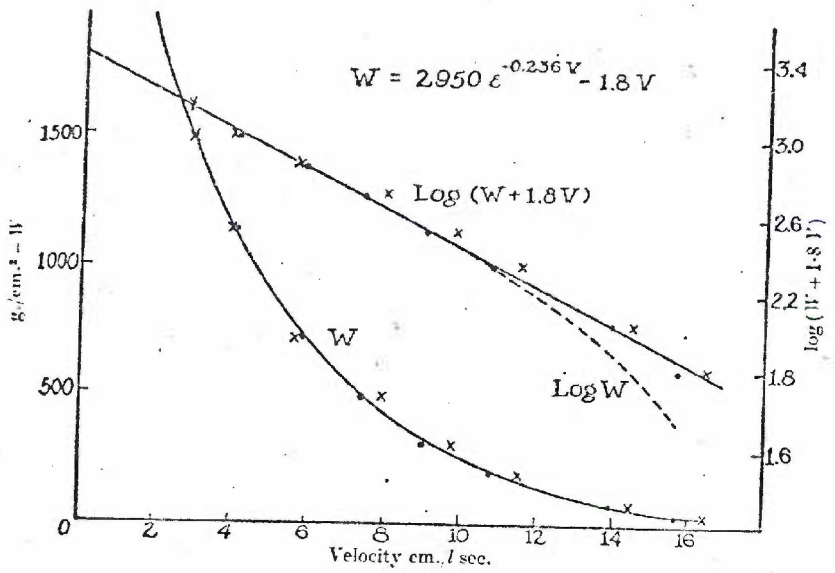
W = 2.950 e^-0.236 V - 1.8 V
Log (W+1.8V)
W
Log W
1500
1000
500
0
2
4
6
8
10
12
14
16
3.4
3.0
2.6
2.2
1.8
1.6
Velocity cm./ sec.

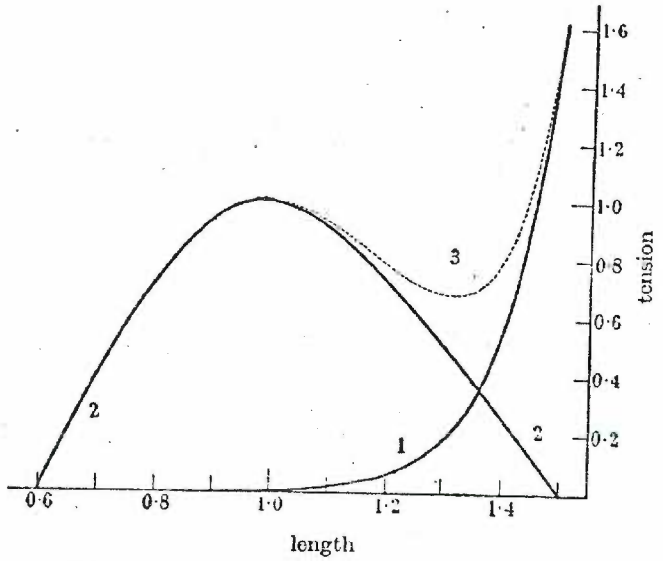
1·6
1·4
1·2
1·0
0·8
0·6
0·4
0·2
tension
0·6
0·8
1·0
1·2
1·4
length
1
2
2
3

the visco-elastance in the model. They introduced the contractile element shown in Figure 2d as an hypothetical element obeying the force-velocity relation.

A.V. Hill (45) three years later confirmed the force-velocity relation of Fenn and Marsh, and found another form for its empirical expression:

$$v = b[P_o - P]/[P+a]$$

P and v are the instantaneous values of muscle force and velocity of shortening respectively, P_o is the isometric force or force at zero velocity. a and b are constants which give the best fit to the observed values; a has the dimensions of force and b the dimensions of velocity. He formulated the above equation (known as the Hill Equation) while investigating the rate of total energy production during shortening. The rate of heat production during shortening was given by $\frac{dH}{dt} = a.\frac{dx}{dt}$ where a is the heat of shortening per centimeter (part of the Fenn effect). Therefore, the rate of total energy (work + heat) would be $[P + a]v$. This appeared to be proportional to $[P_o - P]$, the difference between the actual force and the isometric force of which the muscle was capable. Thus it was only necessary to assume that the chemical energy was available during shortening at a rate proportional to $[P_o - P]$ and that the heat produced was proportional to shortening; then the Hill equation would follow from the first law of thermodynamics (conservation of energy). Thus for 25 years the Hill equation was thought to be more than an empirical fit to the force-velocity relation. In 1964 Hill (46) showed that in frog muscle the heat of shortening is not constant,

but depends upon load; being equal to a only when $P/P_o = 0.5$. Thus at the present time it is only an empirical fit to the force-velocity relation, with no more functional significance than the original relation of Fenn and Marsh. But in the interval of time which passed, it acquired a legitimacy over its rivals, and is still generally used to characterize the force-velocity relations of different muscles.

The velocity of shortening for the unloaded muscle is the intrinsic rate of shortening or V_{max}. V_{max} is equal to $b[P_o/a]$, and is the maximum velocity at which the muscle can shorten. a/P_o, ($= b/V_{max}$), is a dimensionless number, and indicates the degree of curvature of a particular force-velocity relation.

In experiments on frog sartorius, during tetanic contractions at muscle lengths near L_o (length at which active isometric tension is a maximum, see below), the two component model (series elastic component and contractile element) shown in Figure 2d, along with the Hill equation, gives accurate prediction of the observed data. (Although determined upon the whole muscle, the force-velocity relation is presumed to be that of the contractile element.) In other muscles, and under different conditions of muscle length and muscle activation, more variables must be considered.

The Length-Tension Relation.

As the length of a muscle is passively increased, inactive muscle exhibits passive tension. In order to account for this tension, a parallel elastic component is added to the model, either in parallel

with both the series elastic component and the contractile element, as suggested by Hill (47), or in parallel with just the contractile element, as suggested by Aubert (48). These alterations to the model are shown in Figure 2e and f.

Not only does the passive tension of inactive muscle depend upon length, but the isometric tension developed by an active muscle during a tetanus varies with length as shown in Figure 4. The active tension curve is obtained by subtracting the passive tension from the total tension during the contraction. The length at which the active tension is maximum is defined as L_o. The curve of active tension represents the length-tension relation of the muscle, sometimes noted as $P_o(l)$ below. The question arises as to how the force-velocity relation varies with length. Abbott and Wilkie (49) assumed that the Hill equation could be used with P_o replaced by $P_o(l)$ for muscle lengths shorter than L_o. The modified Hill equation was the following:

$$[P + a][v + b] = [P_o(l) + a]b$$

By substituting values of force and velocity obtained at muscle lengths shorter than L_o, they calculated the expected $P_o(l)$ in this region and found it to be in agreement with the length-tension relation obtained from isometric contractions. Since $V_{max} = b \cdot [P_o(l)/a]$, the curves for shorter lengths lie below the curve for L_o, intersecting each axis proportionate to their isometric tensions at that length.

The Active State.

In order to account for the change in muscle activation with time, Hill in 1949 (50) defined the intensity of the active state as the

tension that the contractile element could bear at any given instant without shortening or lengthening. Twenty-five years earlier in experiments conducted with Gasser (51) he had applied abrupt stretches to muscle early in a twitch contraction, and showed that a much greater tension was developed by the stretched muscle than when the muscle was not stretched. He now reapplied this method, trying to adjust the stretch so that the tension immediately after the stretch neither rose nor fell ($dP/dt = 0$). Under this condition the length of the series elastic element immediately after stretch, and therefore the length of the contractile element, would not be changing. The tension of the muscle would be equal to that of the contractile element, and therefore would be equal to the intensity of the active state at that time. He showed that the transition to full intensity of the active state occurred very soon after the muscle action potential.

The time course of decay of the active state cannot be investigated by stretches, but it can be by releasing the muscle a short distance and recording the redevelopment of tension. When dP/dt is zero, one point on the active state curve is determined. Plotting the peak redeveloped tensions for releases at different times in the twitch, the full decay curve can be determined, which has been done by Ritchie and Wilkie (52,53).

The intensity of the active state is compared with the actual developed tension during an isometric twitch in Figure 5. This curve, from a recent publication of Hill (54), shows that the active state is not fully developed until 50 msec. after the muscle action potential.

Figure 5. Time course of the active state after Hill (54). A. P_i is the intensity of the active state of the contractile element; P_n is the tension during a normal twitch. Curves B and C are earlier versions from Gasser and Hill, 1924 (51), and Hill, 1949 (50).

Figure 6. Load-extension curves of the series elastic component after Jewell and Wilkie (56). Frog sartorius 60 mg L_o = 29 mm. Curves were determined at different times in the active state. If SEC was only dependent upon tension, curves could be superimposed by shifting lower curves to right. Shifted curves fall in the envelope bounded by dashed line and the 0.2 sec curve.

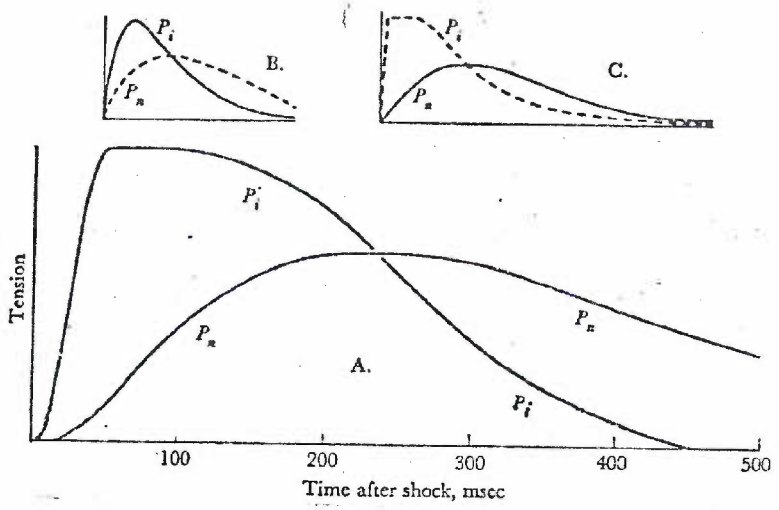
P_i
B.
P_n
P_i
C.
P_n
Tension
P_i
P_n
A.
P_n
P_i
100
200
300
400
500
Time after shock, msec

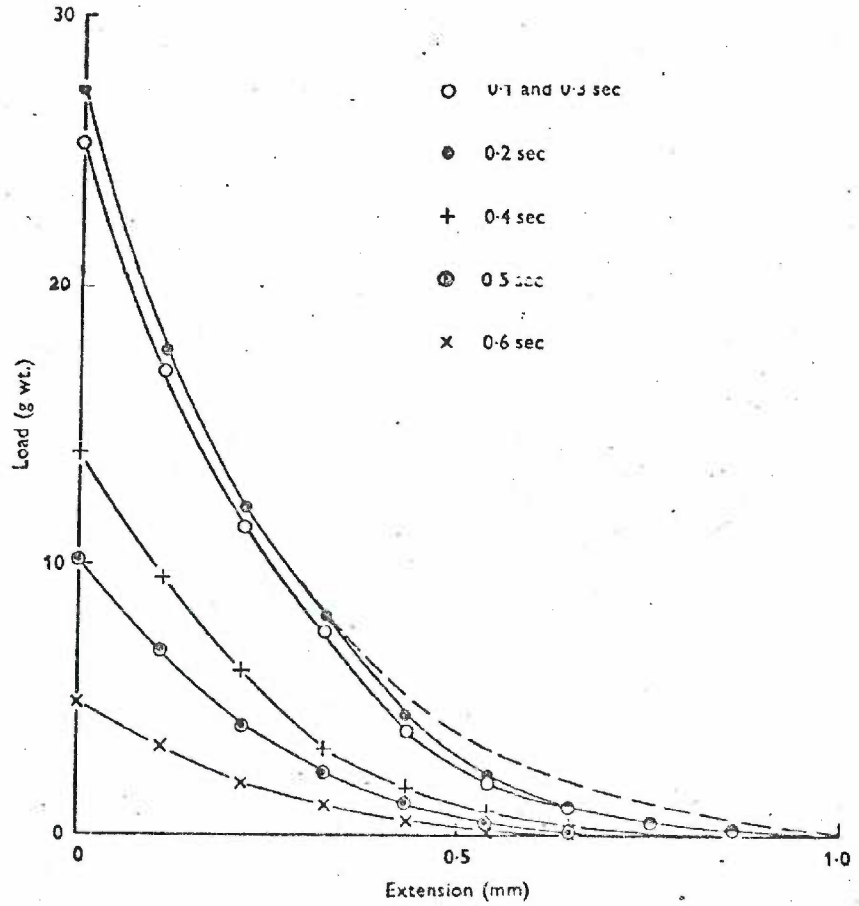
30
20
10
0
Load (g wt.)
0·1 and 0·3 sec
0·2 sec
0·4 sec
0·5 sec
0·6 sec
0
0·5
1·0
Extension (mm)

(The results in 1949 had been interpreted as indicating a more abrupt transition.) The difference between the intensity of the active state and twitch tension early in the twitch occurs because the contractile element must shorten to stretch the series elastic element; late in the twitch (during relaxation) the contractile element is lengthened by the recoil of the series elastance. During lengthening the force-velocity relation is such that forces greater than isometric are produced. Twitch tension at the peak of the twitch is equal to the intensity of the active state at that instant in its decay course. It can be seen that if the stimulus were to be repeated soon enough the decay of the active state could be prevented. Thus tetanic stimulation at a high enough frequency 'fuses' when the active state remains fully active with time.

The Series Elastic Component.

The final development of the classical model involved the characterization of the series elastic component. In 1950 Hill (55) used the Levin-Wyman ergometer to apply 'controlled' releases during an isometric contraction, which then became isotonic. Using the force-velocity relation to determine the internal shortening of the contractile element, he could plot the length change of the series elastance versus the change in tension; the slope at any point of the curve was the compliance ($\Delta L/\Delta P$). He showed that the observed relation could be accounted for by assuming a Gaussian distribution in the rest lengths of parallel fibers making up the series elastic component. Jewell and Wilkie (56) later used a

'quick release' which converts the muscle from an isometric condition to an isotonic condition during a tetanus to determine the compliance of the series elastance. In this case, the release was limited only by the inertia of the muscle level, and contractile element shortening during the interval was negligible. Figure 6 shows the relation between tension and elongation which they determined. The compliance (slope of curve) is high at low tensions, and tends to become constant at higher tensions.

The Relation of the Classical Model to Muscle Ultrastructure.

The classical model in the fully developed form has been used to characterize the contractile properties not only of isolated frog muscle, but a variety of invertebrate and mammalian muscles, as well as cardiac muscle. The model and the properties of the elements have been developed empirically to give the best simulation of the properties of the whole muscle, and are not based upon the ultrastructure of muscle. Of the three relations defining the contractile properties of the contractile element --the force-velocity relation, the length-tension relation, and the intensity of the active state--the last two have been interpreted in terms of the following mechanisms which operate at the ultrastructural level:

1) The length-tension relation at lengths greater than L_o (the length at peak active tension) has been interpreted in terms of the overlap of thick and thin myofilaments at the ultrastructural level. It has been shown that in single fibers the isometric tension disappears at a sarcomere length just suffic-

ient for no overlap of the thick and thin filaments (57). At lengths shorter than L_o the reason for the decrease of tension with decrease in length is unknown. Mechanical interference or interference with muscle activation (via interference with the release of calcium) have been suggested. The evidence supporting this interpretation of the length-tension relation can be found in most recent physiology texts (22).

2) The time course of the intensity of the active state has been related to the process of excitation-contraction coupling. The intensity of the active state has been shown to be proportional to the intracellular concentration of calcium, which increases after release from the sarcoplasmic reticulum in response to a muscle membrane action potential, and decreases as it is taken up by the sarcoplasmic reticulum. The evidence supporting this interpretation has been reviewed by Ebashi and Endo (58).

Models of muscle contraction based upon the ultrastructure of muscle have been developed during the last decade, and have been reviewed recently by Simmons and Jewell (59). They are an attempt to determine a relation between ultrastructure and the contractile properties of muscle. As empirical relations describing muscle contraction they differ from the classical model in two major aspects:

1) In these recent models part of the series elastic component is ascribed to active cross-bridges made between thick and thin filaments. Since in these cross-bridge models the active tension is proportional to the number of active cross-bridges, the

series elastic component is dependent upon the intensity of the active state.

2) In these models the rates of making and breaking active bridges change as determined by the calcium concentration. Since time must pass before the actual number of active cross-bridges changes, the force-velocity relation cannot be established instantaneously upon shifting from one point on the curve to another.

These later models so far have not been used for the comparison of the contractile properties of different muscles, and no advantage is seen in their use as opposed to the classical model.

Measurement of Contractile Properties.

In considering the different measures on contractile properties which have been used to characterize the contractile properties of whole muscles or motor units, a distinction can be made between primary measures and secondary measures. The primary measures are the properties of the classical model previously discussed: the length-tension relation, the force-velocity relation, and the intensity of the active state. The secondary measures are a group of related properties which depend upon one or more of the above properties. They have in common the fact that they are easier to determine than the primary measures, however, they are more difficult to interpret in terms of the model. They include twitch contraction time, fusion frequency, and twitch tetanus ratio. The secondary measures will be considered first, touching upon their inade-

quacies as means to characterize the contractile properties. The primary measures will be considered next, giving the reasons for emphasis upon the length-tension relation and the force-velocity relation, and discussing their validity during reflex activation.

Secondary Measures of Contractile Properties (Twitch-Contraction Time, Fusion Frequency, Twitch-Tetanus Ratio).

The most commonly used measure of contractile properties is the time required to develop peak tension in a simple isometric twitch. This is expecially true of measurements made upon individual motor units of a muscle (page 12). Its relation to the contractile properties of the contractile element of the model can be seen qualitatively from Figure 5, which compares the time course of the active state with that of twitch tension. The peak of twitch tension (where $dP/dt = 0$) must occur on the falling phase of the active state; therefore, the twitch contraction time is particularly sensitive to changes in the duration of the active state. In particular for constant values of twitch-tetanus ratio it can be seen that twitch contraction time and duration of the active state will vary directly. At most the twitch contraction time can only vary over the duration of the decay phase. (It will be noted below that the twitch-tetanus ratio varies with muscle length, so the twitch contraction time could be measured at constant twitch-tetanus ratio.) Under the proper conditions the twitch contraction time is a good measure of relative durations of the active state.

The fusion frequency is sometimes determined along with twitch-contraction times. The stimulus frequency at which the fluctuations in tetanic tension disappear is sometimes used, alternatively the frequency reached when the tetanic tension no longer increases with frequency may be used. At this frequency the period of the stimulus interval is equal to the plateau (period of full activity) of the active state. As such it adds little information to that obtained from the twitch contraction time.

The twitch-tetanus ratio is the ratio of peak twitch tension to the tetanic tension. Twitch-tetanus ratios should be determined when measuring twitch contraction times. The two taken together determine one point in the decay of the active state. For a constant active state duration, the twitch-tension is directly related to the relative speed of force-velocity relation, and inversely related to the compliance of the series elastic component. (See derivation in Appendix 2.1.) Because the compliance of the series elastic component is increased at low tensions, the twitch-tetanus ratio also varies with muscle length. A difficulty with using the twitch-tetanus ratio as a relative measure of the speed of the force-velocity relation is that the series elastic element of individual motor units may be highly variable among units.

The secondary measures of contractility taken together do provide a good estimate of the relative duration of the active state in motor units for which they have been determined. This is fortunate, for as it will be seen below this relation cannot be determined during reflex activation. The secondary measures, however, give very little informa-

tion about the force-velocity relation, and therefore about the intrinsic rate of shortening.

The Validity of the Primary Measures During Reflexes.

The alternative to activation of single motor units proposed is the use of reflex activation to selectively recruit a particular motor unit population. It must be considered whether the primary measure of contractile properties (length-tension relation, force-velocity relation, and active state duration) determined on a reflexly activated muscle is that of the motor units active in the population.

Several characteristics of reflexes would make it difficult to determine the duration of the active state. Reflexes often require temporal summation, the motor units fire asynchronously and the stimulus may be followed by an afterdischarge. A phasic reflex, with synchronous activation of the motor units, would be that form of reflex in which reversal of the order of recruitment would be most probable (see page 9). Therefore, any attempt to determine the duration of the active state during reflex activation would not give a better measure than that obtained by measurement of motor unit twitch contraction times.

During reflex activation of the muscle, the contraction of motor units of the subtetanic fraction will be unfused, that is, their activation will not be constant with time. The model can be used to predict the effect on the measurement of the force-velocity relation, applying the model to individual motor units. The force-velocity relation of a subtetanic unit can be expected to differ from that of a tetanic unit, since it can only shorten maximally for the fraction of time it is active.

The question of whether the force-velocity relation changes (with respect to V_{max}) during the decay phase of the active state is open to question at the present time. The decay of the active state follows the decline in Ca^{++} concentration, so the determination of the force-velocity relation at a Ca^{++} concentration which produces submaximal isometric tension is equivalent to measuring it as a point in the decay of the active state. Podolsky and Teichholz (60) skinned frog fibers, making the fiber permeable to calcium in the bath. With this preparation they found no change in V_{max} at a reduced activation, as measured by the isometric tension. Julian (61), however, using partially glycerinated muscle fibers which were permeable to external calcium, obtained force-velocity relation with a V_{max} one-half the normal V_{max}, at an activation that was 65% of normal.

Rack and Westbury (62) have described a method of obtaining 'smooth' contractions during stimulation of motor units at subtetanic frequencies. The ventral roots which supply the soleus muscle were grouped into five equal fractions which were then stimulated in rotation. Thus all motor units were stimulated at the same rate, but at different times in the stimulus cycle. The contractile properties obtained at subtetanic frequencies under these conditions were markedly different from those obtained at tetanic rates. Figure 7 (63) shows the force-velocity relations obtained at various stimulation frequencies in soleus muscle. As suggested above, the curves obtained have a lower V_{max} for subtetanic stimulation frequencies, decreasing with the decrease in stimulation frequency.

Figure 7. Force-velocity relation during alternate stimulation of ventral roots (asynchronous) at subtetanic frequencies. Stimulation at frequencies indicated was applied to 5 groups of ventral roots in rotation. From Joyce and Rack (63).

Figure 8. Length-tension relation during asynchronous stimulation of ventral roots at subtetanic frequencies. Curves obtained at low frequencies of activation are shifted to right. Vertical lines indicate fluctuations in tension when synchronous stimulation was used. From Rack and Westbury (62).

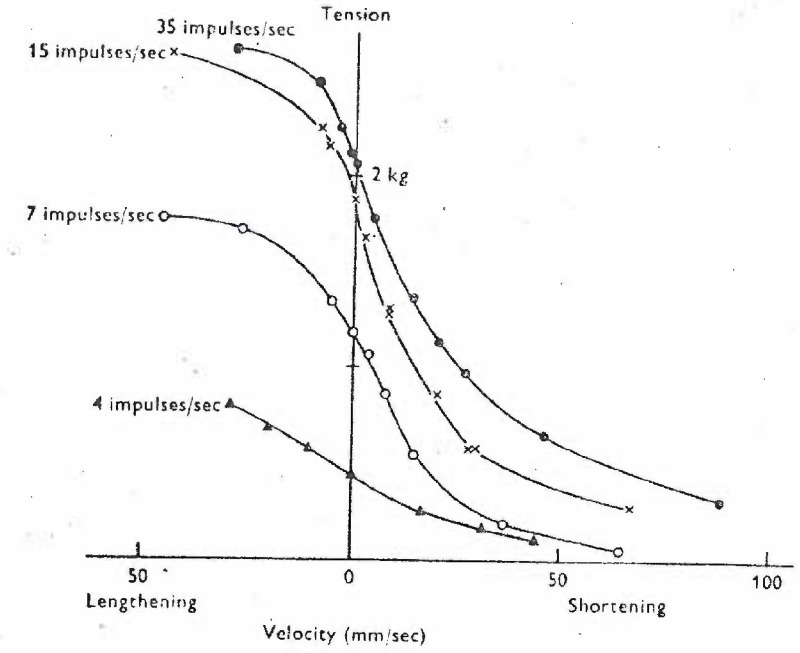
Tension
35 impulses/sec
15 impulses/sec
2 kg
7 impulses/sec
4 impulses/sec
50
0
50
100
Lengthening
Shortening
Velocity (mm/sec)

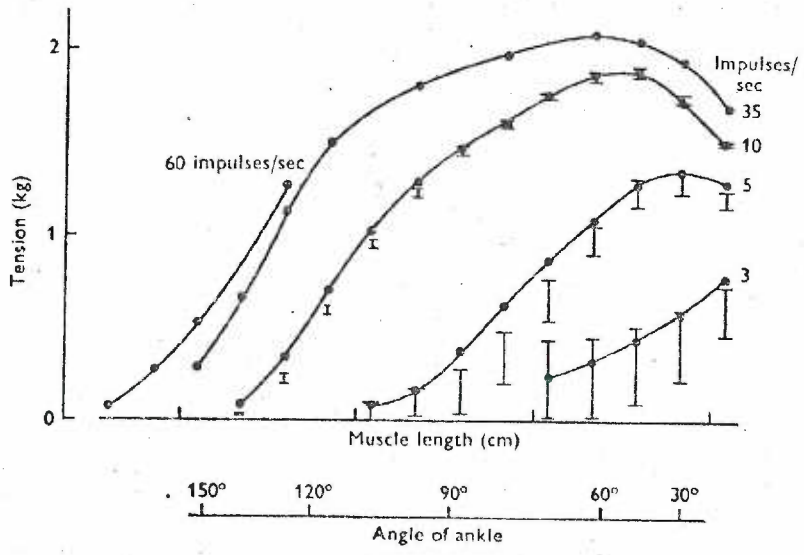
2
1
0
Tension (kg)
Impulses/
sec
35
10
5
3
60 impulses/sec
Muscle length (cm)
150°
120°
90°
60°
30°
Angle of ankle

Figure 8 (62) shows the length-tension relations obtained for stimulation at subtetanic frequencies. As the stimulus frequency was decreased, the curve of increasing tension with muscle length was shifted to the right (toward longer muscle lengths), as was also the peak of the curve to a lesser extent. The authors discussed the effect in terms of a proposed decrease in duration of the active state at shorter muscle lengths. Another explanation is possible, however. It is shown in Appendix 3.1 that the twitch tension will decrease proportionately more than the tetanic tension at muscle lengths shorter than L_o. At low frequencies the average tension is equal to summed twitches in the separate fractions of the muscle and the length-tension relation must vary similarly. The shift of the length-tension relation at low frequencies can be accounted for in part by the classical model, and therefore is not a property exclusive to cat soleus. A similar shift of the length-tension relation could be expected at low reflex levels if there is a significant difference in the firing rates of the motor units as a percentage of their fusion frequencies. Evidence has already been given that the smaller motor units of gastrocnemius (cat) have longer twitch durations and therefore lower fusion frequencies. Thus the actual firing rates of these units would be lower as they were recruited and passed through the subtetanic range.

The Choice of Measurement of the Force-Velocity Relation During Reflex Activation.

The question of the recruitment of 'slow' vs. 'fast' motor units has two parts because the terms have described two different contractile

properties. The part dealing with the duration of the active state has been provisionally answered by the measurement of twitch times of individual motor units, and the identification of their relative excitability via the size principle. The remainder of the question is whether the intrinsic rate of shortening also differs and is related to the motor unit recruitment. The determination of force-velocity relations at different reflex levels is a direct measure of the intrinsic rates of shortening of the motor units recruited at that level, provided that the differences seen cannot be attributed to differences in fusion of motor unit frequencies. The questions of heterogeneity of intrinsic rates of shortening and the relation to recruitment are answered at the same time.

The alternative to using reflex activation would be to measure the force-velocity relation of a single motor unit. At the time the experiment was designed, it was felt that the tension of a single motor unit (especially a small unit) would be too small in relation to the errors which would occur to determine the force-velocity relation reliably for a single motor unit. The errors would arise because of the mass of the muscle (inertial), friction and internal viscosity of the passive muscle. Normally these sources of error would be negligible compared to the forces of even the low level reflex contractions. Even if the technical problems of measuring the force-velocity relation in a single motor unit were overcome (see Discussion, page 143), it is not clear that an advantage would be gained either with respect to the difficulty of the experimental techniques used or in the results obtained.

METHODS

Design of the Experiment

A number of decisions were made which determined the constraints on the experimental apparatus and on the way the experiments were performed. They are considered in the following paragraphs.

Choice of the Experimental Preparation.

The dog was selected as the animal of choice with the intention that the information on the contractile properties would be used in future studies of postural control. The only drawback foreseen to result from this decision was the necessity for increasing the size of the experimental apparatus. It was planned to select collie-shepherd type mongrels, in the range of 35-45 pounds (15-20 kg), which were similar to the animals which had been used in the postural control studies.

Use of Decerebration.

The choice of a decerebrate preparation was dictated by the desire to eliminate anesthetics at the time of the actual experimental runs. The decision was based upon evidence that some anesthetics (i.e., ether and barbiturates) alter the order of recruitment of motoneurons (64). The use of reflex activation enabled the separation of motor unit populations on the basis of their physiological order of recruitment; any alteration of this order would change the active population whose con-

tractile properties were to be studied. Secondarily it was thought that the general facilitation of extensors under decerebrate conditions would be helpful in obtaining maximal reflexes.

Choice of Gastrocnemius.

Gastrocnemius was selected because it was readily accessible, and was an extensor with heterogenous cytochemical properties (based on preliminary determinations of succinic dehydrogenase and glycogen distributions). The mechanical isolation is comparatively simple, requiring the removal of the calcaneous and the section of the other tendons in the Achilles tendon. Fixation of the opposite end of the muscle requires a pin through the distal end of the femur passing behind the lateral and medial condyles. Isolation of the muscle nerves is also simple, which allows their exclusion from the general denervation performed to assure only tension of gastrocnemius is recorded. The soleus, a muscle which is homogeneous in other species, is absent in the dog.

Deafferentiation of L_6, L_7, S_1.

The determination of the force-velocity relation requires that the muscle activation remain constant during muscle shortening. With the dorsal roots intact, the stretch reflex would reduce the reflex activation when shortening began. Sectioning the dorsal roots containing muscle afferents from gastrocnemius (L_6, L_7, S_1) eliminates the stretch reflex. Access to the dorsal roots requires a laminectomy of the lumbosacral vertebral segments, and requires that this section of the spinal

column be stabilized by the experimental apparatus. The deafferentiation appeared to be the major factor responsible for the poor success rate in obtaining usable reflex activation. (See discussion of reflex activation below.)

Use of Crossed Extensor Reflex.

The crossed extensor reflex was not the first choice of reflex activation of gastrocnemius; stimulation of the cut central ends of the dorsal roots seemed more convenient. This was found to result in a mixed excitatory and inhibitory input to the motor pool, which limited the reflex activation which could be obtained. The close proximity of the ventral roots necessitated measures to assure that direct stimulation of the motorneurons did not occur by spread of the stimulus current. These problems were avoided by using the crossed extensor reflex, elicited by stimulation of the peroneal nerve on the contralateral side to the gastrocnemius muscle used. The stimulus causes a reflex flexion of the limb on the stimulated side, and a contraction in gastrocnemius, an extensor, on the opposite side. (The other extensors of this limb are denervated.)

The use of the crossed extensor reflex has several potential advantages. The reflex activation of gastrocnemius is one step removed, reflexly, from the artificial electrical stimulation. It was hoped that the crossed extensor reflex would be as active following deafferentiation as before. Support for this view was Sherrington's observation that the crossed extensor reflex (in vastocrueus, cat) was usually

increased after deafferentiation (65). This was not the result in the present experiments, however. The crossed extensor reflex was reduced, and often eliminated after the section of the ipsilateral dorsal roots. It was observed that with the roots intact the crossed extensor reflex was facilitated by stretch of the interosseous muscles of the ipsilateral paw (positive supporting reaction); the removal of this and other sources of facilitation is a probable cause of the unresponsiveness of the gastrocnemius motor pool after deafferentiation.

The ipsilateral area centralis of the anterior lobe of the cerebellum was ablated in order to facilitate the gastrocnemius motoneurons. When successful, a temporary augmentation of resting tonus was usually the immediate effect, with a concurrent return of the crossed extensor reflex. The facilitation of the crossed extensor reflex often outlasted the tonic activity. By conducting the ablation in stages, the duration of the period of reflex enhancement could be prolonged. The difficulty with the method was the low incidence of successful reflex preparations. However, other attempts at facilitation were unsuccessful.

Use of a Viscous 'Isotonic' Load.

During the period when reflex activation could be obtained, it was necessary to obtain as many runs under different isotonic loads as possible in order to determine the whole force-velocity relation. Thus a means of changing the isotonic load as quickly as possible was needed. Changing weights or springs by hand would be unwieldy, especially ones which could impose the loads necessary. A solution was suggested by the

need for some damping of the muscle lever, to eliminate the 'ringing' or mechanical oscillations following release of the muscle lever. A hydraulic dashpot consisting of piston and cylinder, and a variable flow valve, was substituted for the springs or weights usually used for the isotonic load. Adjustment of the damping valve allowed quick change between runs, resulting in a different isotonic load during muscle shortening, which was inherently highly damped.

The load produced by the dashpot is not a true isotonic load (constant force) but increases with velocity of travel of the piston of the dashpot, and therefore of the muscle lever. This characteristic had one unforeseen advantage. With a true isotonic load a muscle shortens until the isometric tension at that length is equal to the isotonic load and shortening stops. With the viscous load, as the velocity of shortening becomes less at shorter muscle lengths, the load also decreases, and the muscle continues to shorten. The result is that more data points at different muscle lengths can be obtained from each contraction.

It is not completely accurate to say that a 'true' isotonic load eliminates the need to correct for the series elastic component; this was the original reason for using isotonic loads and is true only in the region of L_o where there is little change of isometric tension with muscle length.

'On-Line' Computer Processing of Data.

A minicomputer was part of the system available for sampling and digitizing the data. The choice was made to use the minicomputer to

control the experiment (stimulation, release of muscle) as well as the sampling of the data, and to compute length-tension and force-velocity plots immediately. This decision required additional hardware (computer interfaces) and software (computer programs). However, the ability to see the derived plots in addition to the raw data during the experiment itself permitted more efficient use of those periods of reflex activity which were suitable for force-velocity determinations. This capability was also responsible for the detection of some malfunctions in time to correct them, which would not have been possible after the experiment.

Mechanical Criteria.

The decisions made above basically defined how the experiment would be conducted and the experimental apparatus designed. Additional criteria followed from the necessity to reduce possible errors in the measurement of the contractile properties. These included:

1) The inertial load (effective mass of muscle lever) should not add appreciably to the inertia of the muscle. (The gastrocnemius weighs approximately 60 grams.)

2) The total compliance of the restraints, the muscle lever and the connections should not add appreciably to that of the series elastic component. Some of the deflections under load could be calculated in advance and incorporated into the design. In other cases the best known practice was used, and the resulting compliance actually measured. The design was based on a maximum muscle tension of 40 kilograms.

3) Because muscle lever rotation was measured rather than linear distance, a cosine error was introduced into both length and tension measurement. This error was to be less than 1% for the full range of muscle shortening (8% angle of rotation).

Description of Experimental Apparatus

Mechanical Construction

Slotted Table.

The first step in the establishment of the necessary rigidity was to construct a 'test bed' or table of 6 parallel 2" x 2" alumium T-bars. These T-bars were spaced to give 3/4" separation, resting in milled slots in the two horizontal cross pieces of 3" channel bar in an upright position. The mating surfaces were then heli-arc welded to form a rigid structure, which was then bolted to a supporting structure of angle iron. The result was a table with a flat slotted surface. Passing a bolt through the slot permits a fixture to be held rigidly to the table top at any location in the longitudinal direction and at intervals of 2" in the transverse direction. The rigidity of the connection was determined by the area of surface in contact and the pre-stress in the bolts obtained by the torque used to tighten them. The table as viewed from above is shown in Figure 9.

Animal sling.

The animal was supported in a canvas sling suspended between two

Figure 9. View from above of experimental table and fixtures. Pictured from left to right are the adjustable valve of the dashpot, the muscle lever, the knee fixture, and the animal sling.

Figure 10. Knee fixture. Twist drill passes through distal end of femur, and through axial hole in bolt threaded through leg of the yoke.

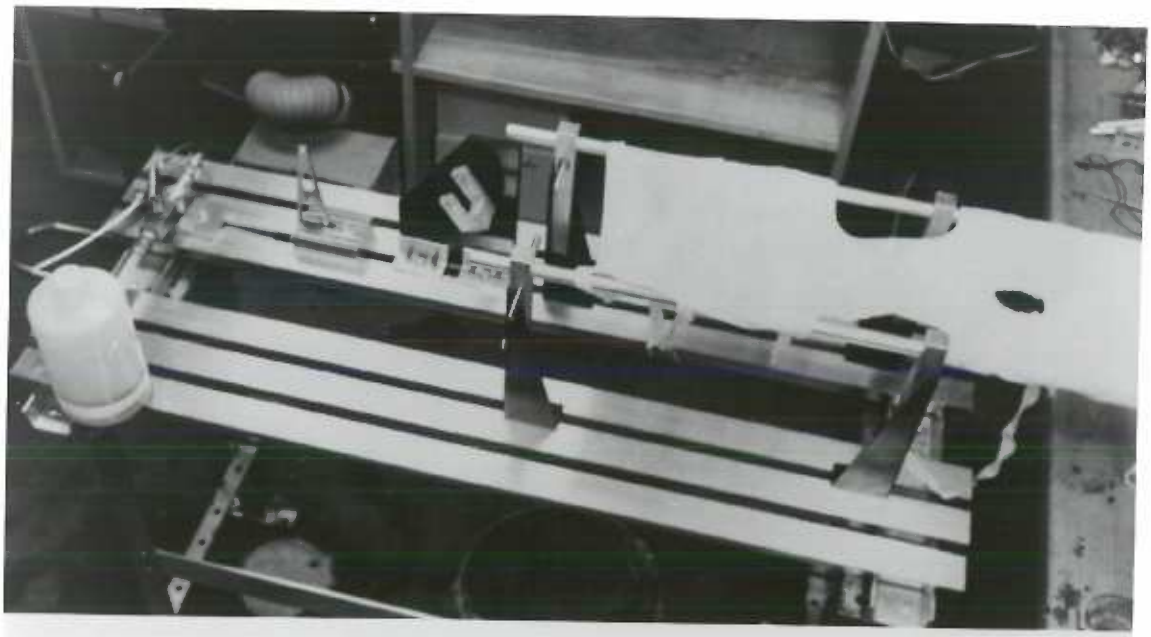

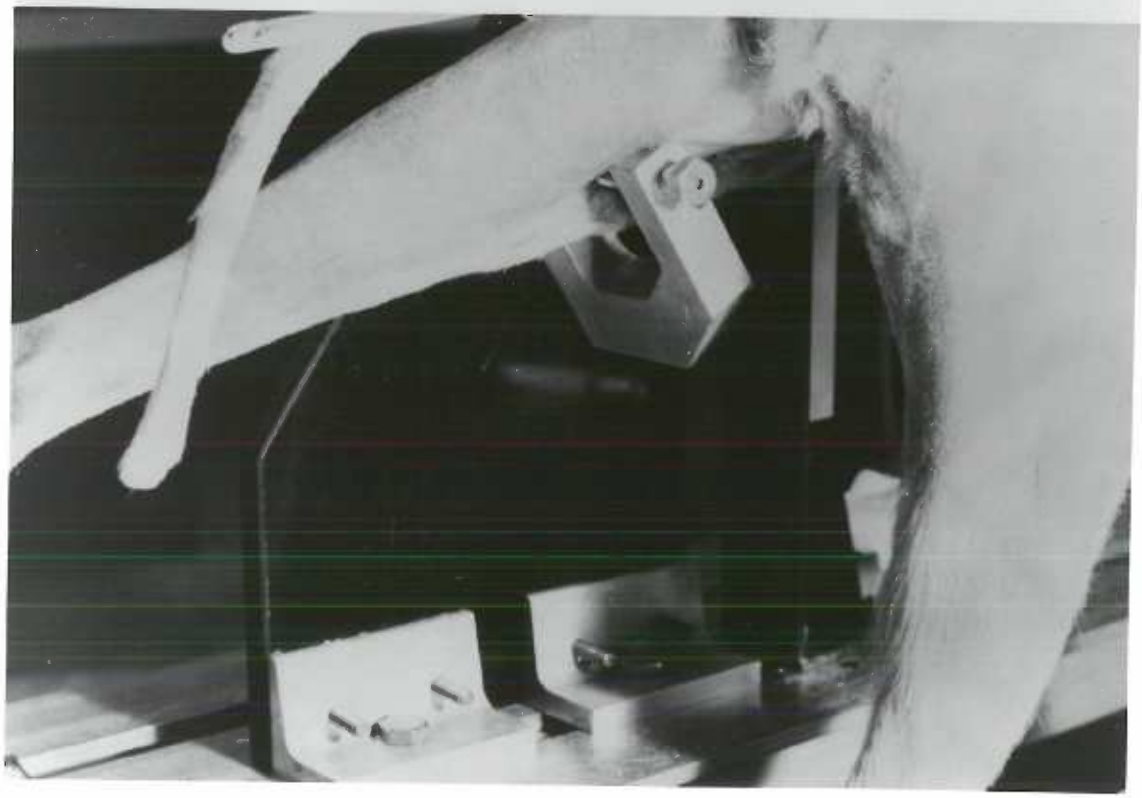

parallel horizontal 3/4" aluminum rods oriented in the longitudinal direction. The sling supported the forepart of the body, and contained openings for the forelimbs and the trachea cannula. Each rod was supported by two corner posts, one fore and one aft. The vertical corner posts were constructed from 1" x 1" aluminum stock, with 3/4" holes drilled in the upper ends through which the horizontal rods were passed. Each post was bolted to an adjustable (steel) bracket (12") via a milled slot to allow adjustment in the vertical direction. The bracket mount mated with the 3/4" slot of the table to allow adjustment in the longitudinal direction. Hip pins formed by grinding points on 8" lengths of 3/8" stainless steel threaded stock were threaded into taped holes in the two aft corner posts. Double nuts on each pin locked the pin once tightened in place in the hip. The hind portion of the animal was supported between the opposing hip pins.

A horizontal cross piece (1/2" aluminum rod) was clamped to the longitudinal rods with adjustable clamps. This provided a support for a vertebral clamp. This clamp was placed on the first dorsal spinous process anterior to the laminectomy. An Allen screw locked the clamp in place on the support rod once in the proper position. The assembled structure may be seen in Figure 9.

Knee fixture.

The gastrocnemius originates from the medial and lateral condyles of the femur. The rigidity of the fixation of the distal end of the femur to the table bed is as critical as the rigidity of the muscle

lever and connections at the other end of the muscle. The force is mainly in the longitudinal direction, creating a torque about a horizontal axis due to the displacement of the force vertically above the table. This torque was resisted with low compliance by making the base of the fixture broad (in the longitudinal direction). The upright was a piece of 1/2" thick bakelite approximating a right triangle 10" x 10". A yoke milled from 3/4" aluminum was bolted to the upright. This yoke straddled the distal end of the femur. The fixation pin was a number 31 twist drill left in place after drilling through the bone. To minimize deflection in the shear direction, it was desirable to imprison the twist drill as close to the bone as possible on either side. On the supported side of the yoke, a button anvil was press-fit, which contained a hole in the center to capture one end of the twist drill. A 1/8" hole was bored along the axis of a 1/2" stainless steel bolt. This bolt was threaded through the opposite arm of the yoke, passing over and capturing the free end of the twist drill. Tightening the bolt clamped the distal end of the femur between the bolt and the anvil, with the twist drill providing the shear restraint. The result is shown in Figure 10.

The distal end of the tibia was positioned and held in place by a boiling flask clamp attached to a movable vertical upright. It served only to provide vertical and lateral support, not restraint in the longitudinal direction.

Muscle Lever (Mechanical).

The muscle lever, shown in Figure 11, was designed to be as rigid as possible consistent with a low moment of inertia. This was accomplished by tapering the lever to distribute the weight closer to the center of rotation. In addition, where the stress was low, metal was removed, reducing inertia with minimal increase in compliance. The strain gages were located at positions where the lever approximates an A-frame truss, which simplified the calculations for obtaining the desired sensitivity. The stress level at this location was somewhat higher than that desirable for the remainder of the lever.

The position of the lever was measured as rotation about its pivot (Precision ball bearings, Fafnir F33KDS). Bending of the lever above this pivot results in an unrecorded deflection. Bending of the lever below the pivot (or deflection of the lever restraint under load) results in a recorded deflection. The latter is a deviation from ideal isometric contraction, but is not an error in measuring muscle length.

The muscle lever release mechanism was a micrometer attached to a pivoted mount. A pawl on the end of the micrometer shaft engaged the lower end of the muscle lever, and allowed for adjustment of initial muscle length. Activation of a solenoid attached to the mount resulted in rotation of the micrometer about the pivot, and disengagement of the pawl in the muscle lever, releasing the lever.

The mount for the muscle lever and the mount for the release mechanism were bolted together to the table, the bolt passing through one of the slots in the table. The lower end of the muscle lever also passed

Figure 11. Muscle lever and release. Upper and lower support blocks are held together by a bolt passing through a slot in the table. Micrometer adjustment sets muscle length before release. Strain gages are in open area of lever immediately above pivot. Piston of dashpot attaches to ball bearing in lower muscle lever. Dual connectors are outputs of potentiometer and strain gage bridge respectively.

Figure 12. Connection between muscle lever and calcaneous. Conical 'keeper' positions the stainless steel sutures on the adjacent calcaneous. Sutures are threaded through tendon behind portion of calcaneous removed with tendon.

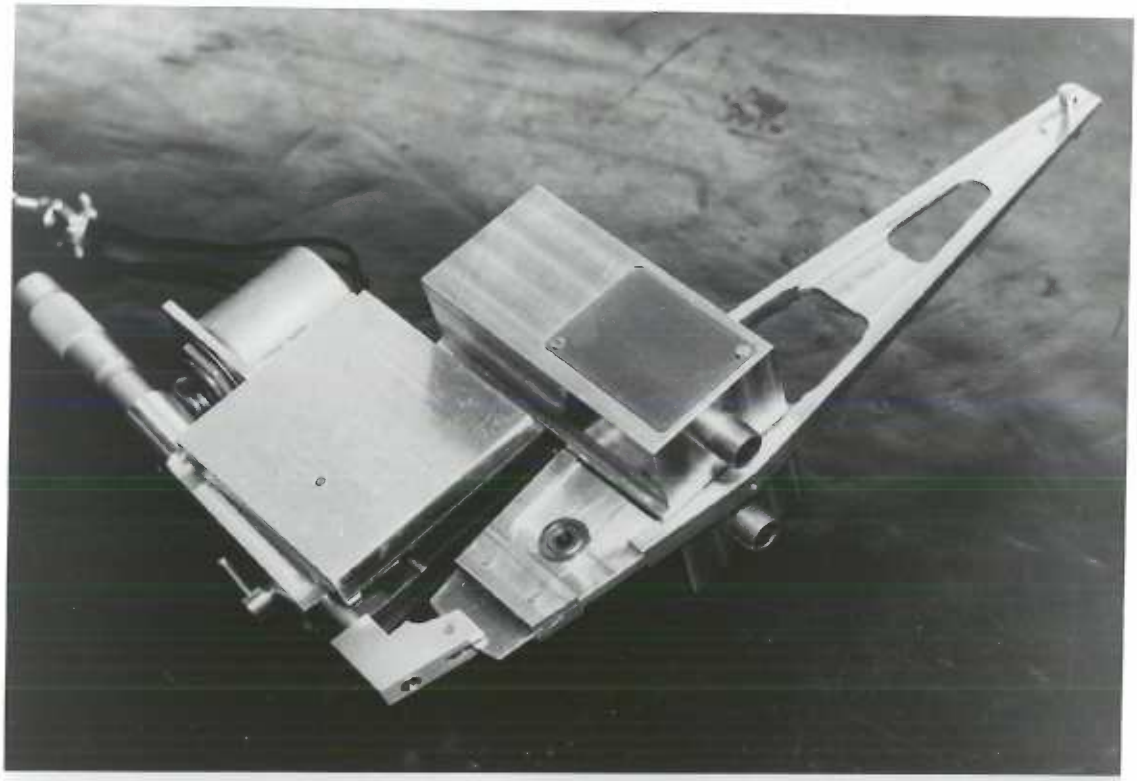

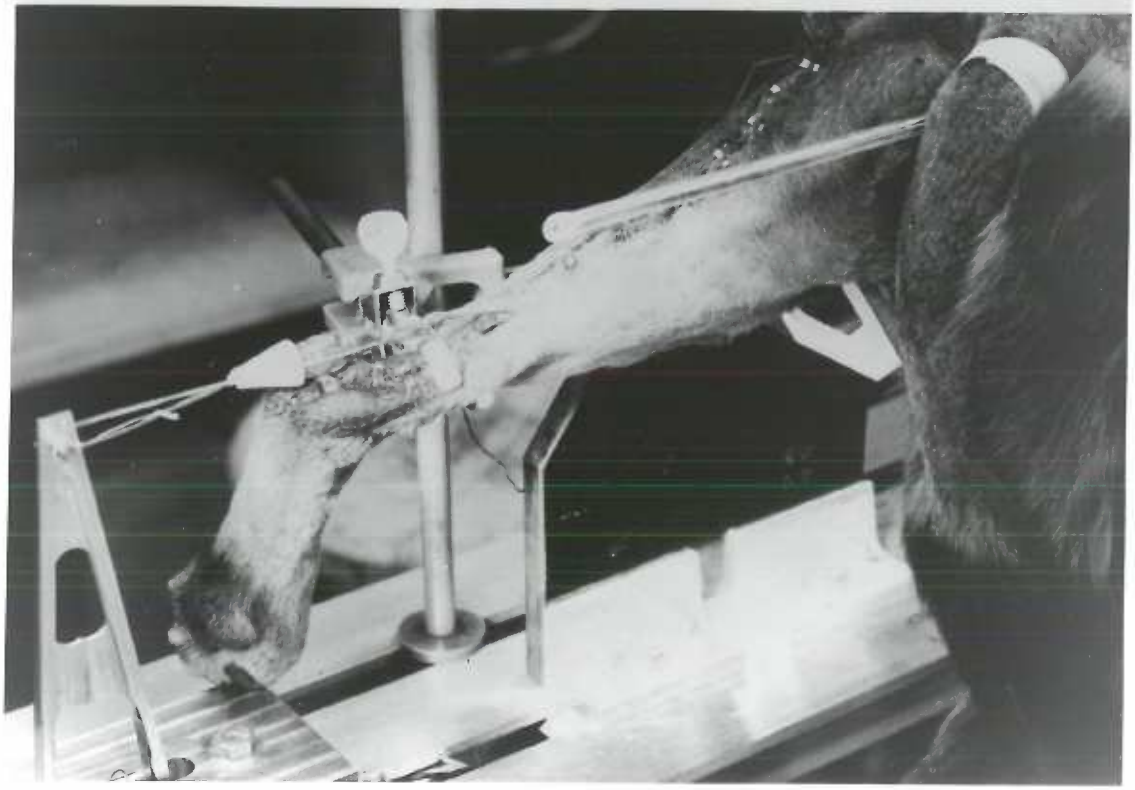

through the slot. Milled ridges on both mounts aligned the mounts with the slot of the table, and therefore with each other. After adjustment was made in the longitudinal direction, the bolt was torqued tight, locking muscle lever and restraint mounts rigidly to the table.

Connection of Calcanean Tendon to Muscle Lever.

A critical part of the external compliance in series with the muscle was the link between the detached tendon (removed with a portion of the calcaneus) and the muscle lever. This connection is shown in Figure 12. A single length of number 0 braided stainless steel suture, doubled in thickness, was used. The suture, attached to a large straight needle (cutting), was threaded once through the tendon behind the attached portion of the calcaneus and passed around a pin located in the upper end of the muscle lever. This pin extends equally on both sides of the muscle lever. A groove in either end of the pin served as a pulley to allow even distribution of the stress between all portions of the connection. After passing around the pin, the suture was threaded through the tendon again, this time at right angles to the first penetration, passed around the pin on the other side of the muscle lever and tied with a square knot. The suture was additionally threaded through individual holes in a 'keeper' which served to position the sutures with respect to the calcaneus, and prevent them from shifting during the experiment. If the load is evenly distributed over all of the sutures, the compliance will be reduced by a factor equal to the number of 'wraps' between tendon and muscle lever, eight in this case. The sutures bear

on the bone, distributing the stress over a larger area than the suture hole in the tendon. Cotton thread ties were used to prevent the sutures from slipping out of the grooves when the muscle is slack, and to position the 'keeper' against the removed portion of the calcaneus.

The Adjustable Dashpot.

The load against which the muscle shortened was developed by a hydraulic dashpot attached to the lower end of the muscle lever. The components of this hydraulic damping system are diagrammed in Figure 13. The dashpot was composed of a piston and cylinder, an adjustable flow valve, a one-way bypass valve, and a reservoir and plumbing. The cylinder was constructed of aluminum, 2" outside diameter with a 1.25" bore. A ridge (to mate to the slot in the table) was milled along the upper length of the cylinder, and the cylinder drilled and tapped, providing the means to rigidly bolt the cylinder to the underside of the table.

The piston was turned from nylon, to fit the bore of the cylinder. An 'O' ring provided a low friction seal between the piston and the cylinder. An aluminum piston arm pivoted within a recess in the piston on a brass pin. The other end of the piston arm formed a yoke spanning the thickness of the muscle lever. The point of attachment was a ball bearing in the middle of the lower end of the muscle lever (Figure 11). The piston arm was coupled to the muscle lever with a pin (1/2" drill rod) through the bearing hub and both arms of the yoke.

Low compliance could only be maintained if the tubing was rigid and the fluid incompressible. The outflow of the cylinder was restricted by

Figure 13. Diagram of hydraulic dashpot. This system was used to apply an adjustable load to the muscle lever during muscle shortening following release of the lever. The calibration of force versus velocity (as appears at upper end of muscle lever) for different settings of the valve is given in Appendix 1.0, Figure 36.

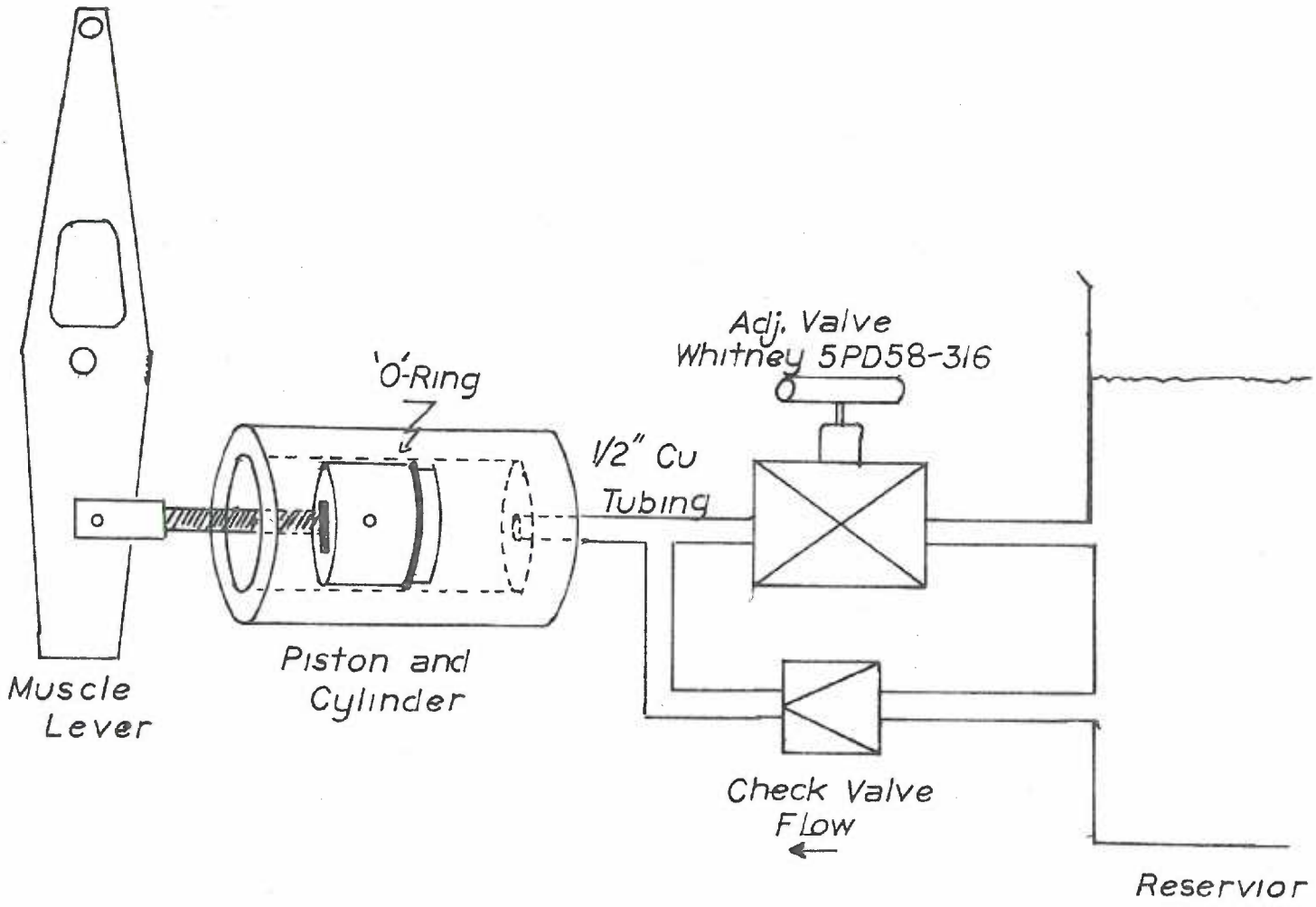

HYDRAULIC DASHPOT

an adjustable valve (Whitney 5PD58-316). One-half inch copper tubing was used here for low compliance and low resistance to flow at high flow rates. The tubing lengths were kept to a minimum. The outflow of the valve empties into a reservoir at atmospheric pressure. On the return stroke of the piston, the adjustable valve is bypassed by a check valve. This bypass limits the negative pressure developed on the return stroke, which if sufficient would allow air to pass the 'O' ring seal. All the fittings were wrapped with teflon tape before being 'plumbed' together. Finally, silicone stopcock grease was used as an additional seal between piston and cylinder. By pumping fluid between cylinder and reservoir, air was purged from the system. Any air remaining trapped in the system results in a step change in length when the mucle lever is released. Values of this instantaneous change in length are included in Table 1.

The 'damping' (force divided by velocity) achieved depends both upon the viscosity of the fluid as well as the constriction of the valve. Vacuum pump oil (DuoSeal, Sargent Welch) was used, and was found to provide the necessary range of damping. A plot of the load seen at the muscle attachment versus the velocity at this point for various turns of the valve is given in Appendix 1.0 (Figure 37).

Determination of Mechanical Constants.

The resulting mechanical constants of the experimental apparatus are given in Table 1. Restraint compliance is the total external compliance seen by the isometrically contracting muscle. Uncorrected compliance is that which results in a muscle length change which is not recorded as movement of the muscle lever.

The uncorrected compliance was estimated as follows: A piece of wood simulated the attachment to the calcaneus and the attachment to the femur. One end was held in the yoke for fixating the femur, and the muscle lever was attached to the other end in the normal manner. Recording both length and tension the micrometer of the muscle lever restraint is used to increase both length and tension. The compliance is the length change divided by the tension change. Since the length change occurs above the pivot of the muscle lever, it is normally unrecorded.

The restraint compliance was determined as follows: The muscle lever restraint was locked in position. While recording both length and tension, a load was applied to the lever (horizontally, via a pulley and weights). Only the change in length due to compliances in structures below the pivot of the lever will be recorded. Therefore, the recorded compliance equals the change in length divided by the tension. The restraint compliance is the sum of this compliance and the compliance determined above.

The 'effective' muscle lever inertia was determined by the following method:

A light spring was attached to the muscle lever. Its compliance was determined by changing the length, and recording the tension change. The lever and spring were allowed to oscillate and the period of oscillation determined. The equation giving the period is as follows:

$$\omega^2 = (2\pi f)^2 = Ks/_{Me}$$

The instantaneous length change after release varied depending upon the care in purging the hydraulic system of trapped air. A minimum value as well as the range of values encountered during the experiments is given in the table.

TABLE 1: Table of Mechanical Constants of Experimental Apparatus

Lower lever + release compliance =	.083 mm/kg @ 8 kg
Upper lever + fixation compliance =	0.07 mm/kg @ 8 kg
Total restraint compliance =	.15 mm/kg @ 8 kg
Isotonic release displacement =	1.7 mm-2.1 mm
Effective mass of lever at attachment =	1.07 grams (mass)
Lever arms:	
Pivot to muscle attachment =	16.5 cm
Pivot to dashpot coupling =	5.0 cm
Pivot to release catch =	9.0 cm
Displacement for 1% cosine error ($\pm$ 8°) =	$\pm$ 23 mm

Instrumentation

Muscle Lever (Tension and Length Transducers).

Force applied to the end of the muscle lever puts one strut of the lever into compression and the other into tension. This allows a simple calculation of the strain for a given force. The dimensions of the struts were designed for 1500 μ strain for a 50 kg force applied to the lever. Two silicon strain gages (PO-500, Whitaker Co.) with a gage factor ($\Delta R\%/\Delta L\%$) of 120 were bonded to each strut, one longitudinally and the other at right angles to this gage. The longitudinal stress produces both a longitudinal strain ($E_L = \frac{S}{Ym}$, Ym = Young's modulus) and a transverse strain of opposite sign ($E_T = \sigma E_L$, σ = Poison's Ratio). The strain gages were wired to form a four active arm Wheatstone Bridge,

with gages sensing compression and tension respectively occupying opposite arms of the bridge. The gages on each half bridge (i.e., left or right half as shown in Figure 33, Appendix 1.0) were on the same strut, and at the same temperature. Thus the ratio of resistances remains constant as the temperature changes, minimizing the zero shift with temperature of the bridge. A schematic of the bridge and amplifier is shown in Figure 33, Appendix 1.0.

Rotation of the muscle lever was amplified by a set of helical gears (Boston Gear) used for minimum backlash with a gear ratio of 8:24 to produce rotation of a single turn resistance potentiometer (Econopot, New England Instrument Co.). The potentiometer formed one-half of the Wheatstone bridge, shown in Figure 33, Appendix 1.0, along with the associated amplifier.

Because rotation of the lever changes the effective length of the lever, there is a cosine error in tension and length measurements, which equals 1% for $\pm$ 8° rotation. This represents $\pm$ 22 mm displacement at the end of the lever.

Measurement of EMG.

The electromyogram (EMG) was recorded via two sintered Ag-AgCl electrodes which were separated 18 mm apart along the longitudinal axis of the muscle.

The differential amplifier shown in Figure 31 (Appendix 1.0) was designed to amplify the EMG. The input differential FET (field effect transistor) pair used is designed to track with low voltage offset.

Good common mode rejection was achieved since the input impedance was large (≈100 Meg) and a cascode configuration was used for both the current source and the differential pair. The amplifier was AC-coupled with a low cutoff frequency of 20 hertz.

The integrated EMG is obtained by rectifying (taking the absolute value of) the instantaneous EMG and filtering with a low pass filter. Phase distortion results unless the filter has a linear phase (or constant delay) characteristic. A Bessel filter (whose network function is determined by the n'th order Bessel polynomial) approximates this characteristic. The 6-pole Bessel filter preceded by a precision rectifier shown in Figure 32 (Appendix 1.0) was used. The cutoff frequency (3DB attenuation) is selectable by switch setting, which selects one of the combinations of resistors and capacitors shown in the included table. The constant time delay between input and output signals (a characteristic of the filter) depends upon the filter setting, varying as the reciprocal of the cutoff frequency. The phase characteristic is linear with increasing frequency within 1% to a frequency 2.5 octaves above cutoff and the attenuation is 50 DB two octaves above cutoff. Thus frequencies in the signal high enough to be shifted in phase (relative to linear) are drastically attenuated.

Experimental Control.

In order to facilitate taking experimental data under computer control, it was necessary to control the periods of stimulation and time of muscle lever release. A programmable stimulator and a programmable bit

switch were designed as peripherals to the computer I/O buss, shown schematically in Figure 34 (Appendix 1.0). The programmable stimulator is programmed by three successive digital words output on the I/O buss. The first determines the value of stimulus voltage, being stored in a latch and input to a D/A (Digital/analog) converter. The second digital word is used to preset a counter, which counts the number of clock pulses to determine the period of the output pulse. The third word selects the output (one of three) to which the output pulse is coupled via an optical isolator. A fourth digital word sets any of eight bit switches. (Each switch is the output of an optical isolater). One of these switches is used to turn on the solenoid driver, also shown in the schematic.

Figure 35 (Appendix 1.0) is a plot of the output voltage of the programmable stimulator for different digital values output to the digital I/O buss.

Data System.

The acquisition of the data and control of the experiment was under direct control of the laboratory data processing system. This system, diagrammed in Figure 14, is an Interdata Model 70 minicomputer with associated peripherals, which include a removable magnetic disk store, magnetic tape recorder, multiverter (analog multiplexer and analog to digital converter), and CRT terminal as a console device. The software included a disk operating system and Fortran compiler as well as machine language assembler. The data handling programs were written in Fortran,

Figure 14. Block diagram of data system. Minicomputer, in center, includes central processor (CPU), core memory, and programmable interval clock (PIC), as well as necessary interfaces. Peripherals shown on left include CRT terminal, disk store, magnetic tape recorder, and plotter. Data inputs and control outputs are shown in right.

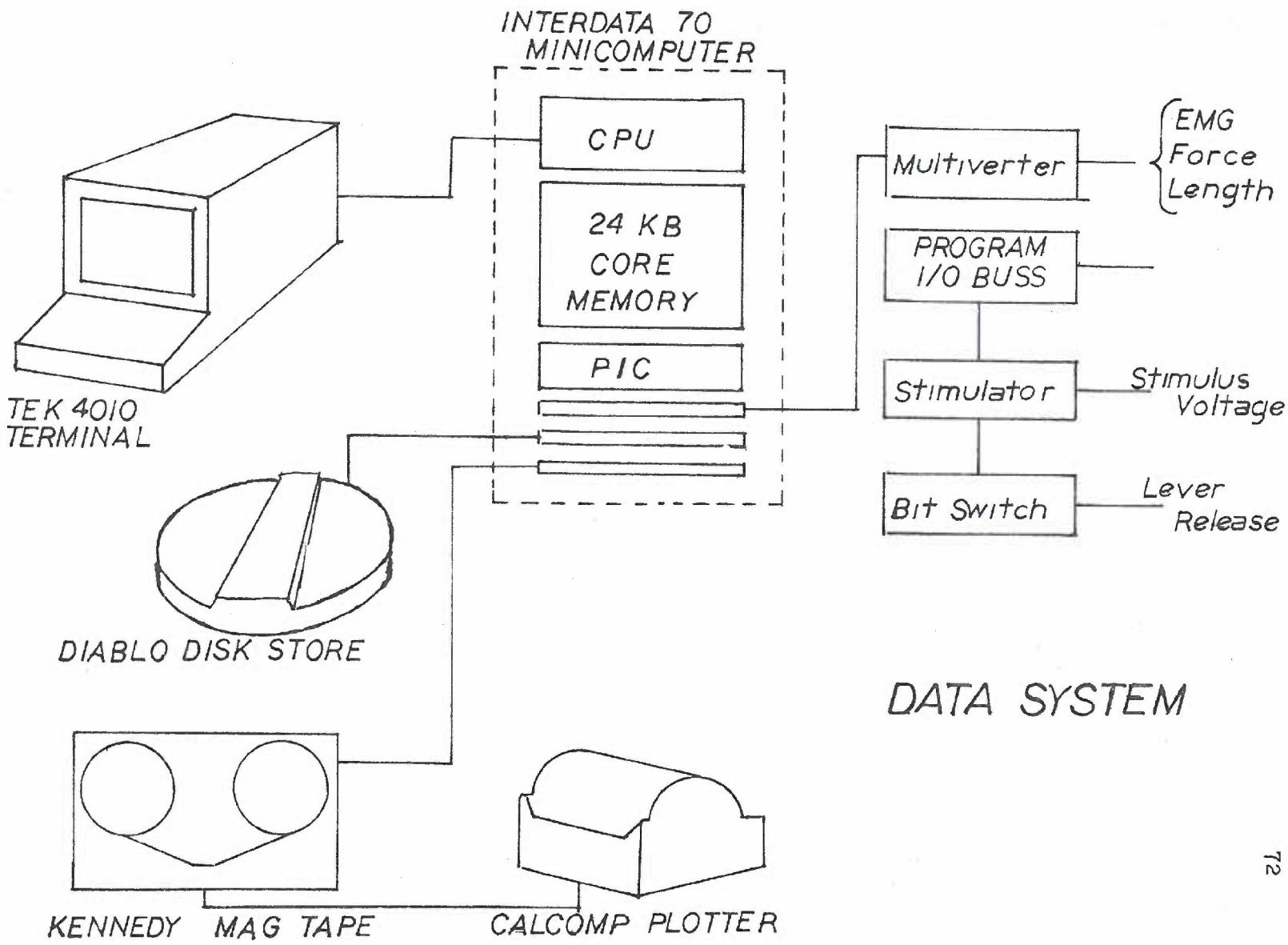
INTERDATA 70
MINICOMPUTER
CPU
24 KB
CORE
MEMORY
PIC
TEK 4010
TERMINAL
DIABLO DISK STORE
KENNEDY MAG TAPE
CALCOMP PLOTTER
Multiverter
EMG
Force
Length
PROGRAM
I/O BUSS
Stimulator
Stimulus
Voltage
Bit Switch
Lever
Release

DATA SYSTEM

or as Fortran callable assembly language subroutines. The programs included experiment control programs, routines for plotting on the CRT, and data processing programs.

Surgical Procedures

Anesthetization.

A preanesthetic dose of 0.5 mg of atropine sulfate was administered I.V. Anesthesia was induced via face mask with a mixture of oxygen and 4% halothane or 50-50% oxygen-nitrous oxide and 4% halothane. After induction, a tracheotomy was performed, and the anesthetic was subsequently administered via the tracheal cannula. Maintenance of an adequate level of anesthesia was usually obtained at 2.5% halothane. The duration of anesthesia was approximately one hour.

Decerebration.

Both common carotid arteries were ligated, with a cannula inserted in the descending portion of one carotid in order to monitor arterial blood pressure. The head was placed in the head holder of a stereotaxic apparatus (David Kopf DKI 1504). A Bovie-type (Burdick SU-4) electrocautery was used to excise tissue and control bleeding. A midline incision of the scalp was made, starting at the forehead and ending beyond the ext. occipital protuberance. First the skin, then the temporal muscle on one side was reflected, scraping the muscle free from the bone. The temporal muscle was excised level with the base of the pinna.

A burr hole was trephined at the lower edge of the parietal bone directly above the external auditory meatus. The burr hole was extended toward the midline of the skull and posteriorly toward the occipital cortex. The diploe was plugged with bone wax at the margins of the burr hole to prevent bleeding or aspiration of air. The dura was removed, and the surface of the cortex was coagulated using a ball electrode with the cautery. A circular loop electrode (3/8" dia.) was used to remove the coagulated parietal cortex overlying the bony tentorium and the colliculi. The last portion of the cortex overlying the brain stem was carefully removed with suction applied through a glass suction tube. The brain stem was transected using a modified weighing spatula. The plane of section passed between the superior and inferior colliculi on the dorsal surface of the brain stem and inclined forward slightly to emerge at the rostral border of the pons on the ventral surface of the brain stem. A piece of gel foam was placed against the posterior surface of the cut. The anesthesia was discontinued, and temporary artificial respiration was applied (Harvard Apparatus small animal respirator) if necessary.

The dura overlying the bony tentorium was excised, carefully avoiding the sinuses, and rongeurs were used to remove portions of the tentorium overlying the anterior lobe of the cerebellum on the exposed side. The skin incision was closed with wound clips when decerebrate rigidity had appeared (usually 1/2 to 3/4 of an hour after discontinuing the anesthesia). If rigidity failed to appear, or the animal was spontaneously active, a second section was made.

Laminectomy.

The animal was removed from the head holder and placed in the experimental apparatus with the forepart (head, shoulders and chest) supported in the sling. The hips were fixed by tightening the threaded hip pins, whose sharp pointed ends were thereby forced into the ileum of the innominate bone immediately rostral to the acetabulum.

A midline skin incision between the L_3 vertebral process and the sacrum was made, and the underlying muscles were exposed. The lateral muscles were retracted, leaving the m. multifidus lumborum next to the vertebral column exposed. The attachments to the spinous processes were cut, and the muscles removed quickly with a large rongeurs. The space was packed with gauze sponges soaked with saline and epinephrine (100,000:1) to control diffuse bleeding. Persistent bleeding was controlled with a hot wire cautery. The most rostral exposed spinous process (L_3) was clamped rigidly, fixing the spinal column. The processes and the lamina of the exposed vertebra were removed with rongeurs, and the bone margins plugged with bone wax. The intervertebral ligaments were cut lengthwise and the extradural fat was removed by suction to expose the spinal roots extradurally.

At a subsequent time the ipsilateral (left) dorsal roots S_1, L_7, and L_6 were sectioned extradurally. The root was first identified at the ganglion (usually visible at the entrance of the roots into the vertebral canal) and then traced to its entrance through the dura. If dorsal and ventral roots were not separate, glass probes with blunt tips were used to separate them sufficiently to cut the dorsal root without damage to the ventral root.

Preparation of contralateral hindlimb.

An incision of the skin overlying the lateral surface of the right (contralateral) hindlimb was made below the knee along the margin of the anterior tibialis muscle (as palpated through the skin). Both branches of the peroneal nerve were exposed (running between ext. digitorum lateralis and fibularis longus muscles). The nerves were cut distally, and freed (side branches sectioned) centrally. Silver wire electrodes were placed on the nerves, and the skin incision closed with skin clips.

Preparation of ipsilateral hindlimb.

Surgery was performed on the left (ipsilateral) hindleg to mechanically isolate the tendon of the gastrocnemius muscle, and to partially denervate the hindlimb, with the exception of the gastrocnemius nerves. The denervation was intended to prevent contraction of muscles, and to eliminate suppressor action of flexor reflex afferents on the extensor reflexes.

Prior to the decerebration an incision under anesthesia was made on the medial surface of the thigh. The superficial branch of the obturator nerve was sectioned as it runs over the adductor muscle. The saphenous nerve was followed until it joins the deep femoral nerve, and both were sectioned.

Following the laminectomy, the yoke of the knee fixture was positioned so the twist drill bit would enter just behind the medial condyle of the femur. After tightening the fixture to the bed, a hand drill was used to drill the bit through the bone (alternating the direction

through a 1/4 turn of the handle). The drill bit was left projecting through the bone (and overlying tissue) and captured in the yoke as previously described (Figure 10).

A longitudinal skin incision from the hip to the calcaneus was made along the back of the thigh. The sciatic nerve was exposed in the popliteal fossa, and followed as far toward the hip as possible. The inferior gluteal and hamstring nerves were sectioned. A stimulating electrode (for direct stimulation) was placed on the sciatic nerve at this location.

A large lymph node and fat pad lies over the heads of the gastrocnemius muscle. The blood vessels on the medial side were tied off and sectioned, and the node reflected laterally, to expose the path of the nerves (gastrocnemius, tibial) without compromising blood flow to the gastrocnemius muscle. The fascia overlying the gastrocnemius was removed to expose the surface of the muscle as well as the entrance of the gastrocnemius nerves and the passage of the tibial nerve. The tibial branches of the sciatic nerve, as well as the peroneal, were cut, preserving the innervation of the gastrocnemius intact. The EMG electrode assembly was positioned on the surface of the muscle, and the skin incision closed with wound clips to hold the electrode in place.

The calcanean tendon is composed of three parts: tendinous extensions from the aponeurosis from the semitendinosus and biceps femoris muscles, the tendon from the plantaris muscle, and the tendon from the gastrocnemius muscle. (There is no soleus muscle in the dog.) All but the latter tendon were sectioned. After marking the rest length in full

extension with a tie around the tendon and clamping the distal tibia, the calcaneus with tendon was removed using large diagonal cutters. The tendon was attached to the muscle lever by the method previously described (see Figure 11). The skin incision was closed, allowing unhindered passage of the tendon through the incision. The exposed tendon was kept moist with saline soaked sponges.

Monitoring of vital signs.

Arterial blood pressure (carotid artery) was measured using a Statham P23AC pressure gage and a Tektronix 564 Oscilloscope with 2C66 carrier amplifier. The rectal temperature was measured and measures were taken to keep the temperature between 36°C and 38°C. Unlike the cat, the decerebrate dog has a tendency toward hyperthermia due to the loss of hypothalamic temperature control and the tonic muscle activity associated with decerebration. Wet cloths and a fan, or a heating pad were used to control the animal's temperature. If the animal did not produce occasional deep inhalations spontaneously, these were provided artificially (by mouth or respirator) via the tracheal cannula to forestall the possibility of atelectasis.

Collection of Data

The determination of the length-tension relation required data from isometric contractions at different muscle lengths, while the determination of the force-velocity relation required isotonic contractions dur-

ing different rates of shortening accompanying variations in load. Thus the experimental runs were of two types, isometric and isotonic, which differed only in that the muscle lever was released during the isotonic run. The data from isometric and isotonic runs were subsequently treated differently in the analysis of the data.

I/O Program.

The actual experimental runs were controlled by the minicomputer operating under a special purpose I/O (input/output) program which supervised the sampling of the data, the release of the muscle lever, and determined the stimulus interval, stimulus pulsewidth, and stimulus voltage amplitude. These parameters could be altered via the CRT terminal (Tektronix 4010) to control the magnitude of the muscle activation, both in the case of crossed extensor reflexes and direct stimulation to the muscle nerve. The terminal was used to initiate the experimental run and the data points collected were plotted out versus time for the measurements of integrated EMG and muscle tension, with muscle length and velocity of shortening plotted as well in the case of isotonic runs.

The temporal sequence of events in an experimental run was organized by the order of instructions in the I/O program while the timing of their execution was determined by the arrival of interrupts from the programmable interval clock (PIC). The interval between interrupts was determined by programming the PIC to count a specific number of clock pulses from a 1 MHz crystal oscillator. Thus by output of commands to different peripherals (PIC, multiverter, programmable stimulator, pro-

grammable bit switch) the timing as well as the sequence of events was determined.

The sampling the the data was the most frequent event, and thus determined the interrupt cycle of the PIC. The data were sampled at intervals of 4 milliseconds, ten successive data points averaged, and the average saved. The data value, expressed in volts at the input of the multiverter, was then multiplied by the proper calibration factor to convert to the units of the variables measured. Velocity was calculated by finding the change of length between successive samples, and dividing by the interval. The data saved for each run comprised 100 values (25 per second) of integrated EMG, muscle tension, muscle length, and velocity of muscle shortening.

The experimental run was organized into a half-second period of no stimulation, a three-second period of stimulation, and ended with a half-second period of no stimulation. During the isotonic runs the muscle lever was released after a half-second of the stimulation, that is, after a half-second of an isometric contraction. The program counted the interrupts from the PIC to decide when to output a command to the programmable stimulator, thus determining the period and frequency of stimulation.

Initialization.

After the surgical protocol was complete, the range of muscle tension and length was roughly determined by direct stimulation of the muscle nerve, and the channel offset adjusted if necessary to assure that

the outputs stayed within the ± 10 volt capability of the multiverter. Following this the channels were 'zeroed' in the following manner: the muscle length was shortened until the active tension had just decreased to zero; here the passive tension was also zero. The input to the EMG amplifier was short-circuited. Then a 'zero' command via the CRT terminal resulted in the sampling of the channels and the saving of these values as channel 'zero' references.

Isometric series.

After adjusting the stimulus level to give a stable, repeatable level of muscle activation (either reflex or direct stimulation) a series of isometric runs was undertaken. Following each isometric run the muscle length was changed by means of the micrometer adjustment on the muscle lever release. A thumb screw locked the adjustment during the subsequent isometric contraction.

Following each run the data taken were displayed on the CRT. If no malfunction was apparent from the data, the data were saved on a disc file. Averages of muscle length, the passive muscle tension before the stimulus, and the total tension during the isometric contraction were computed and saved. After a number of isometric runs had been completed, the data could be recalled, and plotted as curves of passive and active muscle tension versus muscle length. The data were fit by a least squares method (see Analysis of Data) and the constants of the equations determined were saved for later use in the data analysis.

Isotonic Series.

Following the isometric series, a series of isotonic runs was undertaken to provide the data for force-velocity plots. The initial length of the muscle was adjusted depending upon the expected rate of shortening in order to determine the range of muscle lengths for which data would be collected. The damping valve was adjusted in order to establish the isotonic load which would be developed by the dashpot during muscle shortening. Following the initiation of a run an isometric contraction was produced during the first half-second of stimulation. Then the muscle lever was released by the actuation of the release solenoid, and the muscle began to shorten against the isotonic load. Following the run, the data (EMG, force, length, and velocity of shortening) were displayed on the CRT versus time. If there was no apparent malfunction, the data were stored on the disc file. The data were replotted from the disc file on the CRT, substituting the active tension (total tension minus the passive tension) obtained by correcting with the aid of the equation of the passive length-tension curve. Five different muscle lengths were specified at which to select data; the times at which these lengths were reached were indicated on the plot, and these data points could be saved for a force-velocity plot. The sequence was repeated at new isotonic loads (after readjusting the damping valve and resetting the muscle lever) until a range of isotonic loads and shortening velocities sufficient for a force-velocity plot had been obtained. A preliminary force-velocity plot (minus the corrections for series elastance to be described below) using the data could be dis-

played upon the CRT and used to check whether sufficient data had been collected. Isotonic series for different reflex levels and for submaximal direct stimulation of the muscle nerve were collected when possible.

Analysis of the Data

Although preliminary length-tension plots and force-velocity relations were obtained at the time of the experiment, the data from the experimental runs were saved, and plots incorporating a number of corrections were made at a later date. The following section discusses the treatment of the data.

Length-Tension Relation.

The data values of the tension of the inactive muscle (passive tension) and the active muscle (passive plus active tension) obtained from the isometric runs were used to construct plots of active and passive tension. The data for the passive tension were fit by the following exponential relation by determining the values of the constants for best least squares fit:

$$P_{passive} = A + B \cdot e^{+.1x} + C \cdot e^{+.2x} + D \cdot e^{+.3x}$$

where x = the muscle length.

The relation fit to the active tension data was a cubic polynomial in x:

$$P_{active} = A + B \cdot x + C \cdot x^2 + D \cdot x^3$$

The constants for the above relations were saved, and the relations used to make several corrections during the analysis of the force-velocity data.

Compliance of the series elastic component.

An estimate of the compliance of the series elastance was needed to obtain contractile element length and velocity. The length of the series elastic component is a function of the muscle tension; the greater the tension the greater the elongation. Since the total muscle length is measured, the elongation of the series elastic component must be known to determine the length of the contractile element. That is, the force-velocity relation is determined at different contractile element lengths, not overall muscle lengths. The overall muscle shortening velocity is also the sum of shortening of the series elastic component as well as the contractile element; therefore, the estimate of series elastance compliance can be used to correct the velocity. (Note: the latter correction is not needed if the contractions are truly isotonic, but the series elastance must be known to make the length correction.)

The method adopted utilizes the curve of tension development during an isometric tetanus. Under isometric conditions, the overall length of the muscle is constant, therefore the velocity of shortening of the contractile element is equal to the rate of elongation of the series elastic component. The compliance of the series elastic component is $\Delta x/\Delta P$, therefore it can be determined from the time derivative of tension and the velocity of shortening as follows:

$$\Delta x/\Delta P = \Delta x/\Delta t \cdot \frac{\Delta t}{\Delta P} = v/[dP/dt]$$

At a given tension the velocity of shortening may be obtained from the force-velocity relation, and dP/dt directly measured from the curve of tension development.

The method has given abnormally high values compared to those determined by the quick release method. The primary reason for this is that the active state is not maximal until approximately 50 milliseconds after the beginning of the tetanus. For the values determined late in the isometric rise this error should be avoided (54). Because the tension is close to the isometric tension, the correction to obtain contractile element length is small, and the corrected and uncorrected (for series elastance) force-velocity relations are almost equal in this range. Thus the error in determining the compliance of the series elastic element using the uncorrected force-velocity relation is small (and can be reduced by repeating the determination with the new corrected force-velocity relation). As the tension actually approaches the isometric tension, however, the values of dP/dt and velocity become small, which magnifies the effect of errors on their ratio and the determination of compliance becomes unreliable. As a compromise, values between 70% and 80% of the final or isometric tension were used. Isometric contractions of different magnitudes of tension, obtained at different muscle length, permitted determination of values of compliance at different tensions, always at 70%-80% of the isometric rise in tension. The plot of these compliance values versus tension was fit with a curve by adjusting the constants of the following equation:

$$\text{Compliance} = dx/dP = K_o[1 + 5 \cdot e^{-P/K_1}]$$

where the constants, K_o and K_1, have units of mm/kg and kg respectively. The exponential provides the decrease in compliance (stiffening) of the series elastic component which is seen as the tension increases, until

it approaches the limiting value, equal to K_o. In the case of the actual compliance, it becomes infinite when the tension equals zero, that is, the series elastic component becomes slack. Thus, the relation will not be fit clear to zero tension. The equation can be integrated to obtain the length change of the series elastic component, i.e.

$$x_{SEC} = K_o \cdot P - 5 \cdot K_o \cdot K_1 [1 - e^{-P/K_1}]$$

These equations were used to make corrections to the isotonic data (length and velocity) used for the force-velocity relations described below.

Force-Velocity Relation.

In contrast to the responses obtained with direct stimulation, it was unusual to have a reflex response which was stable over time. There were both spontaneous changes in excitability, and changes induced by periods of previous stimulation. Thus reflex responses of equivalent magnitude had to be selected after the fact. The selection of data introduced the potential for the experimenter to bias the sample. In an attempt to avoid this possibility, objective criteria were established to select the data, as follows:

1) The estimate of reflex magnitude must be within $\pm$ 25% of the mean level of the reflexes used in a single force-velocity determination.

2) Within this $\pm$ 25% range the actual values of force were normalized to the mean value in proportion to their estimated reflex levels.

3) The reflex must remain constant during each run as determined by the EMG for the period of time which includes the data points used.

4) Data points were excluded which occurred during periods of large rates of change of force and velocity.

5) Data points were excluded when the active tension component was approximately zero in the presence of passive tension from the parallel elastic component.

Criterion 4) avoided the largest errors due to uncertainty in the correction for series elastance and deviation from steady-state conditions. Criterion 5) avoided the possibility of shortening due to the elastic recoil of the parallel elastic component at velocities greater than V_{max}, producing slack in the contractile element. The data selected from individual runs were stored, and later plotted by a computer program; thus the experimenter was unaware of the effect of an individual data point upon the resulting curve at the time of selection.

Data were collected during each run at five increments of muscle length. These lengths were determined by entering the shortest length and the increment of length into the program. The time of arrival at each length was indicated on the 'quick look' plot of the data run. The program made corrections for the series elastic component length using the equation described in the previous section. If a data sample did not occur at the same time, a linear extrapolation was used to find the values at the correct length. The data at any length could be excluded on the basis of the above criteria. For each determination of

the force-velocity relation, five sets of data, all at different contractile element lengths, were selected.

In addition, the following corrections were made to the values of force and velocity selected at each contractile element length:

1) The passive tension was subtracted to obtain just the active component. This correction changes with length, and is given by the passive length-tension relation.

2) The tension was scaled for changes in activation between different runs, due to changes in reflex activation or direct stimulation of the nerve. A choice of two methods was available:

   a) The integrated EMG was used as a measure of muscle activation. The tension was multiplied by the ratio of the average EMG of all runs used to the EMG magnitude for the particular data point.

   b) The value of the isometric tension developed before release of the muscle was used as a measure of muscle activation. If the final isometric tension had not been reached after one half-second, an exponential extrapolation to final isometric tension was used. The length-tension relation was used to determine what the isometric tension would be at L_o, this defined the degree of muscle activation. The tension was multiplied by the ratio of the average activation of all runs used to the magnitude of activation for the particular data point.

3) The velocity was corrected for the shortening of the series elastic component by calculating the rate of length change by the equation:

$$dx/dt_{SEC} = dP/dt \cdot dx/dP = dP/dt \cdot \text{compliance}$$

where compliance = $K_o[1 + 5.0 \cdot x^{-K_1 \cdot P}]$. Data points which occurred where dP/dt was large were avoided, thus minimizing the errors in this correction.

The corrected values were plotted, muscle force versus shortening velocity. The modified Hill equation of Abbot and Wilkie was used to fit curves to the data following the method in Appendix 2.2. The values of the constants a and b were determined on the basis of best fit of data at all muscle lengths, while values of $P_o(1)$ were determined for the fit at each separate muscle length. The five values of $P_o(1)$ gave five separate curves, each following the equation:

$$[P+a][v+b] = [P_o(1)+a]b$$

The method minimized the total sum of the square error for all the data points. The standard deviation of the fit was defined as the square root of the mean square error; this parameter was used as a measure of how well the data fit the series of curves of the force-velocity relation. For example, it was used to determine if EMG or initial isometric tension was a better estimate to be used to correct for variations in muscle activation in a particular isotonic series.

RESULTS

Comparison of Length-Tension Relations in Reflexly and Directly Activated Muscle.

In the Introduction, it was noted that the length-tension relation was affected by the amount of fusion of the separate motor units within the muscle. When the firing frequency is well below the fusion frequency, the resulting length-tension relation is shifted with respect to that during tetanic stimulation. Thus the comparison of length-tension relations obtained during reflex and tetanic stimulation of the muscle nerve may indicate the degree of fusion within the active motor units during reflex activation. The length-tension relation is also necessary for the corrections due to the passive elastic component and for estimating the level of muscle activation for computing the force-velocity relation.

In order to obtain length-tension relations during reflex activation the reflex must remain stable from run to run during the whole isometric series. For two experiments the reflex was sufficiently stable to allow determinations of length-tension relations. Figures 15 through 18 are the length-tension relations obtained during reflex activation and tetanic stimulation for experiments 18 and 46.

Comparison of the curves obtained during reflex activation with those obtained during direct stimulation of the muscle nerve reveals little difference except for the differences in magnitude of active

Figure 15. Length-tension relation for gastrocnemius muscle, for direct stimulation of the muscle nerve (submaximal, 30 impulses/sec). Experiment 18. Data for passive tension indicated by + symbol. Data for active tension indicated by x symbol. Curves through data fit as described in text.

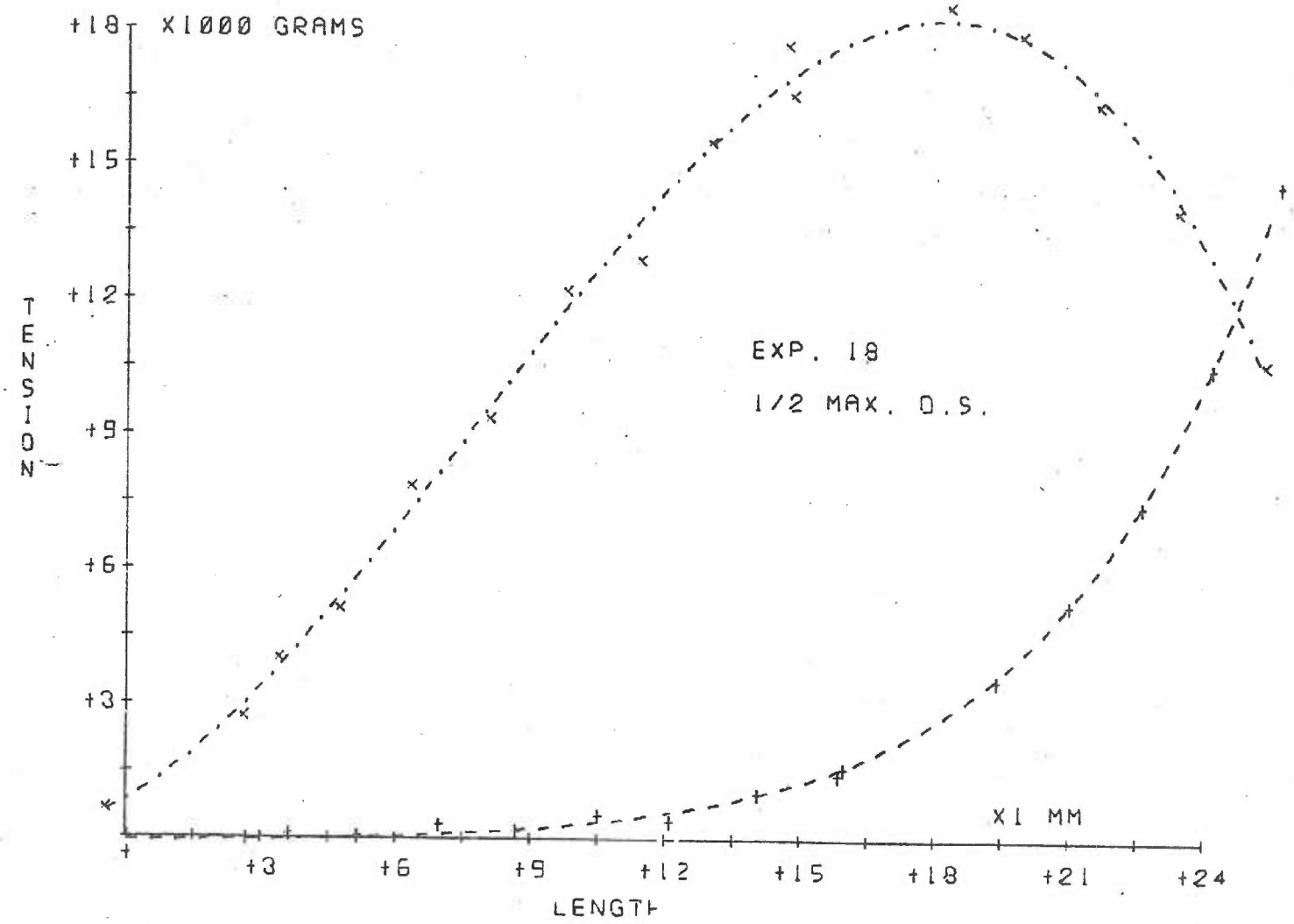
+18
X1000 GRAMS
+15
+12
+9
+6
+3
TENSION
EXP. 18
1/2 MAX. O.S.
X1 MM
+3
+6
+9
+12
+15
+18
+21
+24
LENGTH

Figure 16. Length-tension relation for gastrocnemius muscle, obtained during a crossed extensor reflex equal in magnitude to 14% of maximal tetanic tension. Experiment 18. Data indicated as in Figure 15.

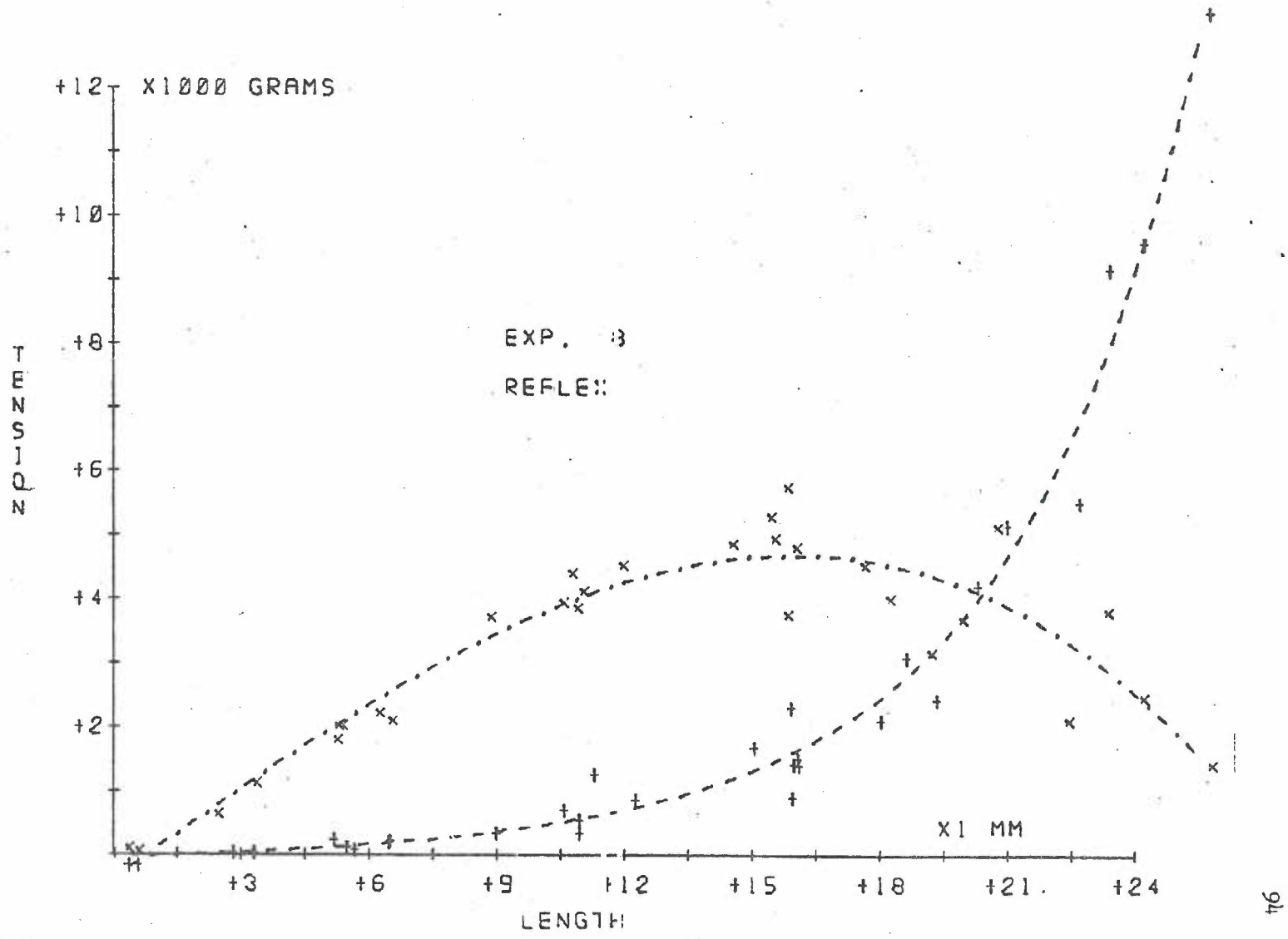
+12 X1000 GRAMS
+10
+8
+6
+4
+2
TENSION
EXP. 3
REFLEX
X1 MM
+3
+6
+9
+12
+15
+18
+21
+24
LENGTH

Figure 17. Length-tension relation for gastrocnemius muscle, for direct stimulation of the muscle nerve (submaximal, 30 impulses/sec). Experiment 46. Data indicated as in Figure 15.

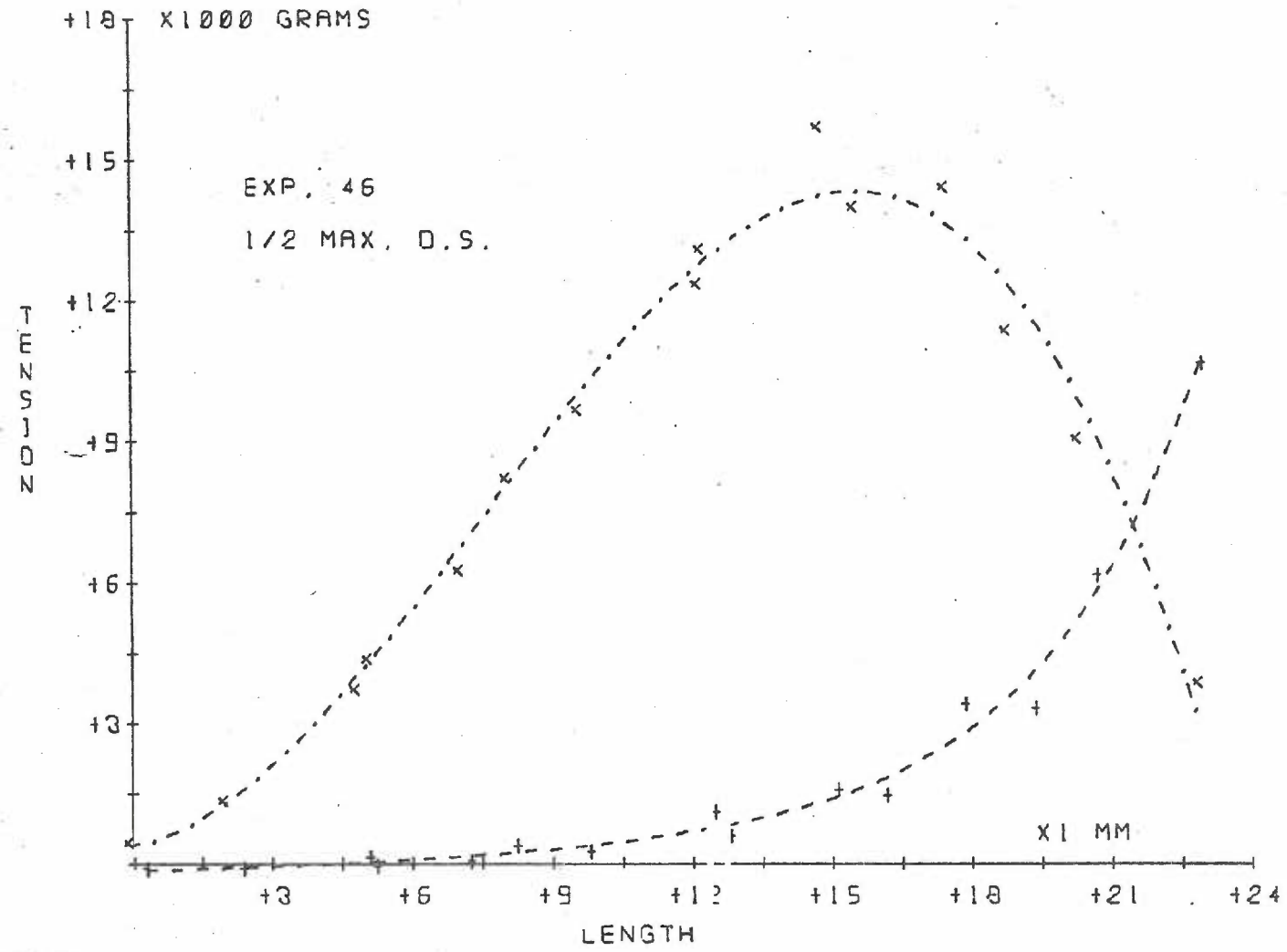
+18
X1000 GRAMS
+15
EXP. 46
1/2 MAX. D.S.
+12
TENSION
+9
+6
+3
X1 MM
+3
+6
+9
+12
+15
+18
+21
+24
LENGTH

Figure 18. Length-tension relation for gastrocnemius muscle, for crossed extensor reflex equal in magnitude to 9% of maximum tetanic tension. Experiment 46. Data indicated as in Figure 15.

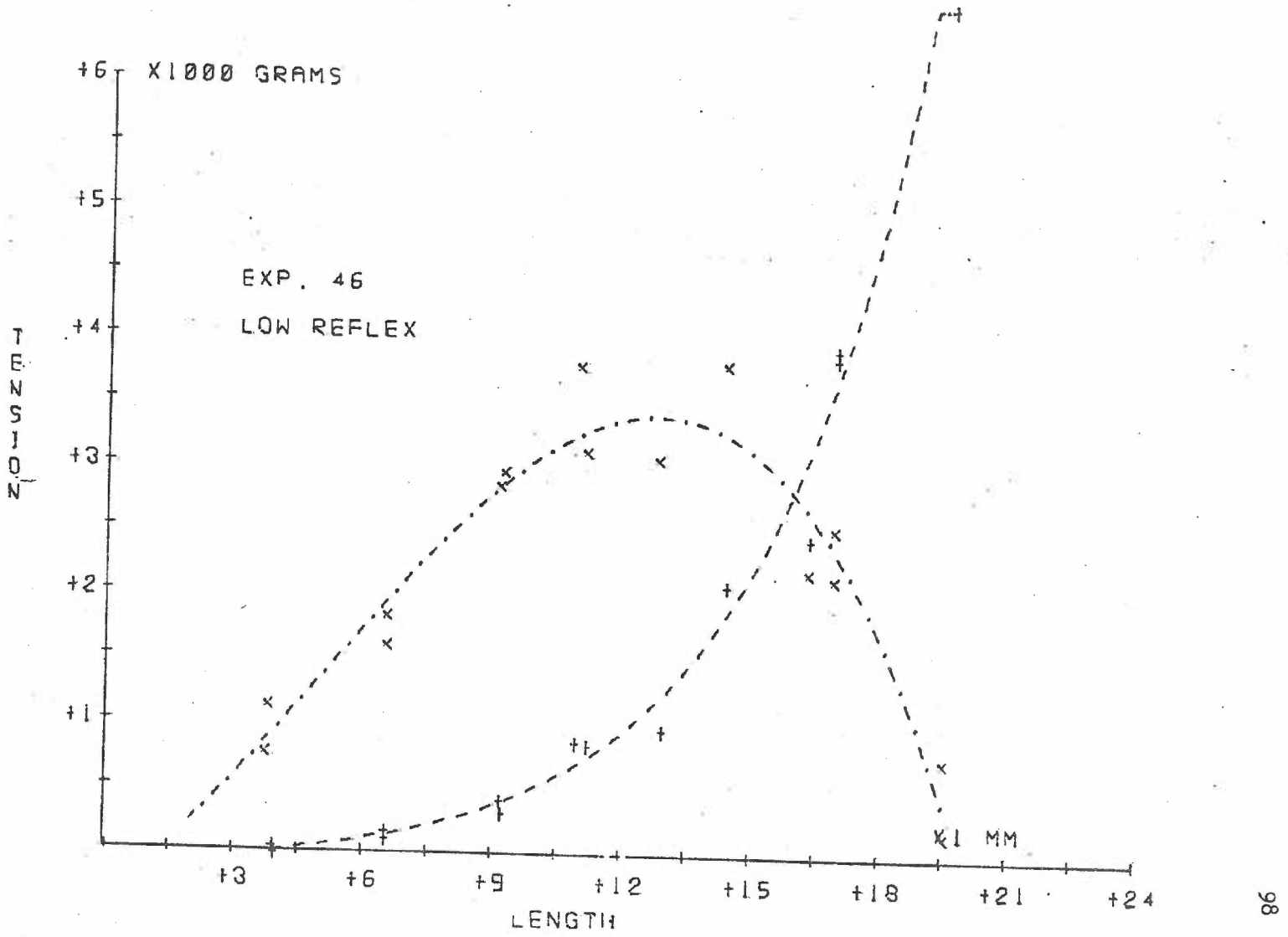
+6
X1000 GRAMS
+5
EXP. 46
LOW REFLEX
+4
TENSION
+3
+2
+1
X1 MM
+3
+6
+9
+12
+15
+18
+21
+24
LENGTH

tension. The reflex curves show a greater scatter of the data points, reflecting the variability of the reflex curve with respect to the direct stimulation curve; both intersect the axis at approximately the same muscle lengths (.0 and 1.5 mm in Exp. 18 and 46 respectively). The peak of the active tension curve, which defines L_o, occurs at a shorter muscle length for reflex activation than for direct stimulation. In experiment 18, L_o lies at 16.5 mm for the reflex curve compared to 18 mm for direct stimulation. The values are 13 mm and 16 mm respectively for experiment 46. However, the length-tension curves have not been corrected for elongation of the series elastance. Because the peak active tension during direct stimulation was much greater than during the reflex, the elongation of the series elastance was greater. The average compliance between 5 kg and 20 kg (see Figure 20) is estimated to be approximately .1 mm/kg. Using this value a difference in L_o of 1.3 mm can be attributed to the different lengths of the series elastance at the different tensions.

It should be noted that the active tension curve is determined on the assumption that the parallel elastic component (PEC) is located in parallel with both the series elastic component and the contractile element as in Hill's model (Figure 2e). If it is located in parallel with just the contractile element as in Aubert's model (Figure 2f), elongation of the series elastic component under active contraction would allow the PEC to shorten, producing a lower passive tension. The calculated active tension obtained by subtracting the initial passive tension (before the isometric contraction) would be lower than the

actual value. Even small errors in the determination of the active tension in the region of L_o can change the actual location of the peak. Thus the resolution of the determination of L_o at low levels of activation is poor, and could account for the remaining differences between the value of L_o determined for reflex activation and direct stimulation.

A comparison of the location of the rising slope of the length-tension relation provides a better resolution of the relative locations of the curves. Along most of the slope the tension due to the parallel elastic component is small. As the tension approaches zero, the elongation of the series elastic component disappears; thus the SEC affects only the slope, and not the intersection of the active curve with the length axis. If the slope midway on the rising portion of the curve, which is approximately linear and at its steepest value, is extrapolated back to zero tension, the relative positions of the curves can be determined with better resolution. The length at which this extension occurs for the reflex length-tension relations was well within .5 millimeter of that for the relations determined during tetanic stimulation of the muscle nerve. This is not a significant difference.

These results should be compared with those of Rack and Westbury (62) obtained with differing degrees of motor unit fusion (Figure 8). Although determined for a different muscle (cat soleus), the active tension rises to a maximum over a range of 2 centimeters, roughly comparable to the present curves. A decrease from 35 to 10 pulses/second resulted in a shift of the length-tension relation of 5 mm toward a longer muscle length.

Thus, when the degree of fusion was determined by the frequency of stimulation, L_o became longer with the departure from complete fusion. Since there was no significant change in L_o in the present experiments, it may be concluded that the motor units were firing at or near their fusion frequency during both reflex and direct forms of excitation and the measurements were made under comparable conditions.

Compliance of the Series Elastic Component.

The compliance of the series elastic component at different tensions is used to determine contractile element lengths and velocities of shortening during isotonic runs. The correction of force-velocity data depends upon the determination of this compliance. The method of determination was previously described in the Methods section (page 84).

Figure 19 is an example of a plot of compliance computed from dP/dt and velocity of shortening at different points during the development of isometric tension in response to a tetanus. Note that the data (the triangles in the figure) approach the dashed curve only as the tension (on the abscissa) approaches its maximum value. This curve describes the relation used to make the corrections for series elastance. The value at approximately 80% of the maximal tension during the step lies close to the curve.

Figure 20 is a plot of compliance values determined only at times of the rise when the tension was 70-80% of the final value of the rise. The points represent different isometric contractions at different

Figure 19. Plot of compliance ($\Delta L/\Delta P$) versus tension as computed during single isometric rise of tetanic tension. Compliance calculated from ratio of velocity (from force-velocity relation) to dP/dt. Compliance of series elastance indicated by Δ symbol. Compliance of lever restraint indicated by $\Diamond$ symbol. Dashed curve is same as in Figure 18. Note values approach curve as tension approaches isometric value (maximum).

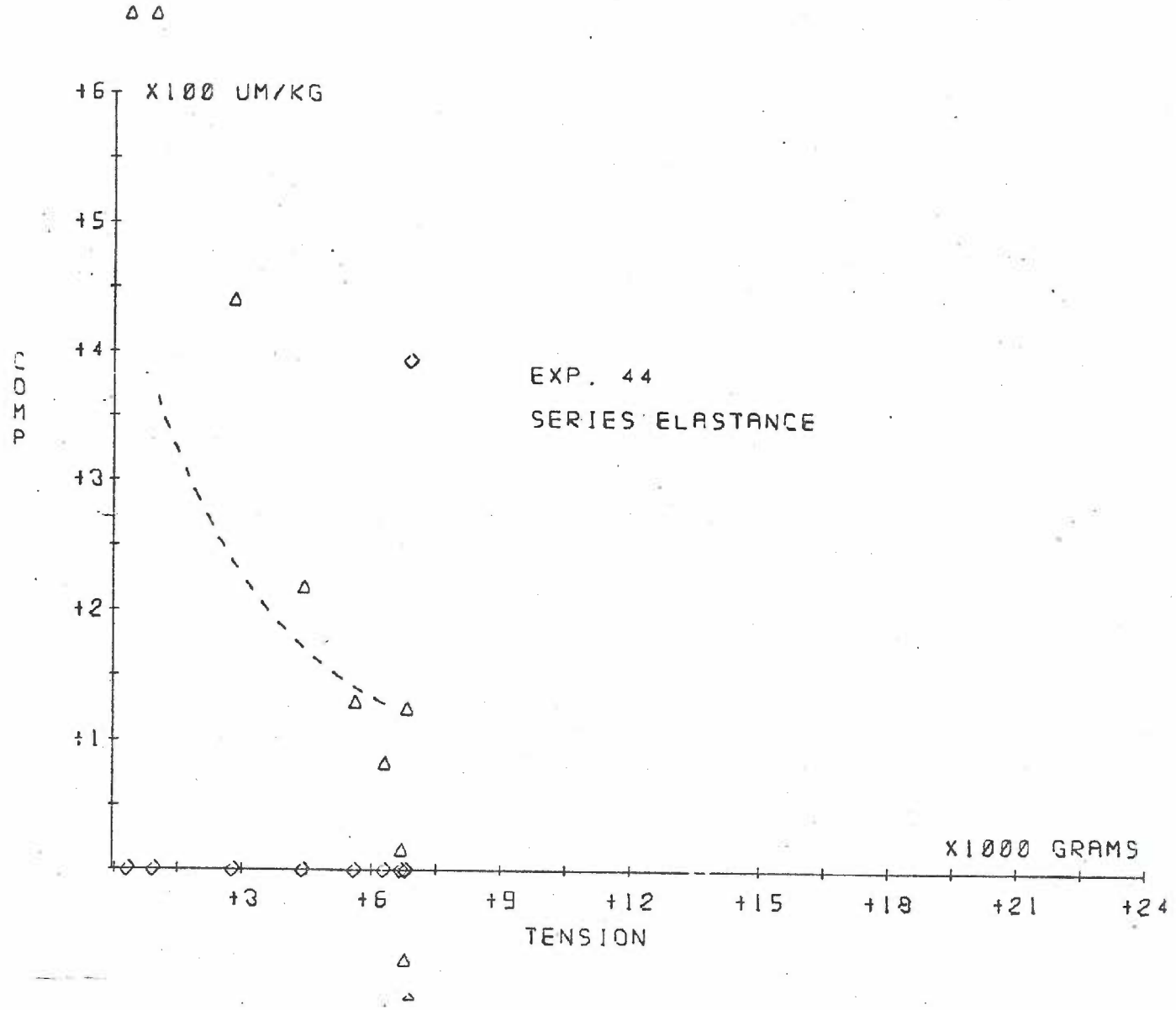
X100 UM/KG
+6
+5
+4
+3
+2
+1
COMP
EXP. 44
SERIES ELASTANCE
X1000 GRAMS
+3
+6
+9
+12
+15
+18
+21
+24
TENSION

Figure 20. Compliance of series elastic component late in isometric tension development during tetanus (70-80% of final tension). Experiment 44. Each data point is from a separate isometric tetanus. Curve A plots the following equation used to correct for series elastance:

$$\frac{dx}{dP} = K_o(1 + 5 \cdot e^{-P/K_1})$$

For K_1 = 3.0 kg

K_o = 80 μm/kg

Note: curve is valid representation of compliance of series elastic component only in region of actual data.

For an explanation of curve B see Discussion (page 137).

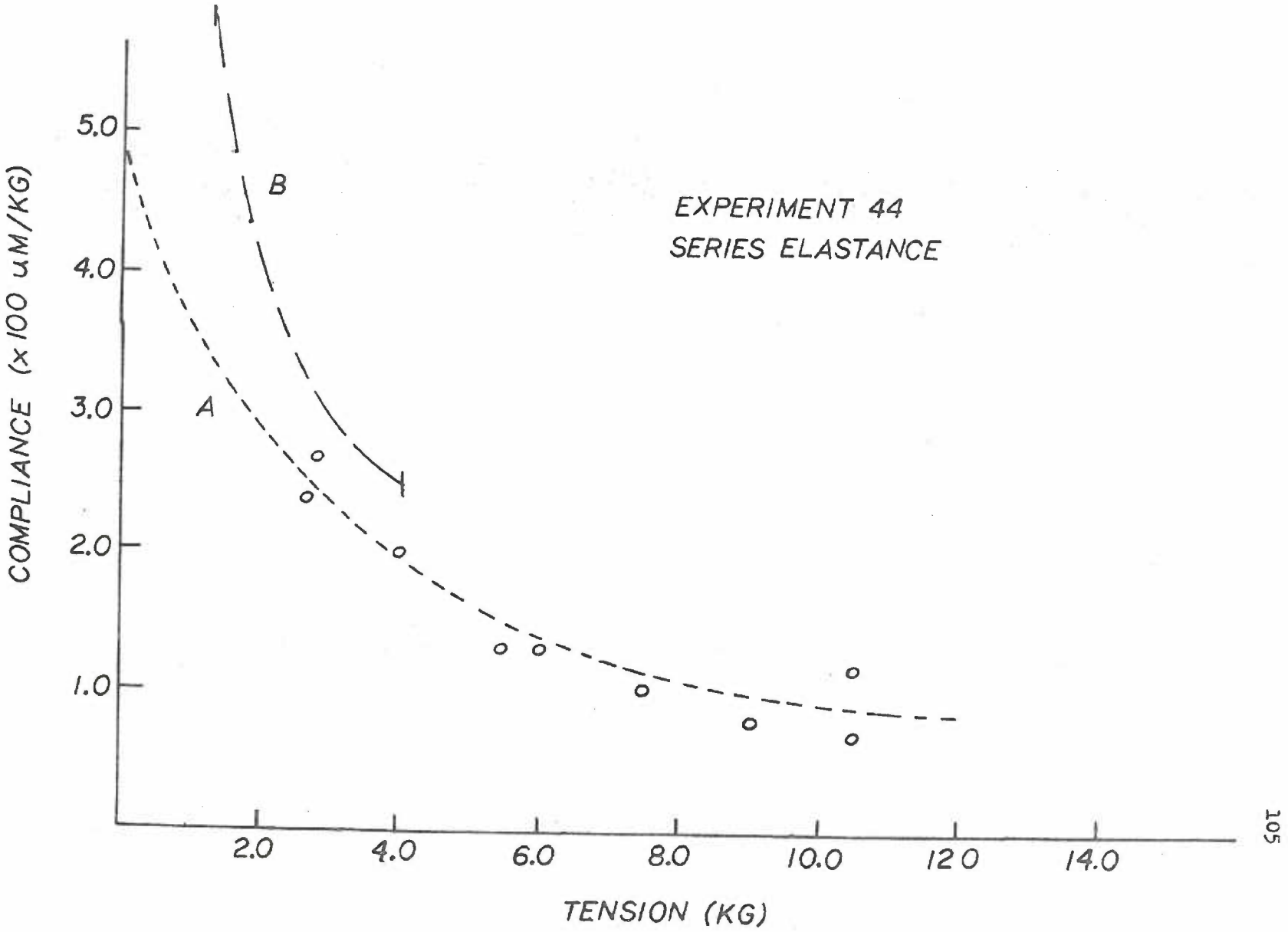
EXPERIMENT 44
SERIES ELASTANCE
COMPLIANCE (x 100 uM/KG)
5.0
4.0
3.0
2.0
1.0
A
B
2.0
4.0
6.0
8.0
10.0
12.0
14.0
TENSION (KG)

muscle lengths during experiment 44. The lengths were all shorter than L_o to avoid errors due to the parallel elastic element. The dashed curve was obtained by selection of K_o and K_1 to fit the relation, $dx/dP_{(SEC)} = K_o\ [1.0 + 5 \cdot e^{-P/K_1}]$, to the data by eye (it was judged sufficient in view of the uncertainties involved in the method). The dashed curve is shown extended to the ordinate axis in order to indicate the values of the above equation at low tension since the correction was made on the basis of these values. The actual values in this region were not determined, therefore the curve represents the actual compliance relation only in the region of the data. The implications of the uncertainty of the compliance of the series elastance will be discussed later.

As indicated in the Methods section, the compliance of the series elastic component was approximated using a procedure involving successive estimates from force-velocity plots in an iterative manner. The compliance values plotted in Figure 20 constitute data points obtained after a single iteration of the procedure and represent a satisfactory convergence, that is, do not differ significantly from values which would be obtained with more iterations. This single iteration was usually sufficient for convergence since the correction to the force-velocity relation (based on the previous estimate of series elastic compliance) was small in the region used for the compliance determination, as previously noted.

Comparison of Force-Velocity Relations in Reflexly and Directly Activated Muscle.

The principle objective of the present study was the determination of the force-velocity relation at different levels of reflex activation and direct stimulation. The assumption was made that submaximal stimulation of the motor nerve would excite the large axons preferentially (4), resulting in a pure large motor unit population as the active fraction of the motor pool. Thus, comparison of reflex force-velocity relations with those obtained during direct stimulation allows comparison of the average force-velocity relation of the motor units recruited during the reflex with that of the large motor units.

Figure 21 shows a force-velocity relation obtained during direct stimulation of the motor nerve at 30 impulses per second (minimum frequency for a 'fused' tetanus). The stimulus was submaximal, resulting in isometric tension at L_o equal to 40% of the maximal tetanic tension obtainable with stimulation at this frequency. The data were obtained by interpolation between the values of force and velocity before and after reaching a specific contractile element length (that is, a correction for elongation of the series elastance was made). Data values were obtained at five lengths less than L_o, 2 mm apart.

The dashed curves drawn through the data obtained at each separate length were obtained by fitting the Hill equation modified by Abbott and Wilkie, $[P + a][v + b] = [P_o(1) + a]b$, using the values of $\underline{a}$, $\underline{b}$, and d $P_o(1)$ obtained by a least squares method. (See Appendix 2.2.) The

Figure 21. Force-velocity relation obtained during submaximal direct stimulation (30 impulses/sec) to muscle nerve. Experiment 44. Symbols indicate different muscle lengths. Dashed curves are plots of the modified Hill equation after Abbott and Wilkie:

$$[P + a][V + b] = [P_o(l) + a]b$$

With $P_o(l)$, a, b determined for the best fit by method described in Appendix 2.2. The following is a summary of the constants for this determination:

$\underline{a}$ = 1,466 grams

$\underline{b}$ = 16.56 mm/sec

Symbol	Length (mm)	P_o (gm)	V_{max} (mm/sec)
+	9.6	1,490	16.8
□	11.2	2,517	28.4
*	12.8	3,729	42.1
Δ	14.4	5,088	57.5
◇	16.0	6,118	69.1

Std. Dev. = 480 gm (as defined in Appendix 2.2).

L_o = 22.0 mm

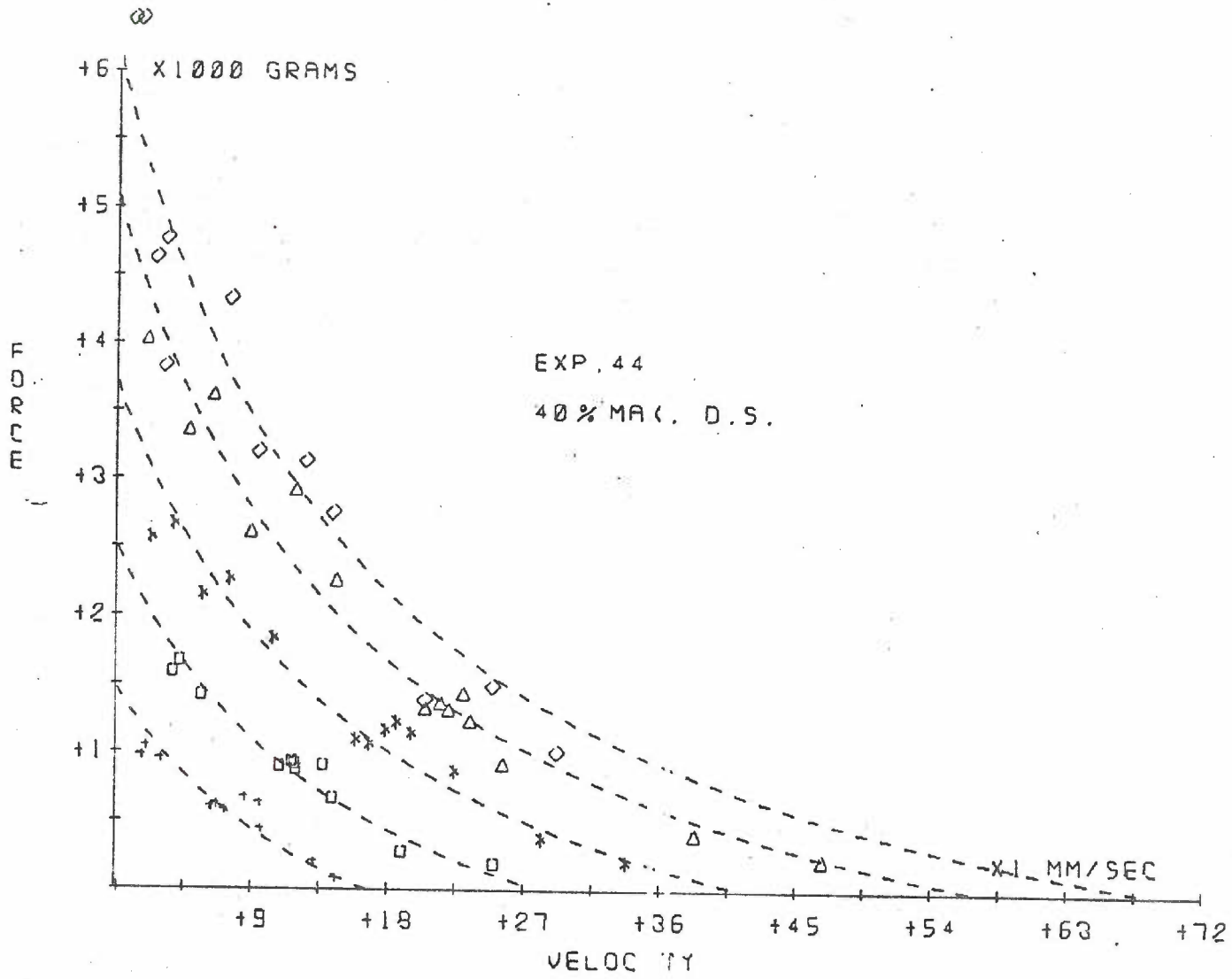
X1000 GRAMS
+6
+5
+4
+3
+2
+1
FORCE
EXP. 44
40% MAX. D.S.
X1 MM/SEC
+9
+18
+27
+36
+45
+54
+63
+72
VELOCITY

close fit of the data to the curves supports the use of the same value of a and b at different muscle lengths shorter than L_o, and the extrapolation of the force-velocity relation to a muscle length of L_o using this relation. ($P_o(1)$ is known from the length-tension relation.) The use of more than one muscle length in the determination of the constants a and b allows a larger statistical base than available at any single muscle length.

Examples of the force-velocity relation obtained at different levels of reflex activation are shown in Figures 22 and 23. In experiment 18 it was possible to grade the reflex activation with the magnitude of stimulation used to elicit the crossed extensor reflex. The result is shown in Figure 22 for a low reflex (14% of maximum tetanic tension) and Figure 23 for the maximal reflex (30% of maximum tetanic tension). The individual force-velocity curves for all the reflex runs and direct stimulus runs are included in Appendix 3.0 (Figures 40-50).

Because the force-velocity relations were not necessarily determined at the same length, were determined at muscle lengths shorter than L_o, and have different corrections for series elastance, it is convenient to extrapolate the relations to L_o based upon the equation of Abbott and Wilkie. The ratio of P_o (isometric tension) at L_o to P_o at any shorter length can be obtained from the length-tension relation. This ratio will be the same for different levels of activation, and can be used to give the value of P_o at L_o for the level of activation present during the determination of force-velocity relation.

Figure 22. Force-velocity relation obtained during a crossed extensor reflex equal in magnitude to 14% of maximal tetanic tension. Experiment 18. Curves determined as in Figure 21. Summary of constants:

$\underline{a}$ = 498 grams

$\underline{b}$ = 5.78 mm/sec

Symbol	Length (mm)	P_o (gm)	V_{max} (mm/sec)
+	5.0	1,559	18.1
⊙	7.5	2,725	31.7
*	10.0	3,583	41.6
Δ	12.5	3,987	46.3
◇	15.0	5,156	59.9

Std. Dev. = 158 gm

L_o = 16.0 mm

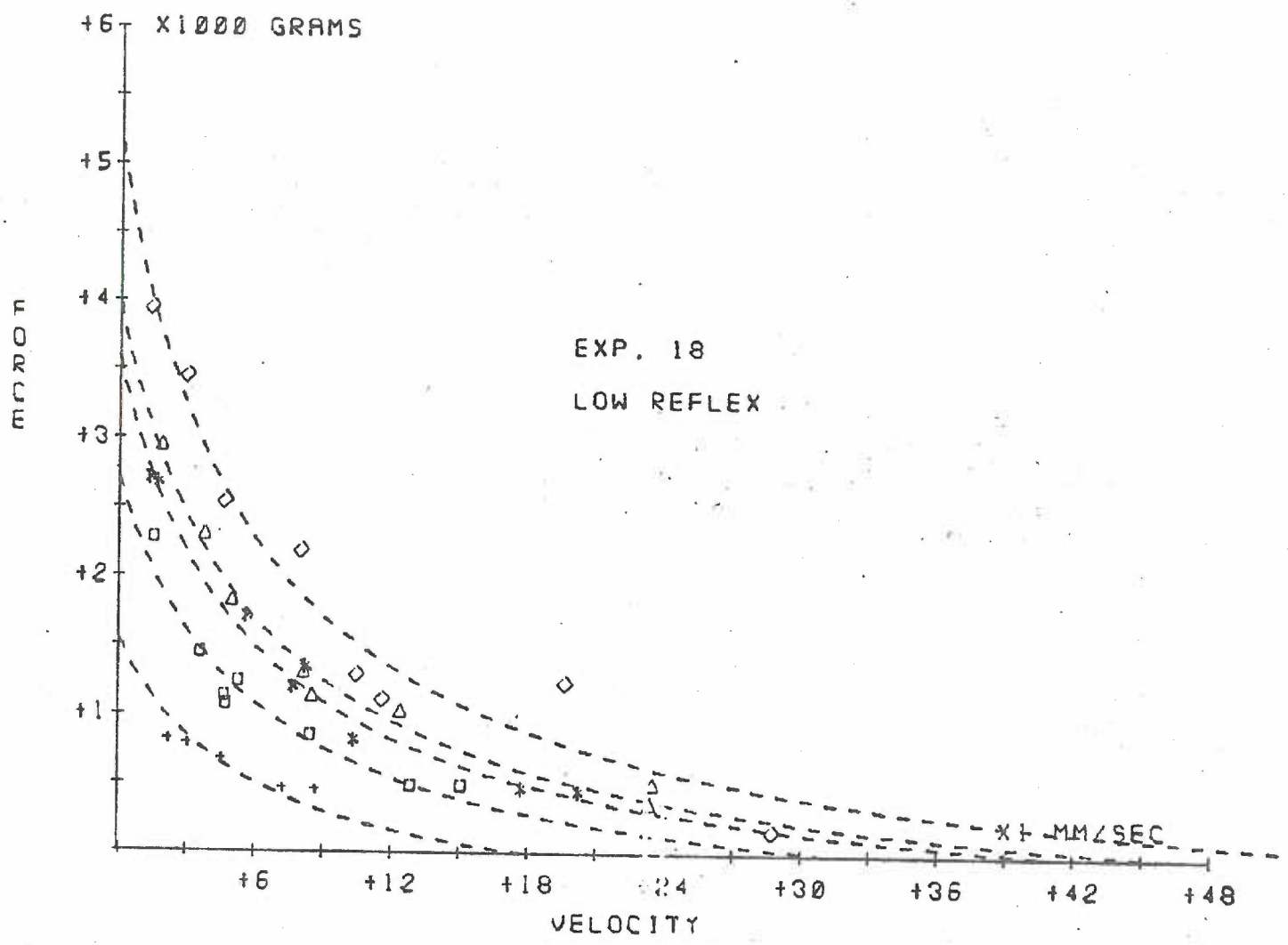
+6
X1000 GRAMS
+5
+4
+3
+2
+1
FORCE
EXP. 18
LOW REFLEX
+6
+12
+18
+24
+30
+36
+42
+48
VELOCITY
MM/SEC X1

Figure 23. Force-velocity relation obtained for a maximal crossed extensor reflex (30% of maximum tetanic tension). Experiment 18. Curves determined as in Figure 21. Summary of constants:

$\underline{a}$ = 1,591 grams

$\underline{b}$ = 19.7 mm/sec

Symbol	Length (mm)	P_o (gm)	V_{max} (mm/sec)
+	5.0	3,414	42.2
□	7.5	5,118	63.3
*	10.0	7,111	88.0
Δ	12.5	8,008	99.0
◇	15.0	9.486	117.4

Std. Dev. = 482 gm

L_o = 16.0 mm

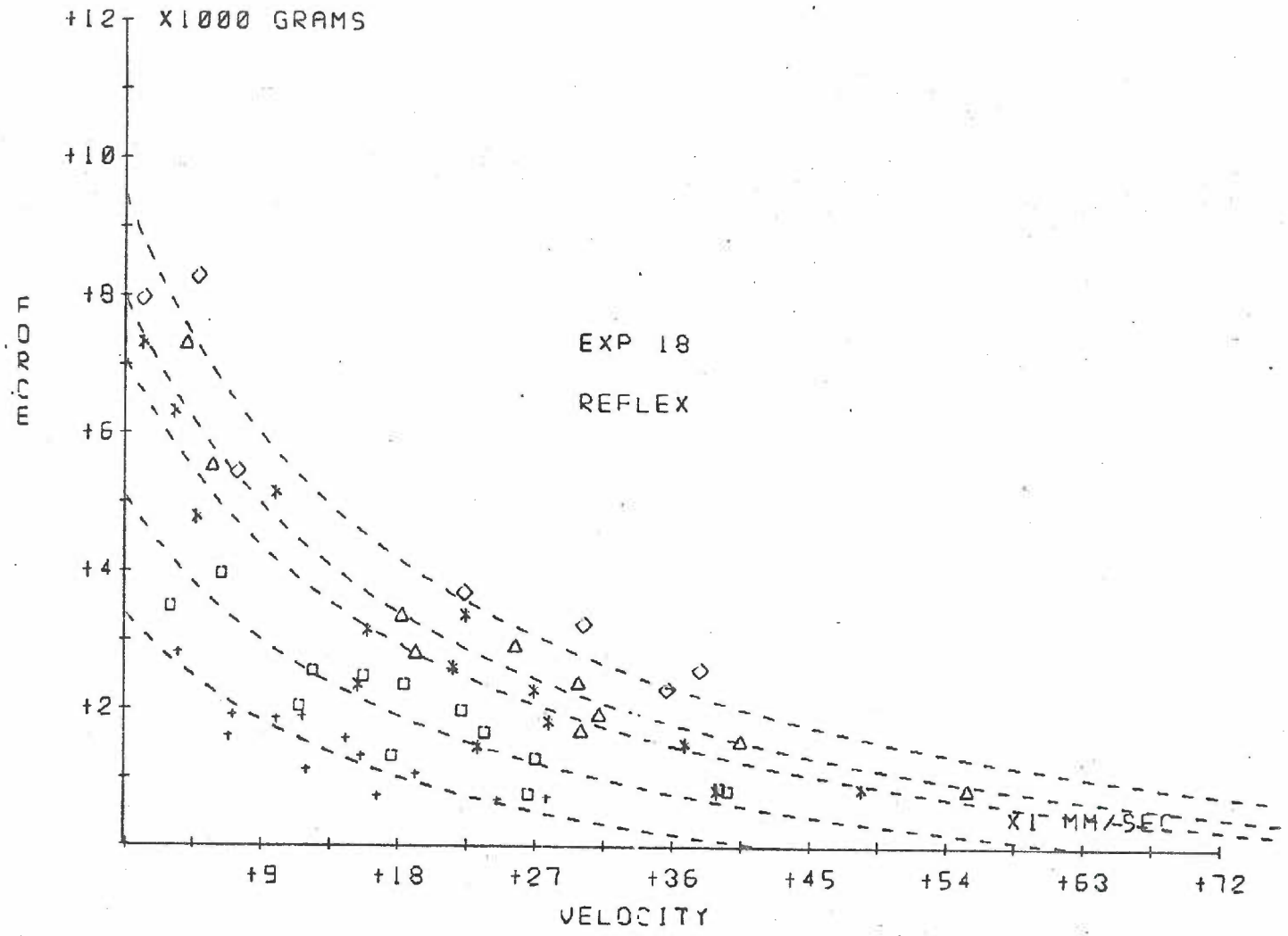
+12
X1000 GRAMS
+10
+8
+6
+4
+2
EXP 18
REFLEX
X1 MM/SEC
+9
+18
+27
+36
+45
+54
+63
+72
VELOCITY

It is more convenient to compare the force-velocity relations determined at different levels of activation if the force is plotted in percent of the isometric value (P_o). Figures 24 through 28 summarize the force-velocity relations obtained for reflex and direct stimulation for each experiment as they would be expected to appear at L_o. Because the individual data points are not plotted, the square root of the mean square deviation of the data from the curve is indicated by a vertical line, which also indicates the upper limit of the velocities of the actual data for each curve.

In general, the experiments are consistent in demonstrating force-velocity relations with low values of V_{max} at low reflexes when compared with those obtained at higher reflexes or during direct stimulation. In particular in Experiment 18 (Figure 24) the force-velocity relation obtained during the maximal reflex (30% of maximum tetanic tension) is superposable upon that obtained during direct stimulation. In Experiment 41 (Figure 26) the force-velocity curves obtained at different reflex levels are shifted toward that for direct stimulation in order of increasing magnitude of the reflex (6%, 18%, and 24% of maximum tetanic tension).

The exception was Experiment 44 (Figure 27) where the force-velocity relations obtained for reflexes of 15% and 20% of maximum tetanic tension were not appreciably different from that obtained during direct stimulation.

Figure 24. Comparison of force-velocity relations for submaximal direct stimulation and crossed extensor reflexes as normalized to L_o. Experiment 18.

Curve A. Reflex equal to 14% of maximal tetanic tension.

Curve B. Reflex equal to 30% of maximal tetanic tension.

Curve C. Submaximal direct stimulation (30 impulses/sec).

Force is in percent of isometric tension (P_o). Vertical line represents 2 standard deviations of fit of data to the curve and is located at upper limit of velocity data for each curve.

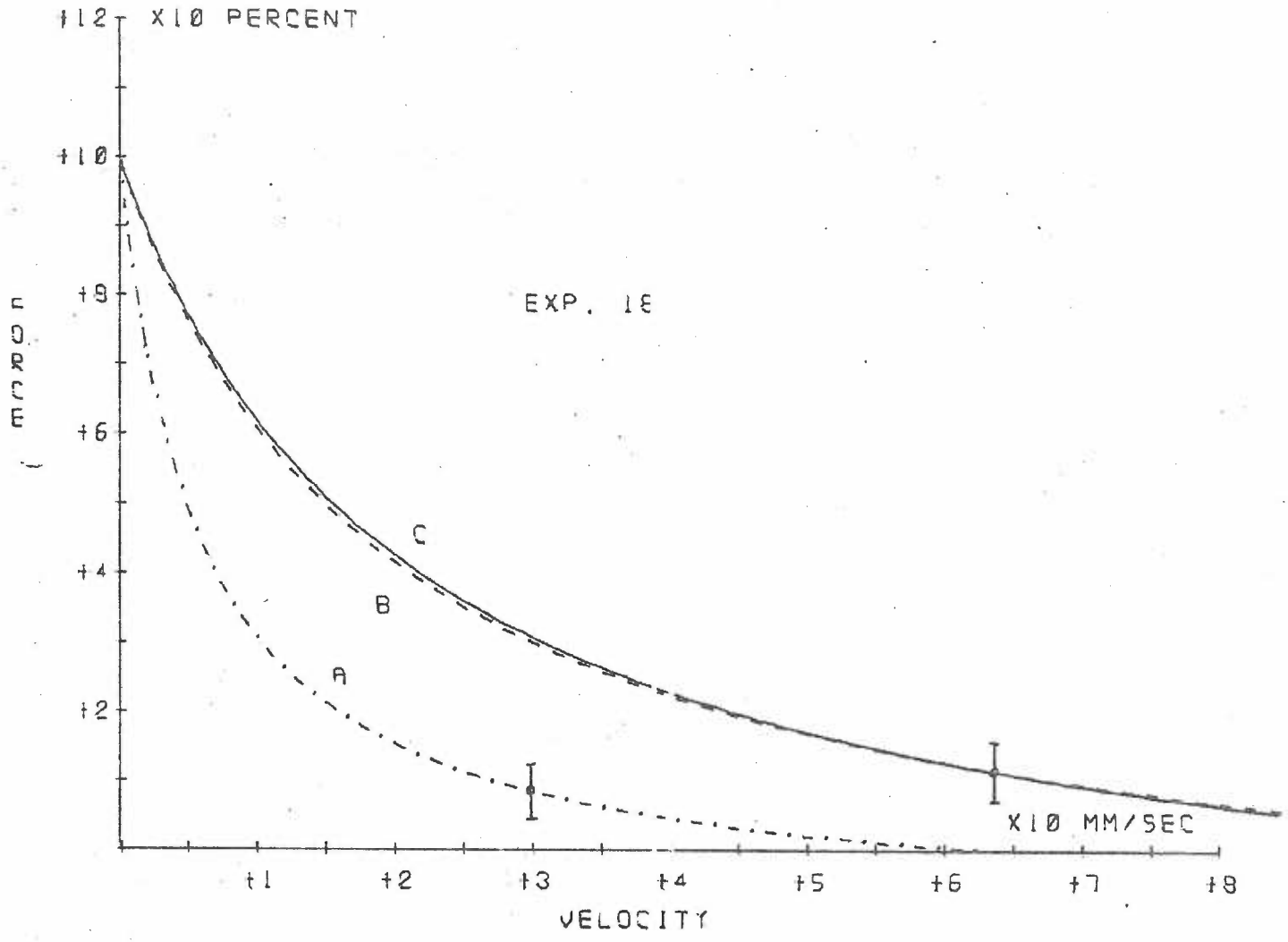
+12 X10 PERCENT
+10
+9
+6
+4
+2
EXP. 1E
C
B
A
X10 MM/SEC
+1
+2
+3
+4
+5
+6
+7
+8
VELOCITY

Figure 25. Comparison of force-velocity relations for submaximal direct stimulation and crossed extensor reflex normalized to L_o. Experiment 24.

Curve A. Reflex equal to 8% of maximal tetanic tension.

Curve B. Submaximal direct stimulation (30 impulses/sec).

Annotation as in Figure 24.

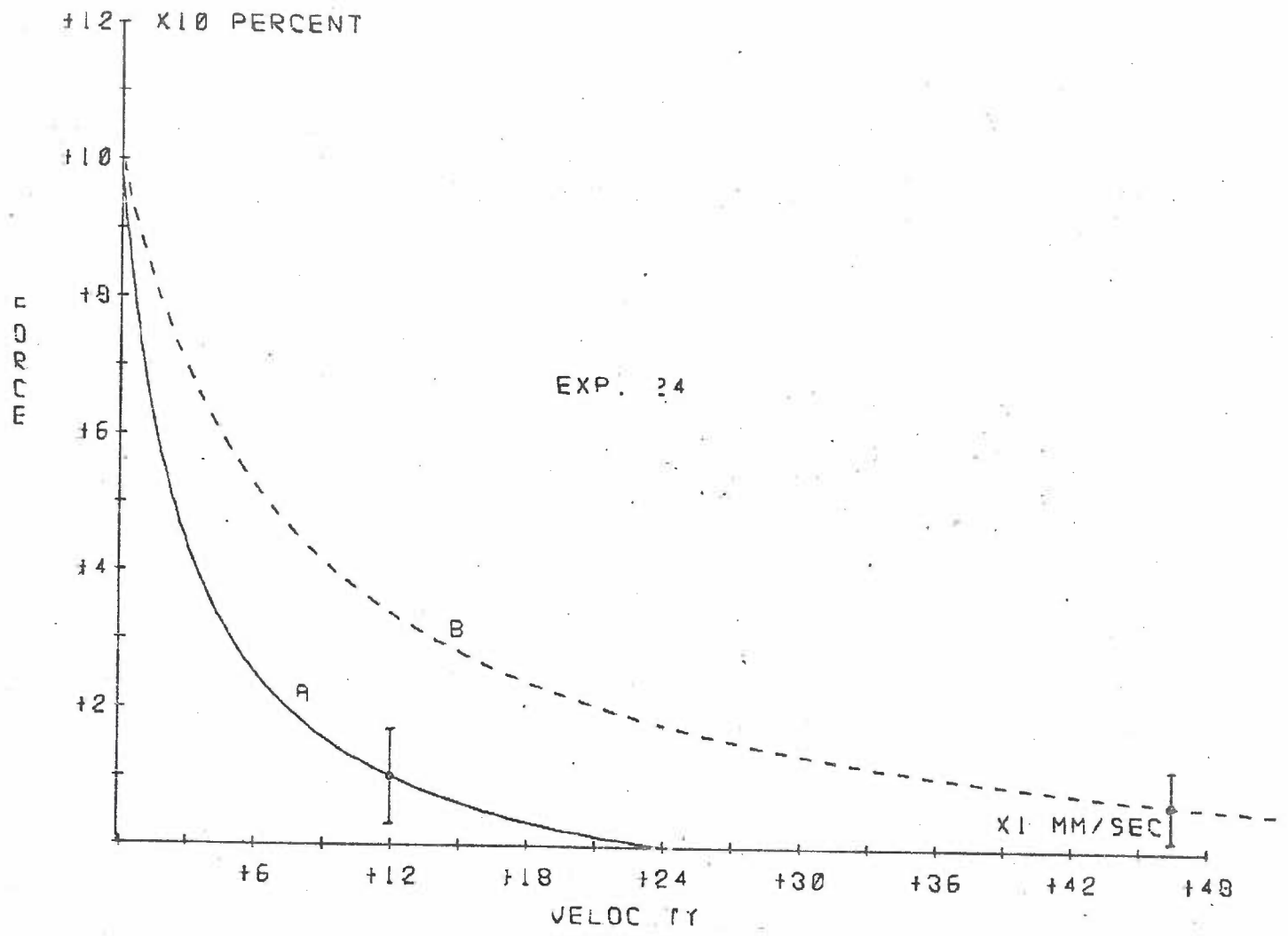
+12
X10 PERCENT
+10
+8
+6
+4
+2
FORCE
EXP. 24
B
A
X1 MM/SEC
+6
+12
+18
+24
+30
+36
+42
+48
VELOCITY

Figure 26. Comparison of force-velocity relations for submaximal direct stimulation and crossed extensor reflexes normalized to L_o. Experiment 41.

Curve A. Reflex equal to 6% of maximal tetanic tension.

Curve B. Reflex equal to 18% of maximal tetanic tension.

Curve C. Reflex equal to 24% of maximal tetanic tension.

Curve D. Submaximal direct stimulation (30 impulses/sec).

Annotation as in Figure 24.

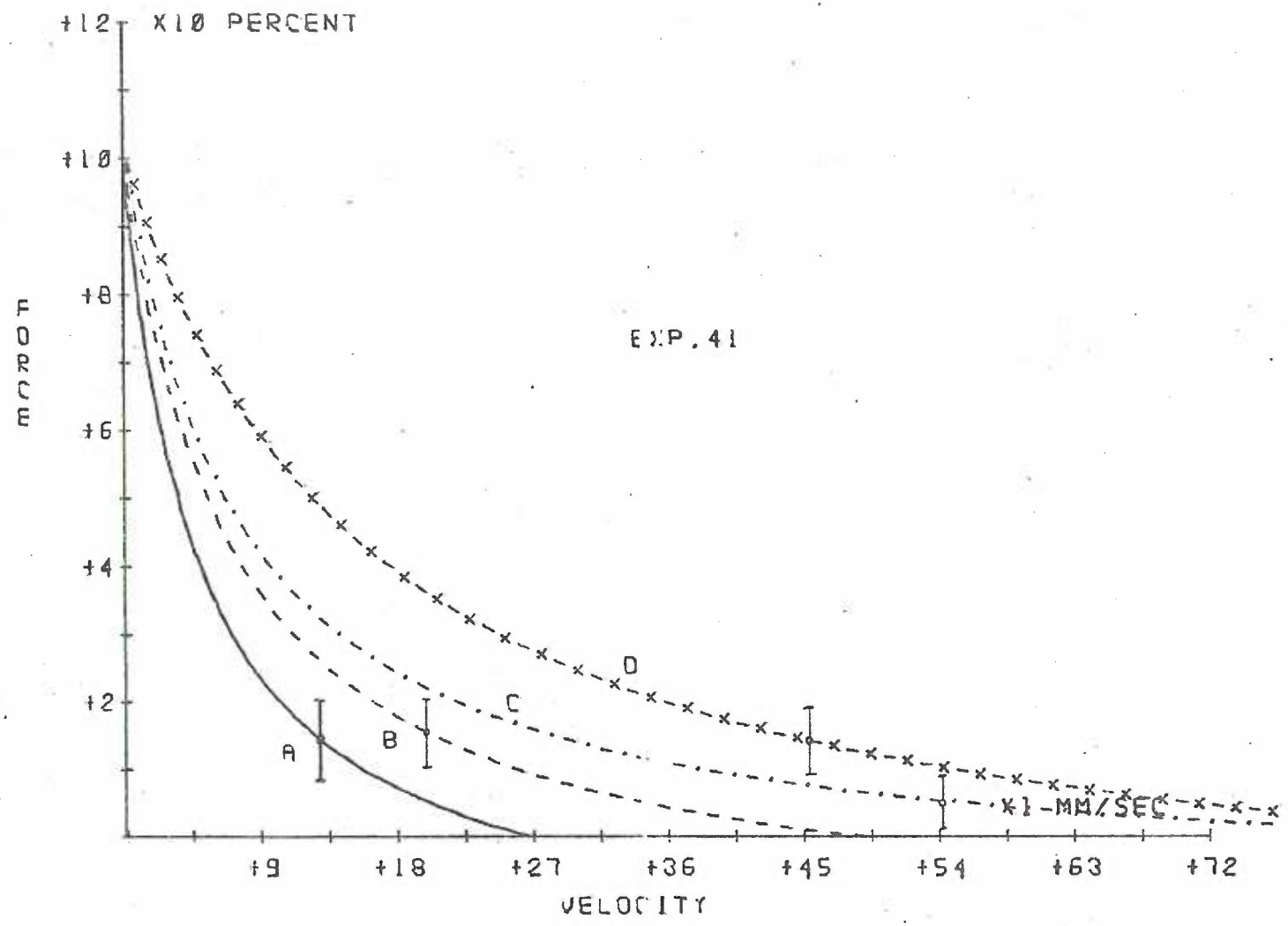
+12 X10 PERCENT
+10
+8
+6
+4
+2
FORCE
EXP. 41
A
B
C
D
X1-MM/SEC
+9
+18
+27
+36
+45
+54
+63
+72
VELOCITY

Figure 27. Comparison of force-velocity relations for submaximal direct stimulation and crossed extensor reflexes normalized to L_o. Experiment 44.

Curve A. Reflex equal to 15% of maximal tetanic tension.

Curve B. Reflex equal to 26% of maximal tetanic tension.

Curve C. Submaximal direct stimulation (30 impulses/sec).

Annotation as in Figure 24.

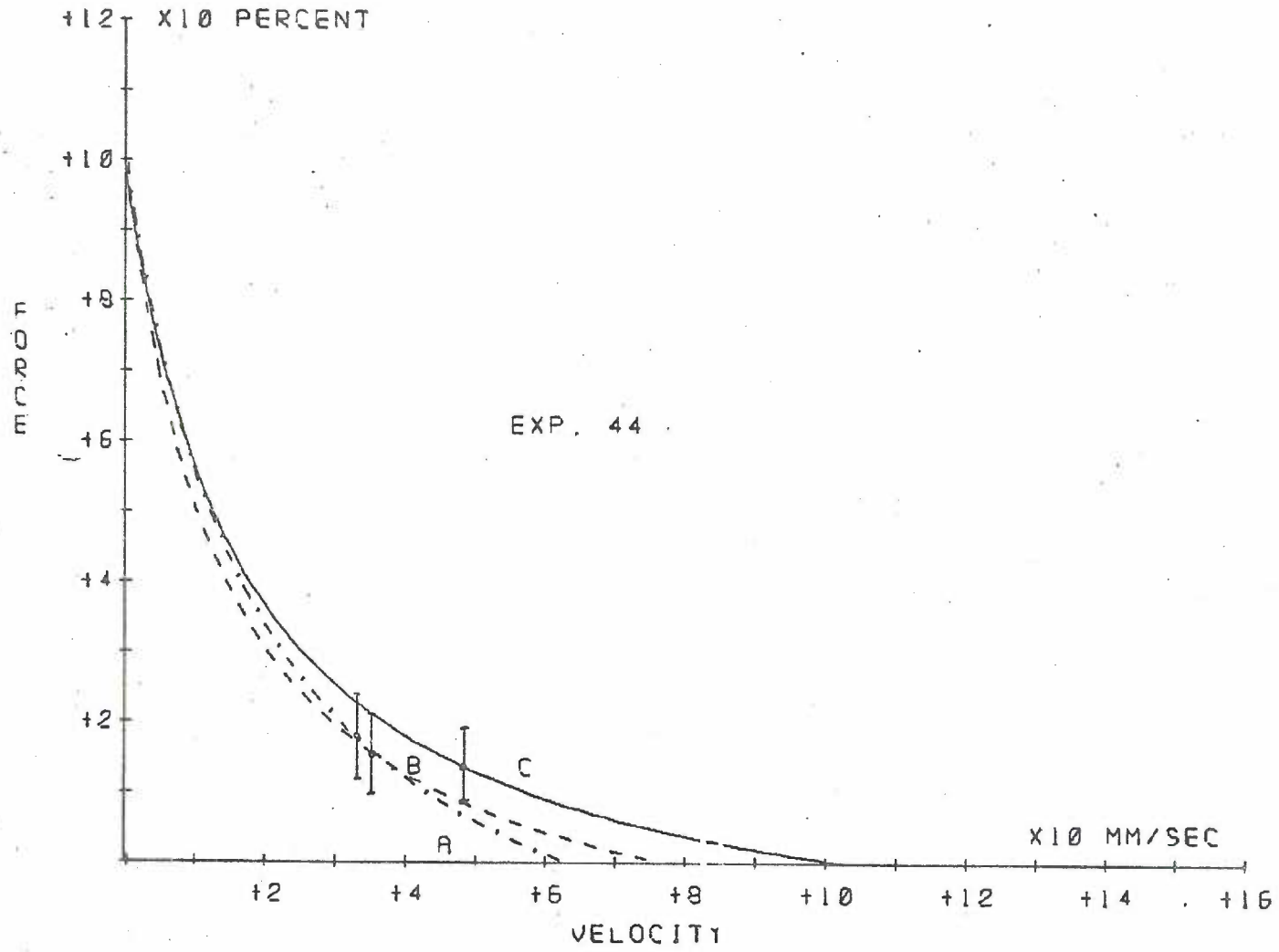
+12
X10 PERCENT
+10
+8
+6
+4
+2
ERROR
EXP. 44
B
C
A
X10 MM/SEC
+2
+4
+6
+8
+10
+12
+14
+16
VELOCITY

Figure 28. Comparison of force-velocity relations for submaximal direct stimulation and crossed extensor reflex normalized to L_o. Experiment 46.

Curve A. Reflex equal to 7% of maximal tetanic tension.

Curve B. Submaximal direct stimulation (30 impulses/sec).

Annotation as in Figure 24.

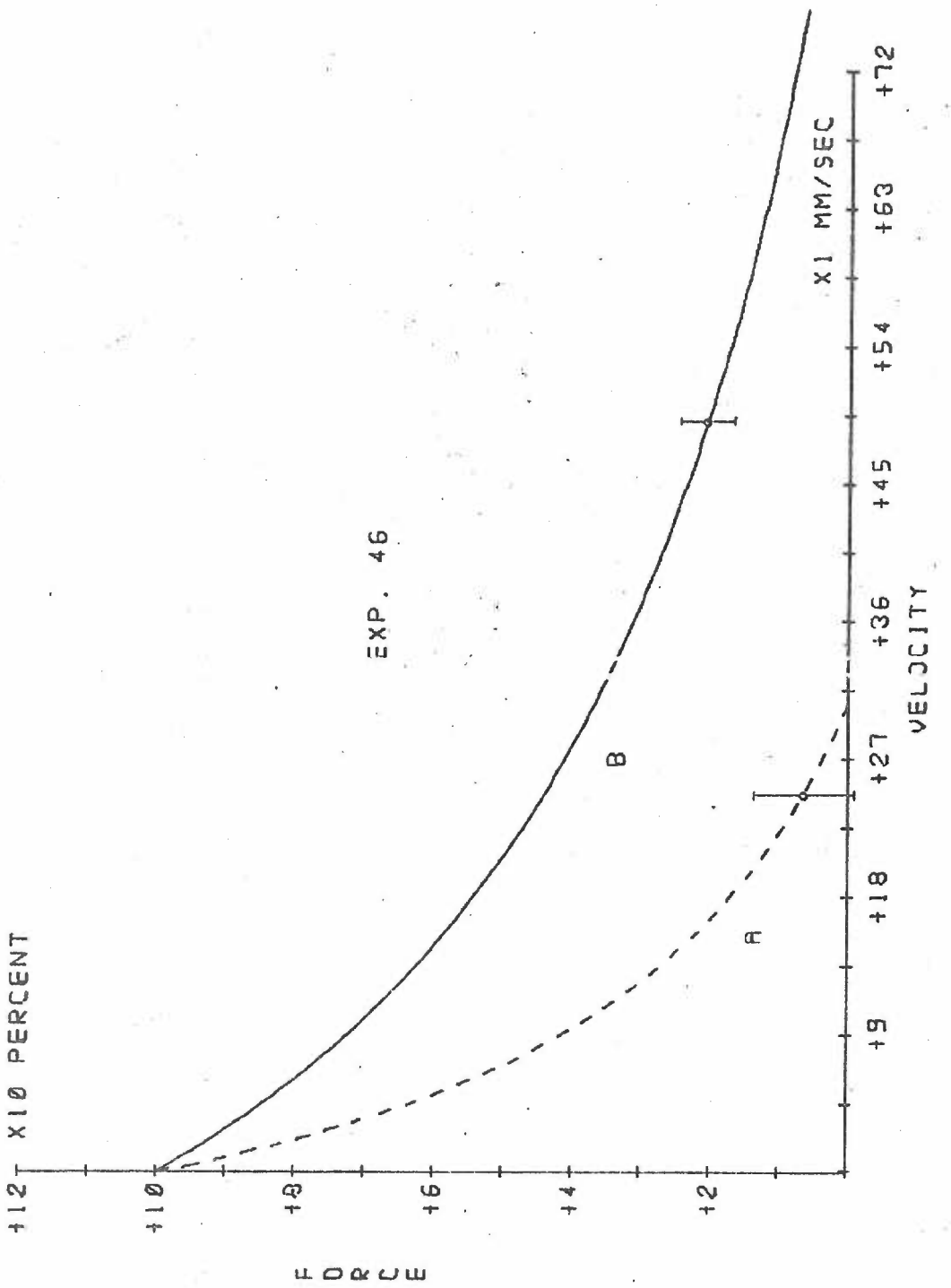
EXP. 46
FORCE
X10 PERCENT
+12
+10
+8
+6
+4
+2
VELOCITY
X1 MM/SEC
+9
+18
+27
+36
+45
+54
+63
+72
A
B

Comparison of Force-Velocity Relations Obtained in Different Experiments.

In order to properly compare the relations obtained from the different animal preparations, it would be necessary to know the fiber length at L_o (not muscle length since gastrocnemius is a pennate muscle). However, the length-tension relation is determined by the relative fiber length, and should vary among the muscles in proportion to the fiber length at L_o. The change in length necessary to go from 10% to 90% of the tension at L_o can be determined accurately, and should be directly related to the fiber length at L_o. Table 2 gives the values of this length change, and the ratio used to 'normalize' the force-velocity relation to the average length, for each experiment. (The ratio is simply the average length change divided by the individual length change).

TABLE 2

Experiment	Δ(10% to 90%)	Ratio
18	12.5	.862
24	10.2	1.06
41	10.1	1.07
44	10.8	1.00
46	10.3	1.05
Average	10.78	

The resulting normalized force-velocity relations obtained from different preparations during direct stimulation are compared in Figure 29. Three of the curves are virtually identical (Experiments 18, 41,

Figure 29. Comparison of force-velocity relations obtained by submaximal direct stimulation in five experiments normalized to L_o and scaled to slope of length-tension relation as described in text.

A. Experiment 24

B. Experiment 18

C. Experiment 41

D. Experiment 44

E. Experiment 46

Annotation as in Figure 24.

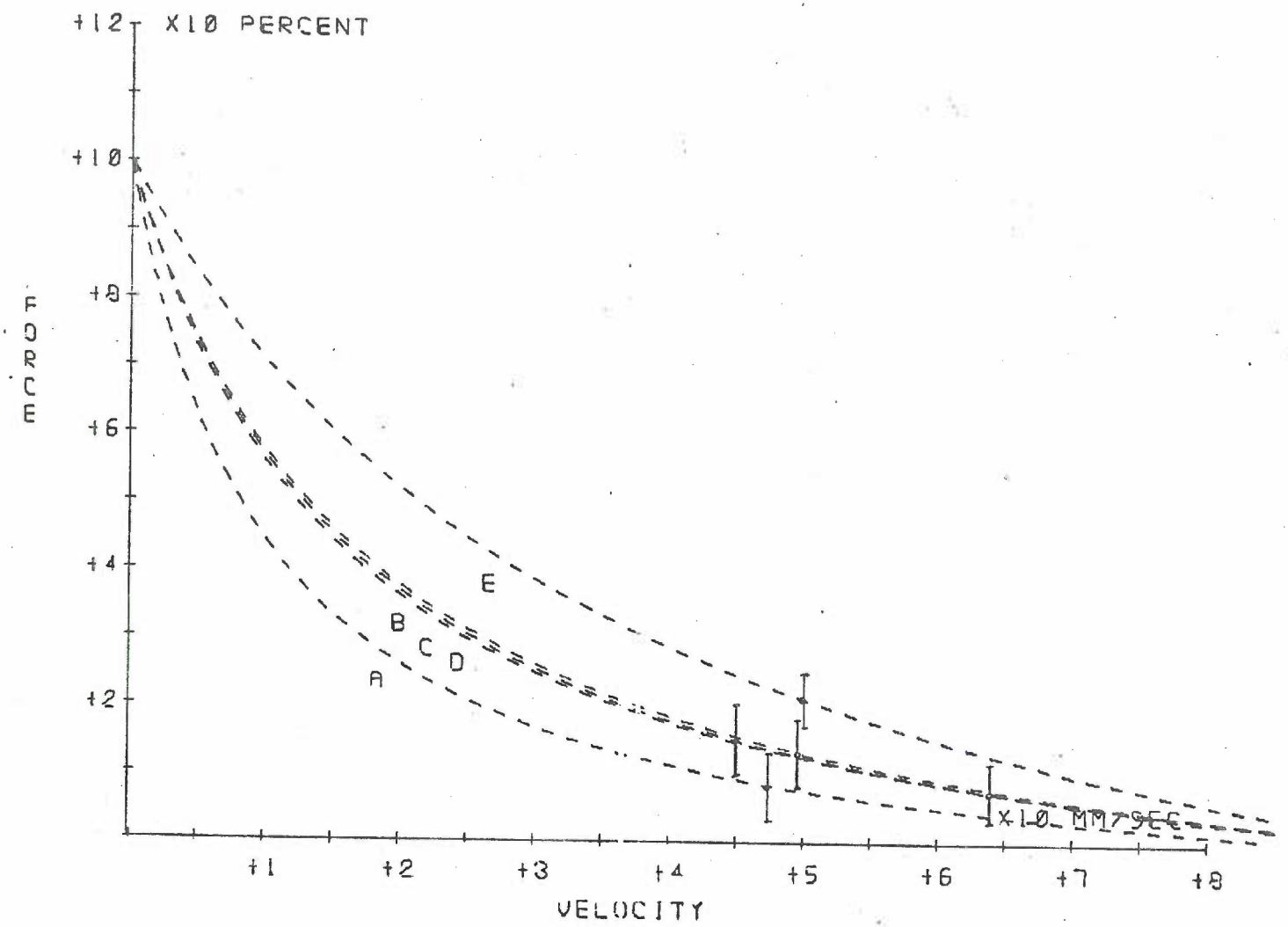
+12
X10 PERCENT
+10
+8
+6
+4
+2
FORCE
E
B
C
D
A
X10 MM/SEC
+1
+2
+3
+4
+5
+6
+7
+8
VELOCITY

44) while the curve from Experiment 46 had a greater curvature and that of Experiment 24 a lesser curvature. The close agreement of the curves, especially with respect to V_{max} (velocity at zero tension) supports both the method of normalization, and the assumption that a homogeneous population of motor units are active, presumably fast large motor units.

The same normalization procedure was used for the force-velocity relations obtained at low reflex levels in three different experiments (all less than 10% of maximal tetanic tension). These curves are compared with the average of the force-velocity relations obtained during direct stimulation (Curve D in Figure 30). The magnitude of the difference between the force-velocity relation at the lowest reflex level and during direct activation can be appreciated from this figure. If only two fiber types (with respect to intrinsic rate of shortening) are present, it is probable that these reflex curves are the same as that for the 'slow' motor units, presumably also the small motor units.

Finally, it is of interest to estimate the velocities of shortening in percent of fiber length at L_o. At the end of Experiment 46, the lateral gastrocnemius was slit lengthwise and the fiber lengths measured in situ for two muscle lengths. Based upon the relation between muscle length and fiber length found (see Appendix 2.3), the estimated intrinsic shortening rates are given in Table 3 for the force-velocity relations at low reflex levels (below 10%) and for submaximal direct stimulation.

Figure 30. Comparison of force-velocity relations obtained for low reflexes (under 10% of maximal tetanic tension) in three different experiments. Normalized as in Figure 29.

A. Experiment 24. (8% max. tetanic tension)

B. Experiment 41. (6% max. tetanic tension)

C. Experiment 46. (7% max. tetanic tension)

D. Average force-velocity curve during direct stimulation (from Figure 29).

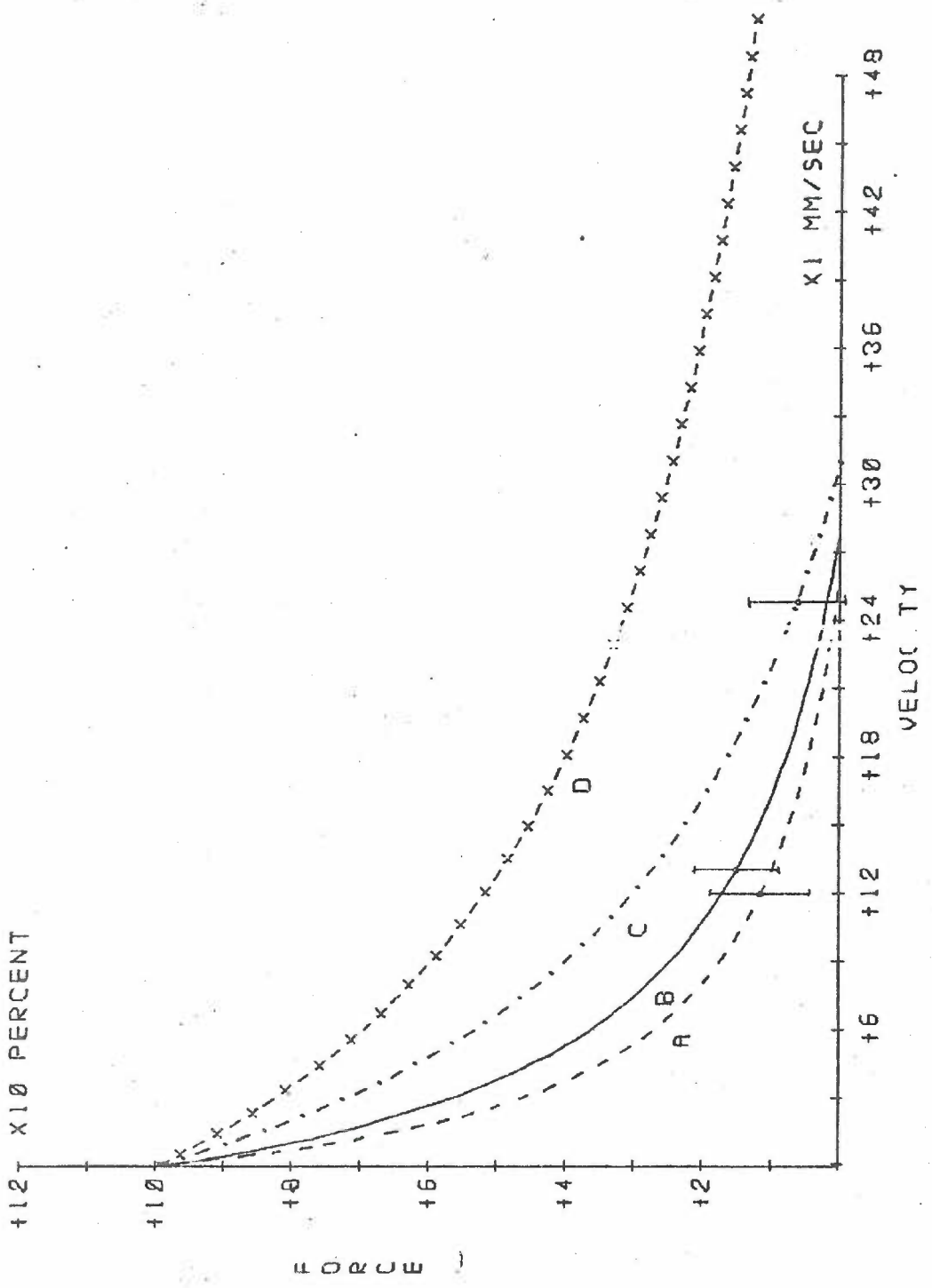
+12 X10 PERCENT
+10
+8
+6
+4
+2
FORCE
+6
+12
+18
+24
+30
+36
+42
+48
X1 MM/SEC
VELOCITY
A
B
C
D

TABLE 3

Estimates of Intrinsic Rates of Shortening

Experiment Direct Stimulation	a/P_o	V_{max} mm/sec	V_{max} Fiber lengths at L_o/sec
18	.18	118.5	2.55
24	.11	87.5	2.30
41	.17	96.3	2.10
44	.16	103.7	1.85
46	.38	95.6	2.11
Average	.20	100.3	2.18
Low Reflex			
24 (8%)	.13	24.1	.70
41 (6%)	.18	26.0	.75
46 (7%)	.37	30.6	.79
Average	.227	26.9	.747

Comparison of Integrated Electromyogram of Reflexly and Directly Activated Muscle.

It was hoped that the integrated EMG (rectified and filtered above 10 Hertz) could be used as one measure of the reflex activation of the muscle. In particular it was expected to reveal changes in the level of activation during muscle shortening in isotonic runs. For this reason, it was of interest to determine the dependence of the measured EMG upon the muscle length, and whether the relation between EMG and the isometric tension differed for reflexly and directly activated muscle.

Plots of EMG amplitude versus muscle length were constructed from data obtained during the isometric runs used to determine the length-tension relation. The variation of EMG amplitude with muscle length was

not the same for different experiments; the differences may have been due to differences in the location of the EMG electrode assembly. The plots of EMG versus length are included in Appendix 3.0 (Figures 51-55). A curve based upon the best fit of a cubic polynomial was fit to the data. This polynomial was used to adjust the values of EMG for changes in muscle length during isotonic shortening.

During one experiment (Experiment 46) the dependence of the EMG amplitude upon muscle length was determined during reflex as well as direct activation of the muscle (Appendix 3.0, Figures 54 and 55). Because the reflex activation was more variable, the scatter in the data was increased. Although the trend of the variation was in the same direction (decreased amplitude at greater muscle lengths), the curves differ in their shape. The differences may be due to a shift of the electrode location between the two determinations, again it may be a real difference between reflexly and directly activated muscle. The two types of activation do differ in the magnitude of EMG for an equivalent muscle activation. The ratio of EMG amplitude to isometric tension at L_o was approximately 60 μV/kg for direct activation and 20 μV/kg for reflex activation. The greater magnitude of the EMG during direct activation probably arises from the fact that the action potentials are in greater synchrony than during reflex activation. Therefore, the action currents of the phases of depolarization and repolarization add rather than cancel.

The repeatability of the EMG measurement might have been improved if implanted electrodes rather than surface (of the muscle) recordings

had been used. They were avoided in order to minimize damage to the muscle. The points observed above should be further clarified before attempting to use the integrated EMG as a quantitative measure of muscle activation.

DISCUSSION

Assumptions Underlying the Interpretation of the Results

The data just presented clearly demonstrate differences in the force-velocity relations of muscle during low levels of reflex activity as compared to muscle during maximal reflexes or during direct stimulation of its motor nerve. These observed differences might be ascribed to differences in the fundamental contractile properties of the motor units under the differing conditions of muscle activation. Before reaching this conclusion, however, several assumptions must be substantiated. One assumption is that the correction for the compliance of the series elastic component is adequate. That is, that the uncertainty in this correction results in an error in determination of the force-velocity relation which is small compared to the above differences. A second assumption is that the activation of the motor units with time is equivalent to that during a tetanic stimulation, that is, the above differences cannot be explained as the result of unfused motor units, which would lead to a lower average value of V_{max} as found by Rack et al. (62,63, also see Figure 7). The error in determination of the force-velocity relations resulting from deviation from these assumptions will be estimated, and compared to the actual differences observed in the following discussion.

Uncertainty of the compliance of the series elastic component.

The uncertainty of the compliance of the series elastic component

during reflex activation arises because the method utilizing the rate of tension development during a tetanus is not valid for reflex activation. This occurs because the onset of activation is not abrupt, and the rate of tension development follows the time course of motoneuronal recruitment instead of being determined solely by the SEC and the force-velocity relation. This mode of activation is quite different temporally from that achieved by the synchronous activation of motor units during direct motor nerve stimulation.

The assumption was made that the series elastic component was common to all of the motor units in the muscle. This is true of the external tendons, and external connections, but not true of the connective tissue of the individual motor units, or for any part of the SEC associated with the intermolecular crossbridges. On this assumption, the compliance curve of the SEC for low reflex activation is the same as that for direct activation at a higher level, and curve A (Figure 20) is used for both. The compliance used at low reflex activation is simply the extrapolated relation fit to the higher values of tension during direct activation, and the uncertainty only that in making the extrapolation.

Another assumption could be made, that the series elastic component was distributed among the motor units. Thus each active motor unit does not stretch the whole of the SEC, but only that fraction associated with it. The elongation of the SEC would depend upon the tension in the motor unit, not the whole muscle. Thus a change in activation would change the total tension by changing the number of active motor units,

but not change the elongation. For example, an activation equal to one third of that used to determine the compliance of the SEC, representing a reduction of active motor units to a third, would reduce the tension to a third for the same elongation. The compliance would be three times as great (one third of the stiffness), being composed of one third of the parallel elements that were formerly active. The compliance curve which would result is plotted in Figure 20 as Curve B. It is given by increasing K_o by a factor of 3 (to 240 μm/kg) and decreasing K_1 by a factor of 3 (to 1.0 kg).

Since the actual SEC is both partly common to all the motor units (stretched by all units) and partly distributed, the actual curve must lie between Curve A and Curve B (note that Curve B is determined from Curve A in the region from 4 kg to 12 kg, the region of the actual data points, and does not depend upon the extrapolation of Curve A). Curve B would represent the worst case in terms of the error which could result, that is, that all of the SEC was distributed. Even another choice for extrapolation of Curve A in this region would most likely lie below Curve B. Thus, determining the change in the force-velocity relation which would occur if Curve B had been used for the correction during low reflex activation gives an upper limit on the uncertainty due to this source. Therefore, the reflex force-velocity relation was redetermined for this value of compliance, obtained by substituting values of 240 μm/kg for K_o and 1 kg for K_1. The same isotonic runs were used to make a force-velocity plot, the constants of the modified Hill equation were determined, and used to calculate the value of V_{max} at L_o. The new

value of V_{max} was 24.8 mm/sec compared with the previous value of 30.6 mm/sec (Table 3). The value of a/P_o at L_o increased from .37 to .44. The magnitude of the change is just under 20%, and therefore is an order of magnitude smaller than the differences observed in V_{max} between low reflex levels and direct activation of the muscle. Furthermore, the direction of the change is toward a smaller value of V_{max}, that is, it would have resulted in a greater difference between the values at low reflex and during direct activation. Thus, the use of Curve A, based on the assumption that the series elastic component was common to all of the motor units, was a conservative one, favoring an underestimate of the actual differences between the force-velocity relations.

Uncertainty in the degree of tetanic fusion.

It was pointed out in the Introduction (page 42) that the apparent contractile characteristics of muscle depend, in part, on the frequency of activation. If the frequency is such as to produce a completely fused tetanus both the force-velocity relation and the length-tension relation are different from those observed when the frequency is below that producing tetanic fusion. Incomplete fusion lowers V_{max} (see Figure 7) and shifts L_o toward a longer muscle length (Figure 8). The data have already been examined with respect to the possible shift in L_o (page 99). It has been concluded that L_o is not significantly different during low reflex activity and direct tetanic stimulation. The question remains whether this rules out a change in motor unit frequency large enough to account for the observed differences in V_{max}.

Figure 7 can be used to obtain an estimate of the change in frequency of the motor units which would be required to account for the three-fold difference in V_{max}, a change from 35 impulses/second to 7 impulses/second. From Figure 8, it can be seen that a length-tension lying midway between the curves for 5 and 10 impulses/second would have been shifted approximately 10 mm, or 40% of the distance over which the tension increases from zero to the maximum at L_o. A shift of 40% of this distance in the present experiments would be 6-7 mm. This would be the shift expected for a change in the frequency of firing of the motor units to explain the differences observed in V_{max}. This is an order of magnitude greater than the differences in position of the length-tension relations during low reflex and direct activation of the muscle (see page 99). The conclusion is that only a small part, if any, of the difference in V_{max} which was seen in the present experiments can be accounted for by a shift in the frequency of activation of the motor units.

With both of the above possibilities eliminated, it can be concluded that the differences in the force-velocity relations observed are due to differences in the intrinsic rate of shortening of the motor units composing the active population in each case. The results will be discussed in terms of this explanation in the following section.

Interpretation of Results in Terms of Heterogeneity of Contractile Properties

The force-velocity relations determined in the present study are the average of the contractile properties of the individual motor units

which are operating under the conditions of activation used in each case. Thus the differences in force-velocity relations which were found in the present study are a measure of the heterogeneity of the motor units within the muscle with respect to the intrinsic rate of shortening. This measure establishes a minimum value for this heterogeneity; the actual heterogeneity must be equal or greater than that indicated by this measure. Only if separate populations, each homogeneous with respect to V_{max}, are activated during the different force-velocity determinations, will the measure determine the full extent of the heterogeneity.

This study was based on the following question: is the contractile behavior, specifically V_{max}, altered by the level of reflex activation? The data imply the following answer. The motor units active at low levels of reflex recruitment have on the average a slower intrinsic rate of shortening than those active at maximal levels of reflex recruitment or those activated by submaximal tetanic stimulation of the muscle nerve. This conclusion does not depend upon an assumption about the order of recruitment during a reflex, although the size principle was important in originally suggesting the question posed. The difference found in intrinsic rate of shortening (V_{max}) at low reflex levels and maximal reflex levels was greater than three-fold. This is a greater difference than the approximately two-fold difference seen in V_{max} between homogeneous fast and slow muscle in the same animal (20). The differences in V_{max} within a heterogeneous muscle are therefore at least as important functionally as those previously observed between whole muscles.

Relation between size and contractile properties of motor units.

The observation of both Burke and Henneman that small motor units in general have lower reflex thresholds than the large motor units means that the units active at low reflex levels were probably small motor units, which were previously shown to have long twitch contraction times. The submaximal stimulus to the motor nerve would activate the larger axons, which are presumed to innervate the large motor units. Thus, by an indirect inference, the high values of V_{max} can be assigned to the larger motor units, previously shown to have short twitch contraction times, and the low V_{max} values assigned to the smaller motor units. The data presented here constitutes the first characterization of the population of motor units with respect to the intrinsic rate of shortening (V_{max}), based upon a direct examination of the contractile properties themselves.

Prior conclusions of a similar nature have been made, based upon the observations of twitch behavior. As noted in the Introduction, however, twitch contraction times are a measure of duration of the active state, not of V_{max}. While V_{max} and duration of the active state are correlated in various whole muscles, it has not been determined that there is a necessary relation. The active state is determined by the process of excitation-contraction coupling, while V_{max} is determined by the contractile mechanism. The former determines the time that the contractile mechanism is 'turned on', V_{max} is the maximum rate of shortening during that period. Semantically it would seem that the terms 'slow' and 'fast' should be reserved for characterization on the basis

of V_{max} only. In this sense it is now accurate to characterize the small motor units as 'slow' and the large units as 'fast'.

Implications as to the order of recruitment.

The results obtained in the present study are consistent with the principle of the recruitment of motor units on the basis of size, with the small motor units having a low V_{max} and the large motor units having a high V_{max}. In Experiment 41 (Figure 26), where a continuous range of reflex values were obtained, the force-velocity relations reveal an increase in speed of contraction as the level of reflex activation increases. This could be due to the recruitment of increasingly faster motor units, or to the mixing of separate populations of slow and fast units. The increased curvature of curve C (reflex equal to 24% of maximal tetanic tension) with respect to curve D (direct stimulation) is suggestive that it results from a mixture of motor units with the force-velocity relation of curve A, and that of curve D. That is, that curve A represents the force-velocity relation of small units, and curve D that of the large motor units. The intermediate curves would then result as large motor units began to be recruited. While originally it had been hoped that the various force-velocity relations could be analyzed to reveal the underlying distribution of values of V_{max} for the motor units, the method had neither the accuracy nor the resolution to do this. Thus the actual distribution of motor units with differing intrinsic rates of shortening has yet to be determined.

The measurement of the intrinsic rate of shortening of single motor units, necessary to determine the actual distribution within a muscle, appeared unfeasible at the beginning of the present study. Recently A. V. Hill (54) has suggested a method which may be found to have the required sensitivity. In the method the muscle lever is forcibly moved faster than the muscle can shorten, that is, faster than V_{max}. It is then stopped, and the time of the first detectable development of tension is determined. The distance shortened and the time are known; from this the intrinsic rate of shortening of the fastest fibers can be determined. The method does not allow the whole force-velocity relation to be determined, only the intrinsic rate of shortening of the fastest of the active fibers. Since a single motor unit is presumably homogeneous, this method used with only a single motor unit active (stimulation of a single motoneurone or ventral root fiber) would determine the V_{max} of the unit. The distribution of motor units with various values of V_{max} could be obtained by sampling a large number of motor units.

Functional Implications of the Results of the Present Study

The results of the present study emphasize the necessity of determining the contractile properties of muscle while activated in a physiological manner, in this case via reflex activation. Previous determinations of the force-velocity relation using artificial stimulation of muscle or muscle nerve are incapable of showing the lower value of V_{max} characteristic of low levels of reflex activation. Yet it is this range

of muscle activity which is most frequently utilized in postural control and fine control of movements.

The previous studies of Rack et al. are important for they point out the difference in contractile properties of muscle whose motor units are firing asynchronously with respect to each other, rather than synchronously. This situation is still artificial in that all motor units are firing at the same rate, and tension is graded only by changing the frequency, not by recruitment of new units. Thus their study resulted in the phenomena observed in Figures 7 and 8, that is, changes in the force-velocity relation and length-tension relation with frequency, which are of theoretical interest, but do not appear to be significant during normal physiological function, at least in the range of reflex activation used in the present study. It appears that on the average the firing rate of the motor units is near their fusion frequency at both low and high reflex levels. This is what would be expected in the scheme of recruitment of Sherrington. Only the units which were just recruited would be firing well below their fusion frequency; after recruitment an increase in excitation would increase the frequency towards fusion. Thus, the present results emphasize the importance of recruitment as a mechanism for modulating the muscle output during motor control.

SUMMARY AND CONCLUSIONS

The investigation was conducted to determine whether motor units recruited at different levels of reflex activity differed in their contractile properties, specifically V_{max}, the intrinsic rate of shortening. This hypothesis implies 1) that the motor units composing the muscle are heterogeneous with respect to contractile properties, and 2) that the recruitment of motor units during a reflex is selective with respect to these differences in contractile properties. This hypothesis was tested by comparing the force-velocity relations determined during low reflex activity with those obtained during maximal reflexes and during tetanic stimulation of the muscle nerve. The reflex used was a crossed extensor reflex elicited in the dog's gastrocnemius muscle by stimulation of the contralateral peroneal nerve. The length-tension relation was also determined during low reflex and direct activation of the muscle. The force-velocity relations were corrected on the basis of an estimate of the compliance of the series elastic component.

A three-fold difference in V_{max} was found between the force-velocity relations obtained during low reflex activity (6-8% of maximum tetanic tension) and those obtained during submaximal tetanic stimulation of the muscle nerve, the latter resulting in the larger value of V_{max}. The values of V_{max} obtained at intermediate levels of reflex activity were closer to those obtained during direct activation; with the values generally increasing with increasing level of reflex activity. The force-velocity relation obtained during a maximal reflex (30% of

maximal tetanic tension) was not significantly different from that obtained during direct activation.

The length-tension relations obtained during low reflex activation and direct activation showed no significant shift with respect to each other. This finding was interpreted to mean that the differences found in the force-velocity relation could not be accounted for by the presence of unfused motor units in the active population during reflex activation. Therefore, the differences must reflect differences in V_{max} of the motor units which were active.

The results obtained can be interpreted in terms of the size principle of Henneman to indicate that the small motor units, which are recruited at the lowest threshold in the reflex, are the slowest, having a low value of V_{max}. The large motor- units, active during submaximal direct stimulation, are fast, having a higher value of V_{max}. These units are recruited at high threshold during reflex activation, and play a predominant role in the determination of the force-velocity curve during the maximal reflexes.

BIBLIOGRAPHY

1. Creed, R.S., Denny-Brown, D., Eccles, J.C., Liddell, E.G.T., and Sherrington, C.S. Reflex Activity of the Spinal Cord. London: Oxford University Press, 1932 (pages 117-125).

2. Bronk, D.W. The energy expended in maintaining a muscular contraction. J. Physiol. (Lond.) 69:306-315 (1930).

3. Henneman, E., Somjen, G., and Carpenter, D.O. Functional significance of cell size in spinal motorneurons. J. Neurophysiol. 28: 560-580 (1965).

4. Erlanger, J., and Gasser, H.S. Electrical Signs of Nervous Activity. Philadelphia: University of Pennsylvania Press, 1937 (pages 16-43).

5. Henneman, E., Somjen, G., and Carpenter, D.O. Excitability and inhibility of motorneurons of different sizes. J. Neurophysiol. 28:599-620 (1965).

6. Somjen, G., Carpenter, D.O., and Henneman, E. Response of motoneurones of different sizes to graded stimulation of supraspinal centers of the brain. J. Neurophysiol. 28:958-965 (1965).

7. Mendel, L.M., and Henneman, E. Terminals of single Ia fibers: location, density, and distribution within a pool of 300 homonymonous motoneurons. J. Neurophysiol. 34:171-187 (1971).

8. McPhedran, A.M., Wuerker, R.B., and Henneman, E. Properties of motor units in a homogeneous red muscle (soleus) of the cat. J. Neurophysiol. 28:71-84 (1965).

9. Wuerker, R.B., McPhedran, A.M., and Henneman, E. Properties of motor units in a heterogeneous pale muscle (m. gastrocnemius) of the cat. J. Neurophysiol. 28:85-99 (1965).

10. Henneman, E., and Olson, C.B. Relations between structure and function in the design of skeletal muscle. J. Neurophysiol. 28: 581-598 (1965).

11. Wyman, R.J., Waldron, I., and Wachtel, G. Lack of fixed order of recruitment in cat motoneuron pools. Exp. Brain Res. 20:101-114 (1974).

12. Grimby, L., and Hannerz, J. Recruitment order of motor units on voluntary contraction: changes induced by proprioceptive afferent activity. J. Neurol. Neurosurg. Psychiatry 31:565-573 (1968).

13. Henneman, E., Clamann, H.P., Gillies, R.D., and Skinner, R.D. Rank order of motoneurons within a pool: law of combination. J. Neurophysiol. 37:1338-1349 (1974).

14. Burke, R.E., Jankowska, E., and Bruggencate, G.T. A comparison of peripheral and rubro-spinal synaptic input to slow and fast twitch motor units of triceps surae. J. Physiol. (Lond.) 207:709-732 (1970).

15. Grützner, P. Zur Anatomie and Physiologie der quergestreiften Muskeln. Rec. Zool. Suisse 1:665-684 (1884). Ref. in Close (20).

16. Denny-Brown, D.E. The histological features of striped muscle in relation to its functional activity. Proc. R. Soc. Lond. [Biol.] 104:142-156 (1929).

17. Gordon, G., and Phillips, C.G. Slow and rapid components in a flexor muscle. Q. J. Exp. Physiol. 38:35-45 (1953).

18. Burke, R.E. Motor unit types of cat triceps surae muscle. J. Physiol. (Lond.) 193:141-160 (1967).

19. Burke, R.E., Levine, D.N., Tsairis, P., and Azjack, F.E. III. Physiological types and histochemical profiles in motor units of the cat gastrocnemius. J. Physiol. (Lond.) 324:723-748 (1973).

20. Close, R.I. Dynamic properties of mammalian skeletal muscles. Physiol. Rev. 52:129-197 (1972).

21. Padykula, H.A., and Gauthier, G.F. Morphological and cytochemical characteristics of fiber types in normal mammalian skeletal muscle. In: Exploratory Concepts in Muscular Dystrophy and Related Disorders. A.T. Milhorat (Ed.) Amsterdam: Excerpta Med. Found., 1967 (pages 117-128).

22. Zieler, K.L. Mechanism of muscle contraction and its energetics. In: Medical Physiology, Vol. 1, 13th ed. V.B. Mountcastle (Ed.) St. Louis: C.V. Mosby, 1974 (pages 77-120).

23. Edström, L., and Kugelberg, E. Histochemical composition, distribution of fibres and fatiguability of single motor units. J Neurol. Neurosurg. Psychiatry 31:424-433 (1968).

24. Barnard, R.J., Edgerton, V.R., and Peter, J.B. Effect of exercise on skeletal muscle. I. Biochemical and histochemical properties. Am. J. Physiol. 28:762-766 (1970).

25. Englehardt, W.A., and Ljubimova, M.N. Myosine and ATPase. Nature 144:668-669 (1939).

26. Cain, D.F., and Davies, R.E. Breakdown of adenosine triphosphate during a single contraction of a muscle. Biochem. Biophys. Res. Commun. 8:361-366 (1962).

27. Barany, M. ATPase activity of myosin correlated with speed of muscle shortening. J. Gen. Physiol. 50:197-216 (1967).

28. Close, R. Dynamic properties of fast and slow skeletal muscles of the rat during development. J. Physiol (Lond.) 173:74-95 (1964).

29. Close, R. Force-velocity properties of mouse muscles. Nature 206:718-719 (1965).

30. Close, R. Force-velocity properties of kitten muscles. J. Physiol. (Lond.) 192:815-822 (1967).

31. Barany, M., and R.I. Close. The transformation of myosin in cross-innervated rat muscles. J. Physiol. (Lond.) 213:455-474 (1971).

32. Close, R. Dynamic properties of fast and slow skeletal muscles of the rat after nerve cross-union. J. Physiol. (Lond.) 204:331-346 (1969).

33. Padykula, H.A., and Herman, E. The specificity of the histochemical method for adenosine triphosphate. J. Histochem. Cytochem. 3: 170-195 (1955).

34. Guth, L., and Yellin, H. The dynamic nature of the "so-called fiber types" of mammalian skeletal muscle. Exp. Neurol. 31:277-300 (1971).

35. Guth, L., and Samaha, F.J. Erroneous interpretations which may result from applications of the 'myofibrillar ATPase' histochemical procedure to developing muscle. Exp. Neurol. 34:465-475 (1972).

36. Yellin, H. Unique intrafusal and extraocular muscle fibers exhibiting dual actomyosin ATPase activity. Exp. Neurol. 25:153-163 (1969).

37. Burke, R.E., and Tsairis, P. Anatomy and innervation ratios in votor units of cat gastrocnemius. J. Physiol. (Lond.) 234:749-765 (1973).

38. Henneman, E., and Olson, C.B. Relations between structure and function in the design of skeletal muscle. J. Neurophysiol. 28: 581-598 (1965).

39. Levin, A., and Wyman, J. The viscous elastic properties of muscle. Proc. R. Soc. Lond. (Biol.) 101:218-243 (1927).

40. Blix, M. Die Länge und die Spannung des Muskel. Skand. Arch. Physiol. 3:295-318 (1892). Ref. in Levin and Wyman (39).

41. Fick, A. Neue Beiträge zur Kenntniss von der Warmeentwicklung im Muskel. Pflüger's Arch. 51:541-569 (1892). Ref. in Levin and Wyman (39).

42. Fenn, W.O. The relation between the work performed and the energy liberated in muscular contraction. J. Physiol. (Lond.) 58:373-395 (1924).

43. Hill, A.V. The maximum work and mechanical efficiency of human muscles, and their most economical speed. J. Physiol. (Lond.) 56: 19-41 (1922).

44. Fenn, W.O., and Marsh, B.S. Muscular force at different speeds of shortening. J. Physiol. (Lond.) 85:277-297 (1935).

45. Hill, A.V. The heat of shortening and the dynamic constants of muscle. Proc. R. Soc. Lond. (Biol.) 126:136-195 (1938).

46. Hill, A.V. The effect of load on the heat of shortening of muscle. Proc. R. Soc. Lond. (Biol.) 159:297-318 (1964).

47. Hill, A.V. The earliest manifestation of the mechanical response of striated muscle. Proc. R. Soc. Lond. (Biol.) 138:339-348 (1951).

48. Aubert, X. Le couplage energetique de la contraction muscularire. Brussels: Editions Arscia, 1956 (page 233).

49. Abbott, B.C., and Wilkie, D.R. The relation between velocity of shortening and the tension-length curve of skeletal muscle. J. Physiol. (Lond.) 120:214-229 (1953).

50. Hill, A.V. The abrupt transition from rest to activity in muscle. Proc. R. Soc. Lond. (Biol.) 136:299-420 (1949).

51. Gasser, H.S., and Hill, A.V. The dynamics of muscular contraction. Proc. R. Soc. Lond. (Biol.) 96:398-437 (1928).

52. Ritchie, J.M. The effect of nitrate on the active state of muscle. J. Physiol. (Lond.) 126:155-168 (1954).

53. Ritchie, J.M., and Wilkie, P.R. The effect of previous stimulation on the active state of muscle. J. Physiol. (Lond.) 130:488-496 (1955).

54. Hill, A.V. First and Last Experiments in Muscle Mechanics. Cambridge: University Press, 1970 (pages 85-109, 56-75).

55. Hill, A.V. The series elastic component of muscle. Proc. R. Soc. Lond. (Biol.) 137:273-280 (1950).

66. Jewel, B.R., and Wilkie, P.R. An analysis of the mechanical components in frog's striated muscle. J. Physiol. (Lond.) 143:515-540 (1958).

57. Gordon, A.M., Huxley, A.F., and Julian, F.J. The variation in isometric tension with sarcome length in vertebrate muscle fibres. J. Physiol. (Lond.) 184:170-192 (1966).

58. Ebashi, S., and Endo, M. Calcium ion and muscular contraction. Prog. Biophys. Mol. Biol. 18:125-183 (1968).

59. Simmons, R.E., and Jewell, B.R. Mechanics and models of muscular contraction. In: Recent Advances in Physiology, 9. R.J. Linden (Ed.) Edinburgh and London: Churchill Livingstone, 1974 (pages 87-147).

60. Pdolsky, R.J., and Teichholz, L.E. The relation between calcium and contraction kinetics in skinned muscle fibres. J. Physiol. (Lond.) 211:19-35.

61. Julian, F.J. The effect of calcium on the force-velocity relation of briefly glycerinated frog muscle fibres. J. Physiol. (Lond.) 218:117-145 (1971).

62. Rack, P.M.H., and Westbury, D.R. The effects of length and stimulus rate on tension in the isometric cat soleus muscle. J. Physiol. (Lond.) 204:443-460 (1969).

63. Joyce, G.C., and Rack, P.M.H. Isotonic lengthening and shortening movements of cat soleus muscle. J. Physiol. (Lond.) 204:475-491 (1969).

64. Somjen, G., Carpenter, D., and Henneman, E. Selective depression of alpha motoneurons of small size by ether. J. Pharmacol. Exp. Ther. 148:380-385 (1965).

65. Sherrington, C.S. On plastic tonus and proprioceptive reflexes. Q. J. Exp. Physiol. 2:109-156 (1909).

APPENDICES

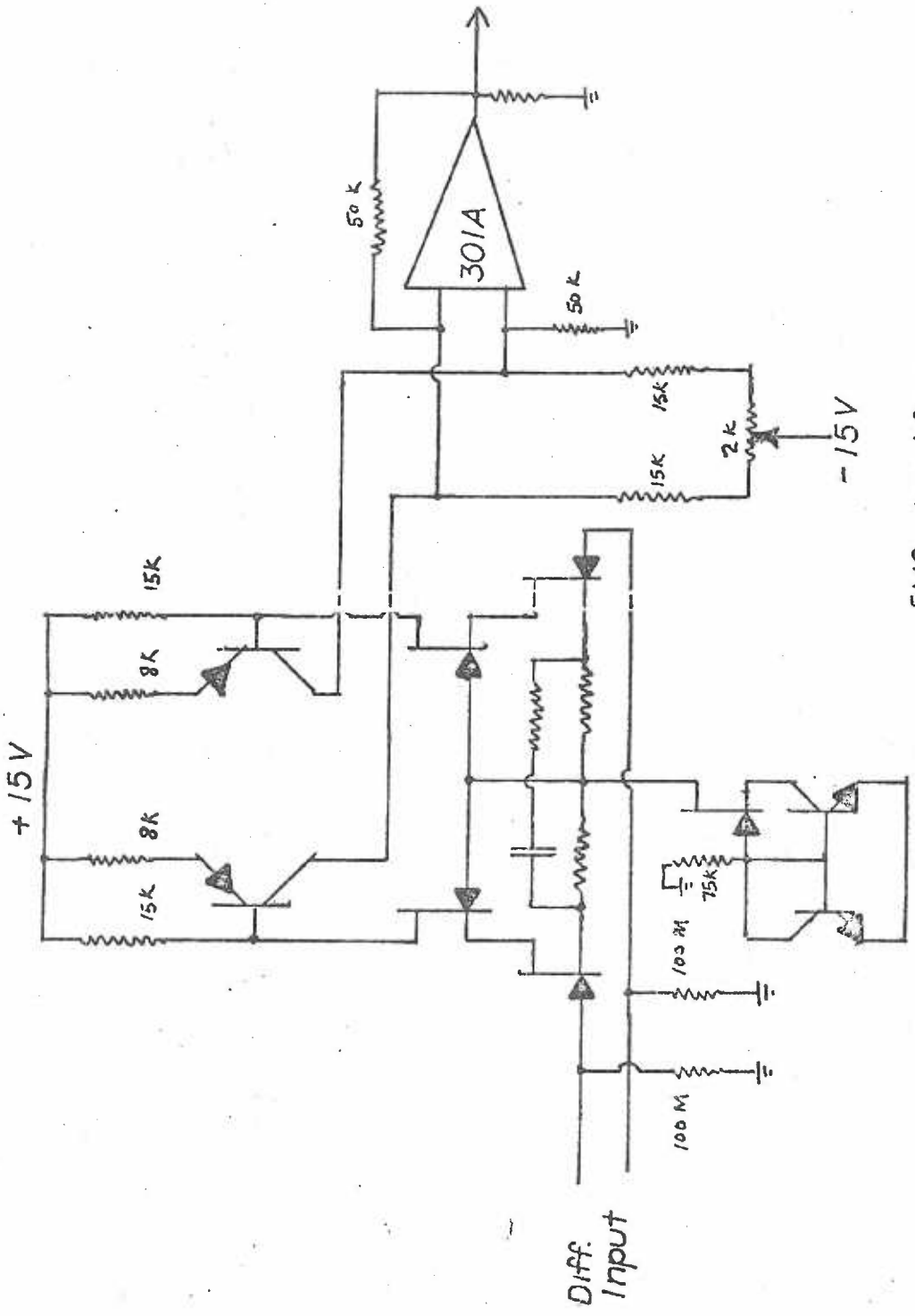

EMG Amplifier
FIG. 31

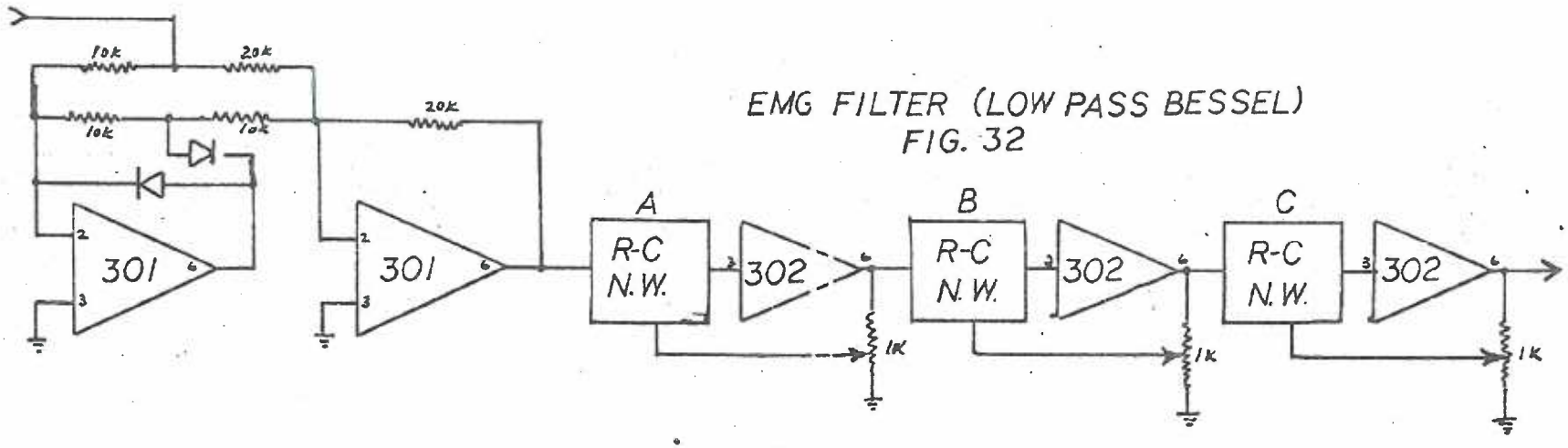

EMG FILTER (LOW PASS BESSEL)
FIG. 32

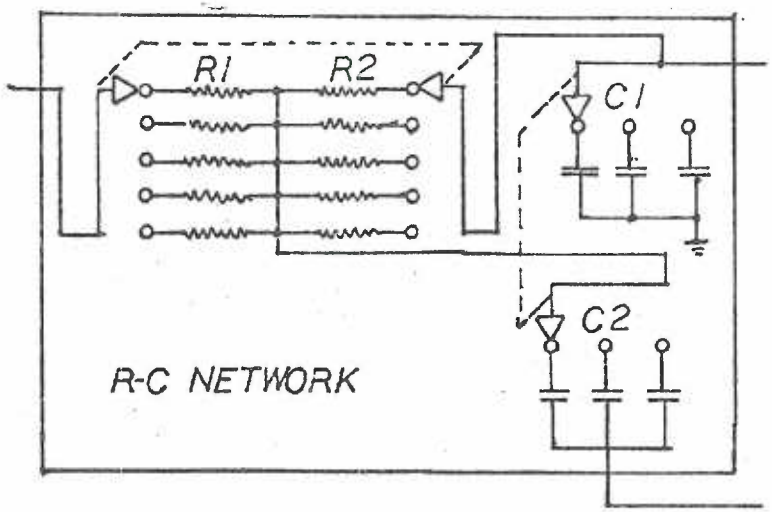

	R1	R2
X10	1MEG	499K
X16	619K	309K
X25	402K	200K
X40	249K	124K
X63	158K	78.7K

1% Tol

	C1A	C2A	C1B	C2B	C1C	C2C
X1	26,000	13,000	36,000	3,600	20,000	9,100
X10	2,600	1,300	3,600	360	2,000	910
X10)	260	130	360	36	200	91

CAP in PF, Polystyrene 5%

'D = 40 MSEC for 10 HERTZ cutoff frequency
= 400 x 1/FC MSEC

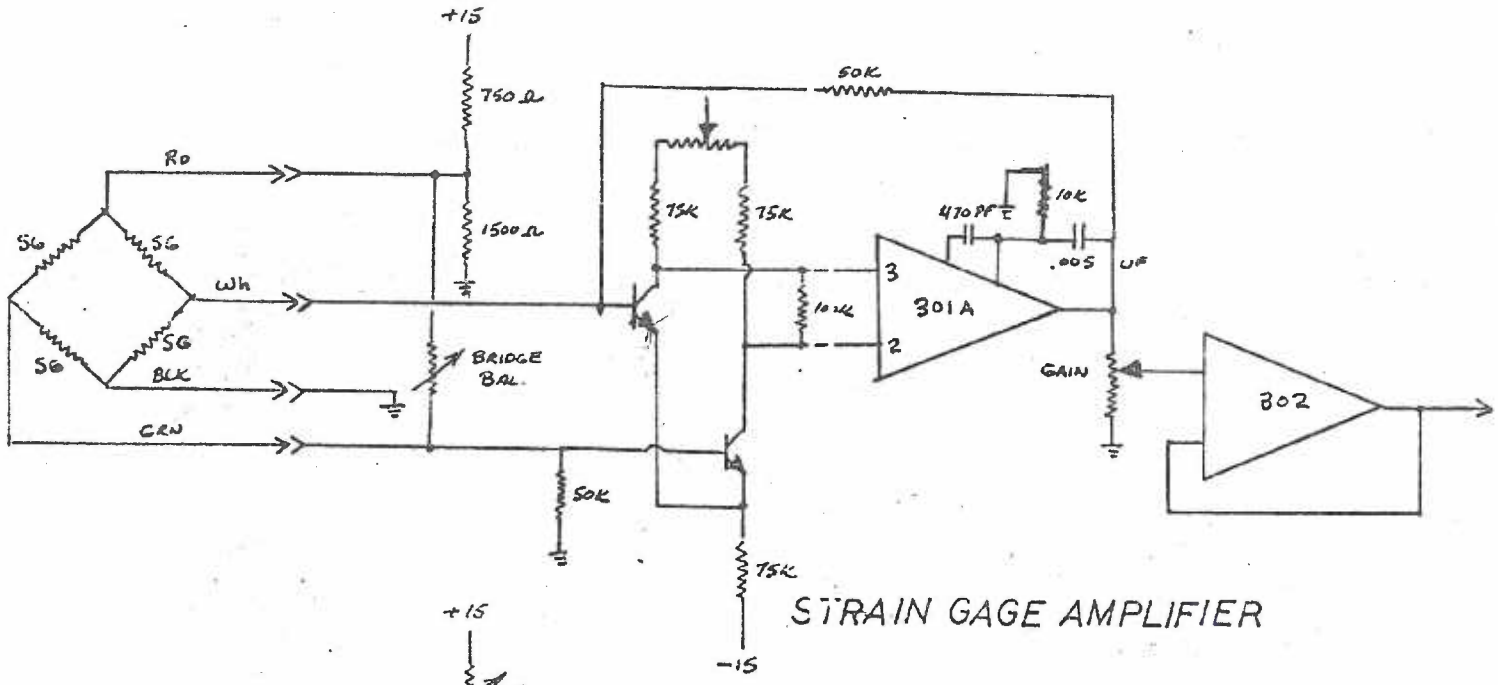

STRAIN GAGE AMPLIFIER

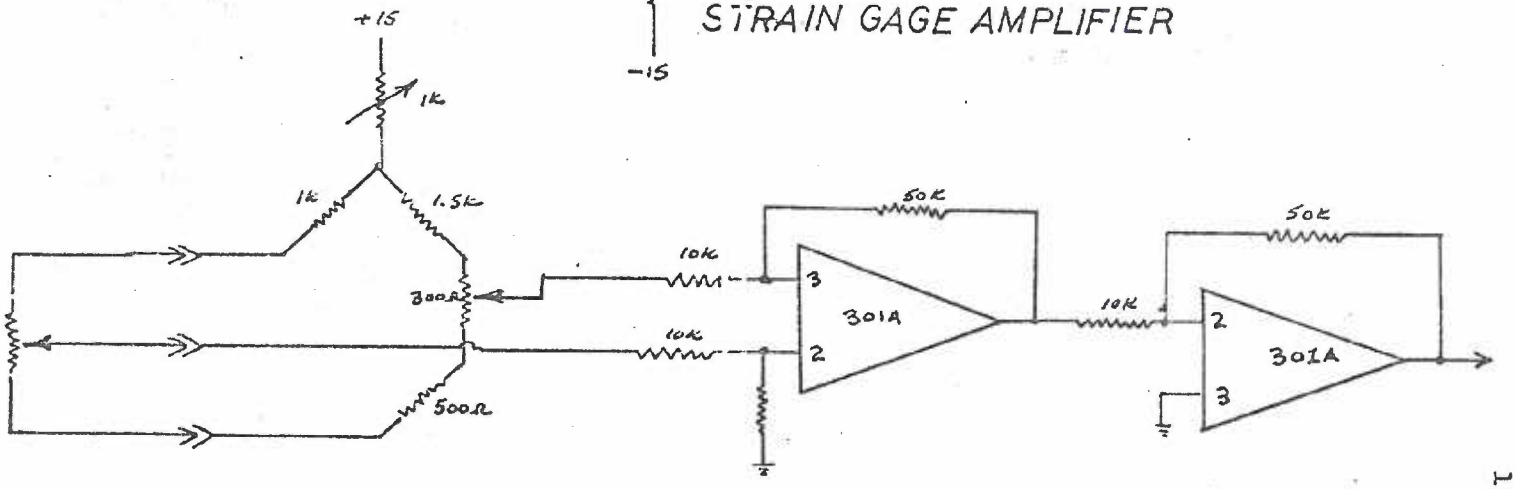

POTENTIOMETER AMPLIFIER

FIG. 33

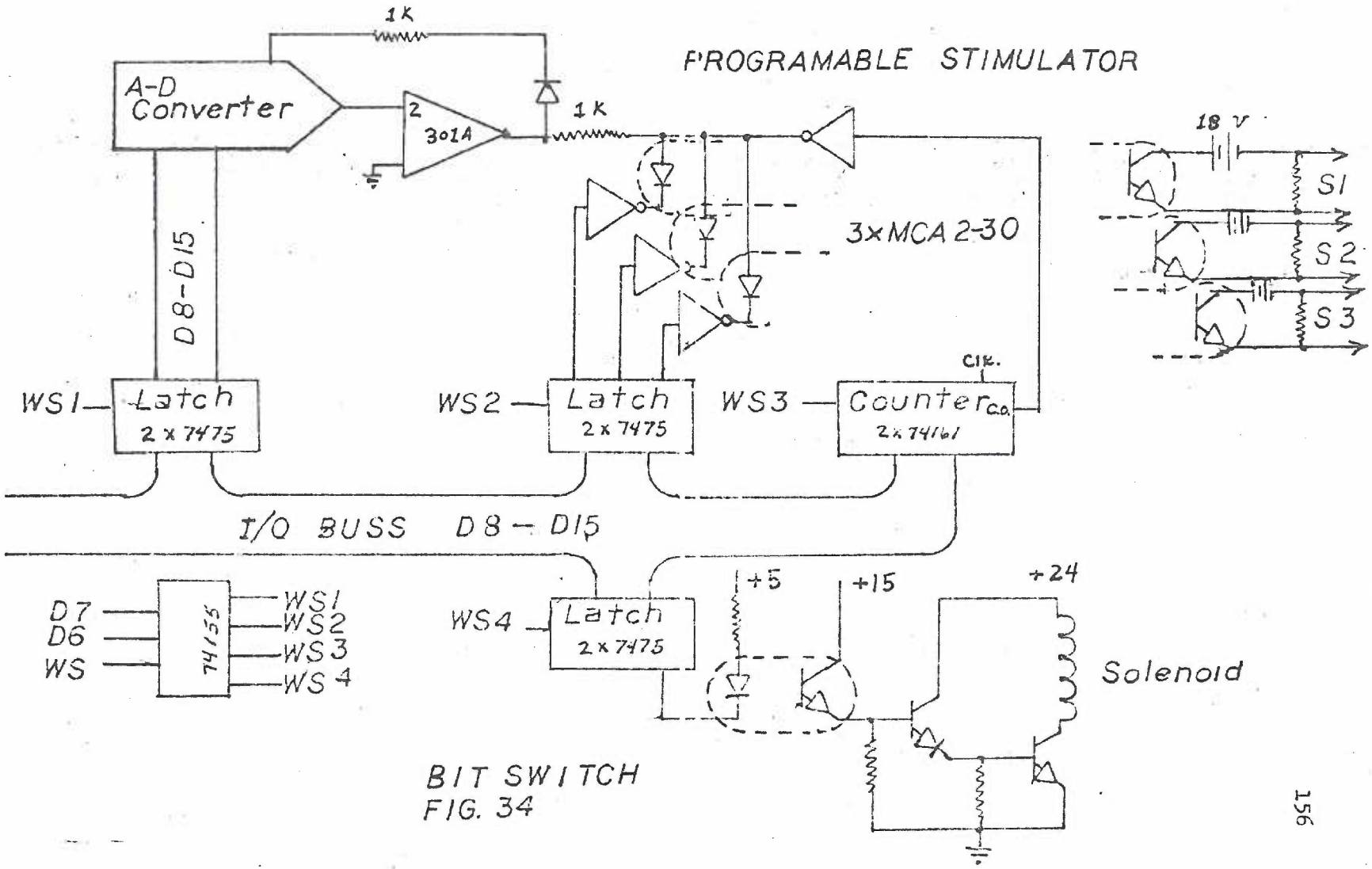

BIT SWITCH
FIG. 34

Programmable Stimulator
Calibration
FIG. 35

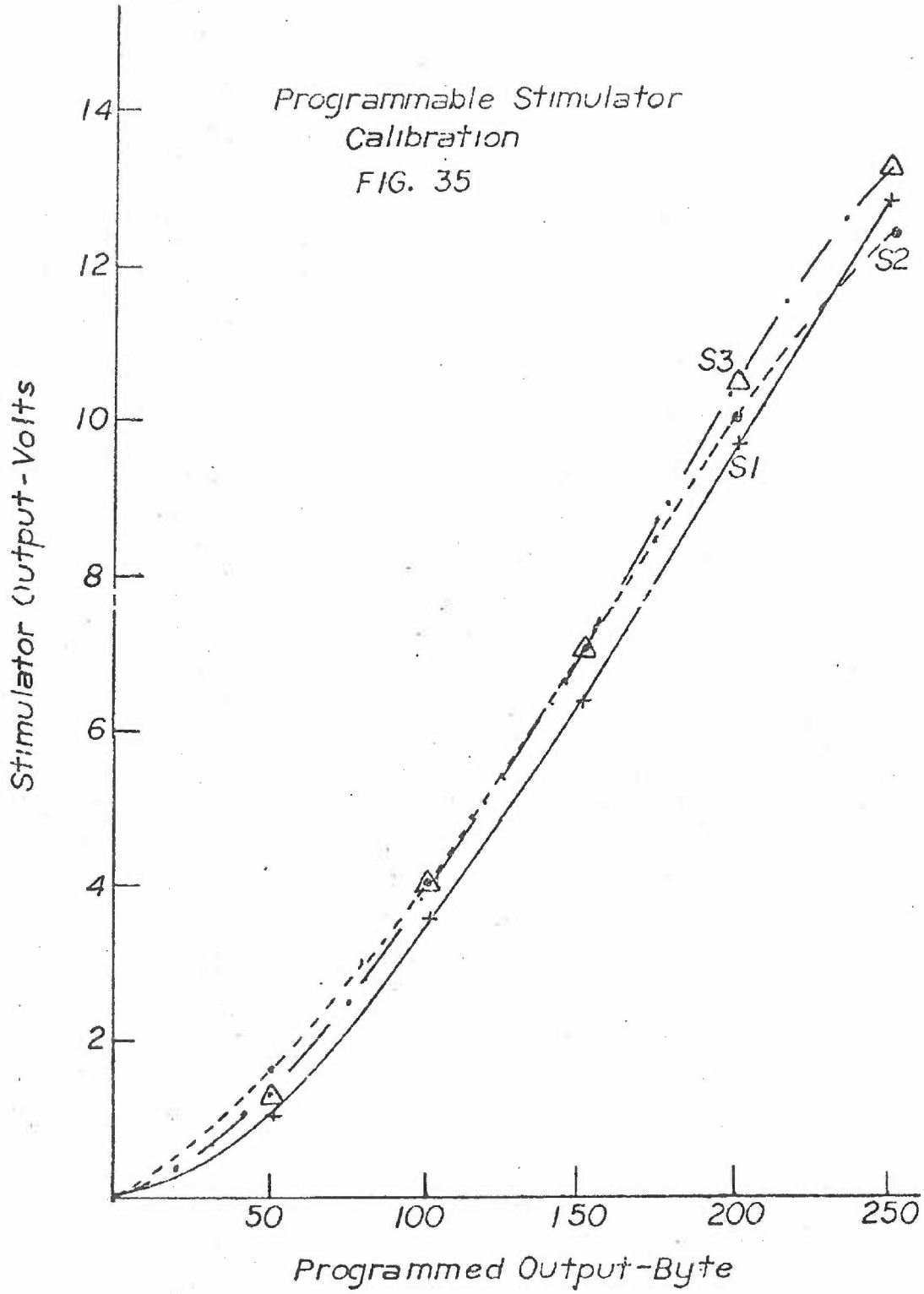

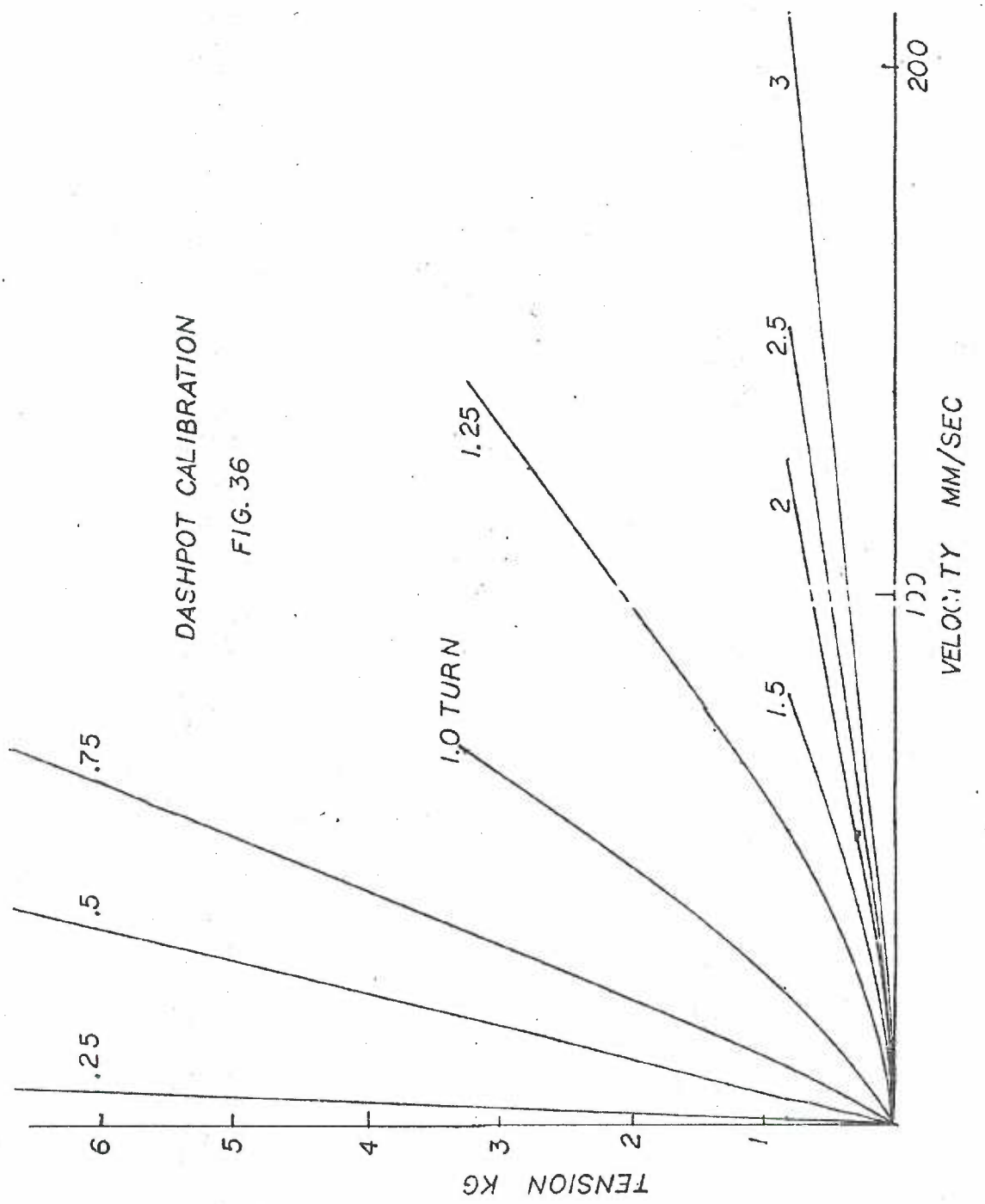
DASHPOT CALIBRATION
FIG. 36
TENSION KG
VELOCITY MM/SEC
1.0 TURN
.75
.5
.25
1.25
1.5
2
2.5
3
100
200
1
2
3
4
5
6

Appendix 2.0. Derivations

Appendix 2.1. Derivation of twitch tension from classical model (relation to force-velocity relation, SEC, and active state).

It will be assumed that the muscle length is equal or shorter than L_o and that the parallel elastic component can be neglected. The model used is that in Figure 2d (page 25). For an isometric twitch contraction the total length remains the same; that is, $x_{SEC} + x_{CE}$ = constant. Therefore, $\frac{dx_{SEC}}{dt} = \frac{-dx_{CE}}{dt} = v_{CE}$, the velocity of shortening, and the compliance of the SEC, $G(P) = \frac{dx_{SEC}}{dP}$, is a function of the tension (P). Therefore $\frac{dP}{dt} = [-dx_{CE}/dt]/[dx_{SEC}/dP] = v_{CE}/G(P)$ and $P(t) = \int[v_{CE}/G(P)]dt$. v_{CE} is a function of muscle length, muscle tension and activation of the muscle. At the full intensity of the active state the Hill equation modified by Abbott and Wilkie can be used: $v_{CE} = \frac{[P_o(1)-P]b}{[P+a]}$

substituting $V_{max} = P_o(1) \cdot \frac{b}{a}$ and $R = \frac{P}{P_o(1)}$

$$v_{CE} = \frac{[1-R] \cdot V_{max}}{[\frac{P}{a} + 1]}$$

where R is the ratio of tension to the isometric tension. $P_o(1)$ (isometric tension) depends upon the intensity of the active state, and V_{max} possibly does. During the plateau of the active state the intensity is maximal, and most of the shortening occurs during this period because R is low. Therefore the tension developed during the plateau can be used to qualitatively determine the effect of V_{max} and G(P) on twitch tension.

$$P(t_1) = \int^{t_1} \frac{[1/G(P)] \cdot [1-R] \cdot V_{max} \cdot dt}{[\frac{P}{a} + 1]}$$

First the factor [1-R] in the numerator, and the factor $[\frac{P}{a} + 1]$ in the denominator must be considered. R cannot be any greater than the twitch-tetanus ratio, therefore is usually less than .25. During the integration it varies between 0 and .25, therefore, its average value is .125. Thus the change in the average value of the factor [1 - R] will be one eighth of the change in R, or twitch-tetanus ratio. $\frac{a}{P_o}$ at L_o will be close to .25, therefore, $\frac{P}{a}$ at the end of the integration will equal 1. At shorter muscle lengths $\frac{P}{a}$ is reduced proportional to $P_o(1)$. Thus the average value of $[\frac{P}{a} + 1]$ is 1.5 at L_o, and approaches 1.0 at short muscle lengths. At short muscle lengths the factor $[\frac{P}{a} + 1]$ is not strongly dependent upon $P_o(1)$. Therefore, at short muscle lengths the integral will vary as

$$\int^{t_1} \frac{1}{G(P)} \cdot V_{max} \cdot dt$$

Changes in the duration of the active state (t_1) will increase the twitch-tension because of the longer time to elongate the series elastic component. The twitch tension is directly proportional to V_{max}, and inversely proportional to the compliance of the series elastic component. At short muscle lengths V_{max} will vary as $P_o(1)$, and if the compliance, G(P), was constant, the twitch-tetanus ratio, $\frac{P(t_1)}{P_o(1)}$, would also be constant. G(P) depends upon the tension, however, being more compliant

at low tensions. Therefore, as the twitch tension is reduced at short muscle lengths, the average value of G(P) is greater, and the twitch-tetanus ratio decreases as the muscle length becomes shorter. That is, twitch tension will decrease faster than $P_o(l)$ as the muscle length is shortened. This would appear as a shift of the length-tension curve of twitch-tension toward longer muscle lengths, and may represent part of the effect seen by Rack and Westbury (62).

Appendix 2.2. Method of curve fitting force-velocity data.

The general method least squares fit assumes that the relation is a linear combination of functions of the independent variable, i.e.,

$$Y(x) = A + Bf_1(x) + Cf_2(x)$$

If $Y'(n)$, $X'(n)$ are actual pairs of data points then sum of square error $= \sum_n [Y'(n) - Y(x'(n))]^2$

The constants A, B, C, etc. can be chosen to minimize this function by taking derivatives with respect to the constants and setting to zero, i.e., $\sum_n Z\,[Y'(n) - Y(x'(n))] \cdot \frac{d}{dA}[Y'(n) - Y(x'(n))] = 0$

This procedure results in a set of simultaneous equations which can be solved by matrix methods or other means.

The constant A can be eliminated by subtracting the mean value from each data value, i.e.,

$$Y^*(x) = Y - \overline{Y} = Bf_1(x^*) + Cf_2{}^*(x).....$$
$$= B[f_1(x) - \overline{f}(x)] + C[f_2(x) - \overline{f_2}(x)].....$$

Thus sets of data which differ only by a constant can be combined after expressing them as deviations from the mean.

The force-velocity data consists of sets of data taken at different muscle lengths, and are fit by a series of relations differing only by a

constant, i.e.,

$$P = P_o(k) - AB \cdot v - B \cdot P \cdot v$$

Where $P_o(k)$ is different at each muscle length (equals isometric tension) $AB = \frac{a}{b}$ and $B = \frac{1}{b}$ in the Hill equation. Eliminating P from the right hand side,

$$P = P_o(k) - AB \cdot v - B \cdot [P_o(k) - AB \cdot v] \frac{v}{[1 + B \cdot v]}$$

The equation is no longer linear with respect to the constants. The last term in fact contains products of all the constants, and the derivatives with respect to the constants would be messy.

We will use an iterative procedure, changing only one constant at a time, and assume the change between iterations is small.

Substitute U(v) for $P \cdot v = (P_o(k) - AB \cdot v) \frac{v}{1 + B \cdot v}$

$$P = P_o(k) - AB \cdot v - B \cdot U$$

Where each value of U is calculated anew after each iteration.

Find AB

$$P + B \cdot U = +P_o(k) - AB \cdot v$$

$$P^* + B \cdot U^* = -AB \cdot v^*$$

where $P^* = P - \overline{P}$, $U^* = U - \overline{U}$, $v^* = v - \overline{v}$

and $\overline{P}(k) = \sum_{n(k)} \frac{P(n(k))}{n(k)}$ (mean value)

$$AB = -\sum_k \sum_{n(k)} [P^* \cdot v^* + B \cdot U^* \cdot v^*] / [\sum_k \sum_{n(k)} v^* \cdot v^*]$$

B = 0.0 on first iteration, current value on successive iterations (AB, $P_o(k)$ used to compute U are current values).

Find $P_o(k)$

$$P_o(k) = \frac{\sum_{n(k)}[P(n(k)) + AB \cdot \sum_{n(k)} v(n(k))]}{n(k)}$$

Find B

$$P + AB \cdot v = P_o(k) - B \cdot U$$

$$P^* + AB \cdot v^* = -B \cdot U^*$$

$$B = -\sum_k \sum_{n(k)} [P^* \cdot U^* + AB \cdot V^*U^*] / [\sum_k \sum_{n(k)} U^* \cdot U^*]$$

Find sum of the squares

$$\text{SumSQ} = \sum_{k,n} [P - P']^2 = \sum_{k,n} [P - P_o(k) + AB \cdot V + B \cdot U]^2$$

The iteration is continued until the change in the SumSQ is less than 2% (1% change in the standard deviation).

The standard deviation of the data from the curve is defined as

$$\text{Std. Dev.} = \sqrt{\text{SumSQ}/\sum_k n(k)}$$

The method above gives the best fit where the variance of the values of tension is constant with tension. A large part of the variance is due to non-repeatibility of the level of reflex activation, this variance is proportional to tension. Errors in making corrections for the passive tension, etc., tend to be independent of the active tension. To be a rigorous statistical measure the variance of the values at high tensions should be equal to the variance at low values of tension. Because the variance of values at low tensions (close to V_{max}) is actually less,

the values of V_{max} determined are probably better than would be expected on the basis of the calculated standard deviations.

Appendix 2.3. Estimation of ratio between muscle and fiber shortening.

The gastrocnemius is a penate muscle, that is, the fibers lie at an oblique angle to the longitudinal axis of the muscle; thus the change in muscle length is not equal to the change in fiber length. At the end of Experiment 46 fiber lengths were measured in situ at two muscle lengths.

Relative Muscle Length	Fiber Length
4.5 mm	20 mm
17.2 mm	30 mm

ΔL (Fiber)/ΔL (Muscle) = $\frac{10.0}{12.7}$ = .79

At L_o = 15 mm, the fiber length = 28.3 mm

The ratio of muscle length (Exp. 46)/average muscle length = 1/1.036*

Therefore, ratio = $\frac{.79}{1.036 \times 28.3 \text{ mm}}$ = .027 fiber lengths/mm

= change in fiber length per mm change in standardized muscle length

*From Table 2

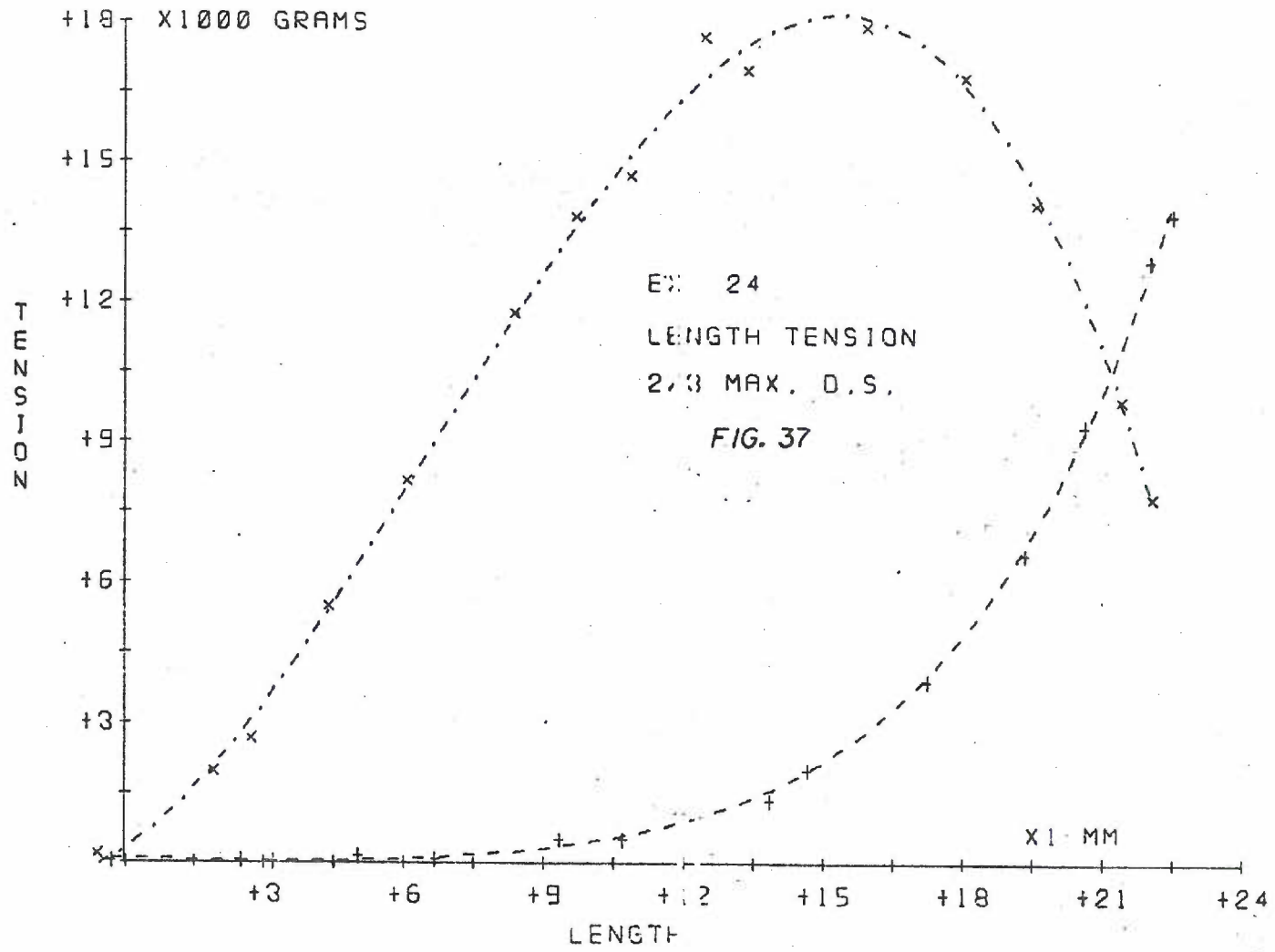
+18
X1000 GRAMS
+15
+12
+9
+6
+3
TENSION
EX 24
LENGTH TENSION
2.3 MAX. O.S.
X1 MM
+3
+6
+9
+12
+15
+18
+21
+24
LENGTH

FIG. 37

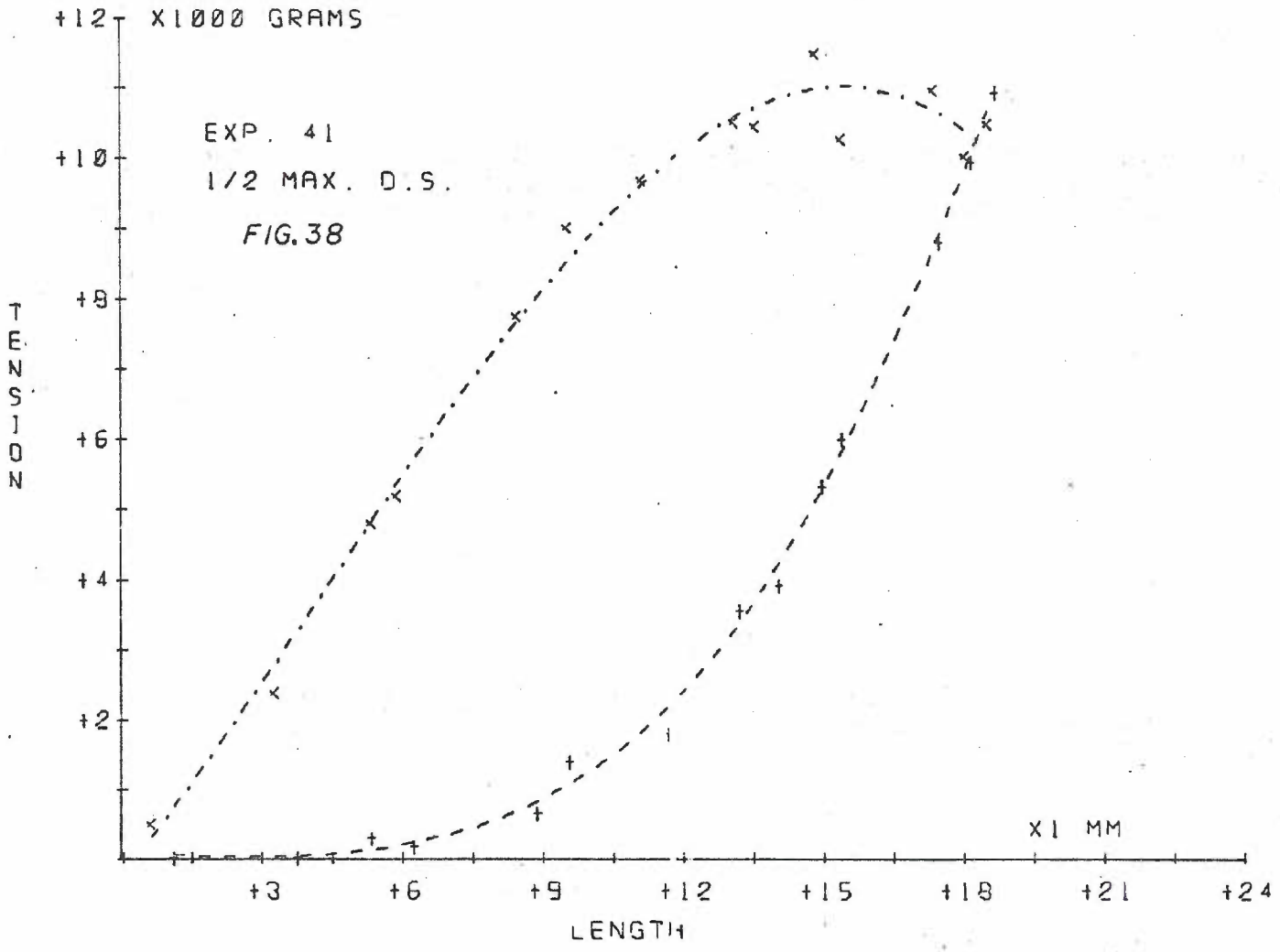
+12 X1000 GRAMS
EXP. 41
1/2 MAX. D.S.
FIG. 38
+10
+8
+6
+4
+2
TENSION
X1 MM
+3
+6
+9
+12
+15
+18
+21
+24
LENGTH

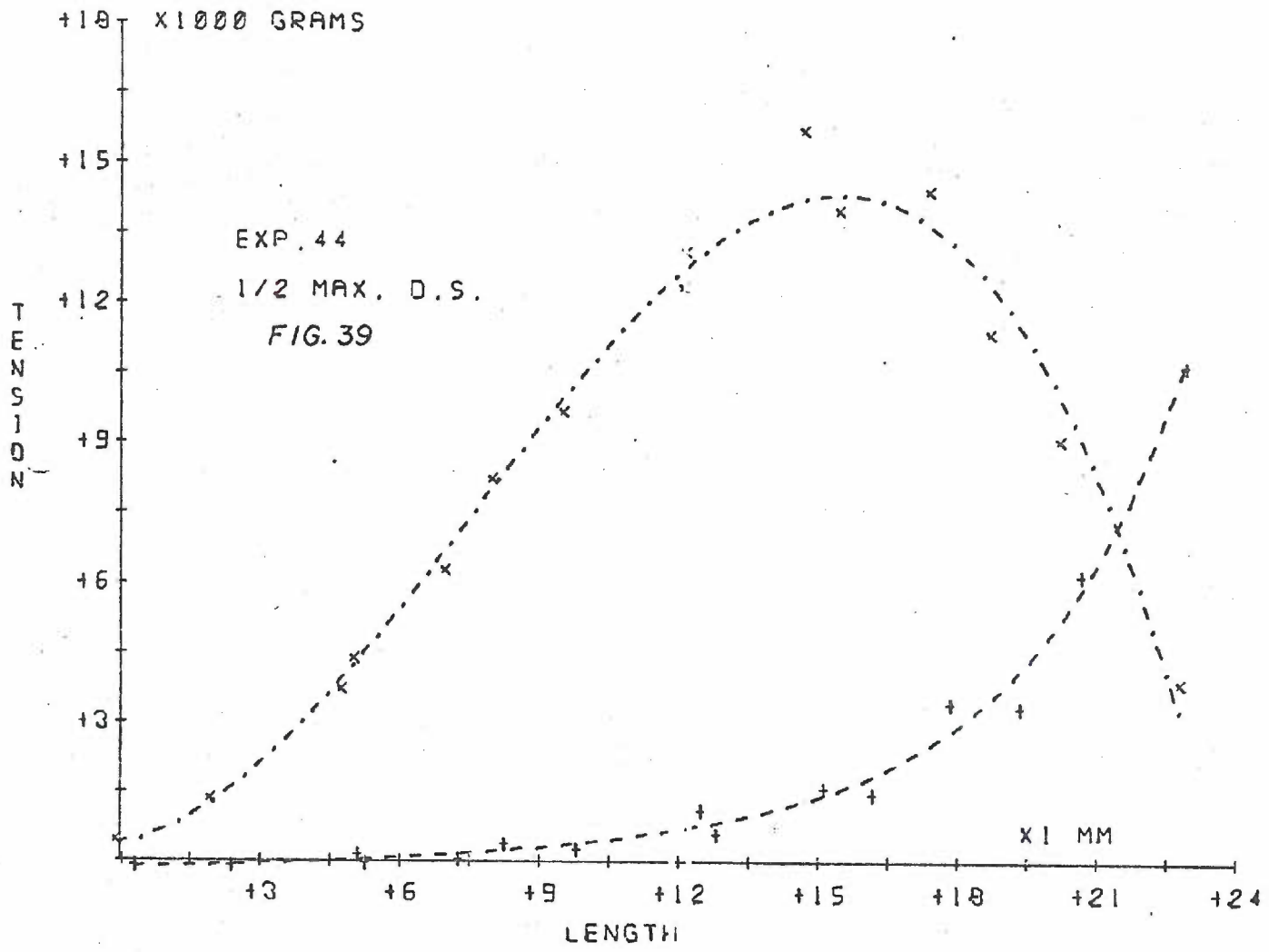
+18
X1000 GRAMS
+15
EXP. 44
1/2 MAX. D.S.
FIG. 39
+12
TENSION
+9
+6
+3
X1 MM
+3
+6
+9
+12
+15
+18
+21
+24
LENGTH

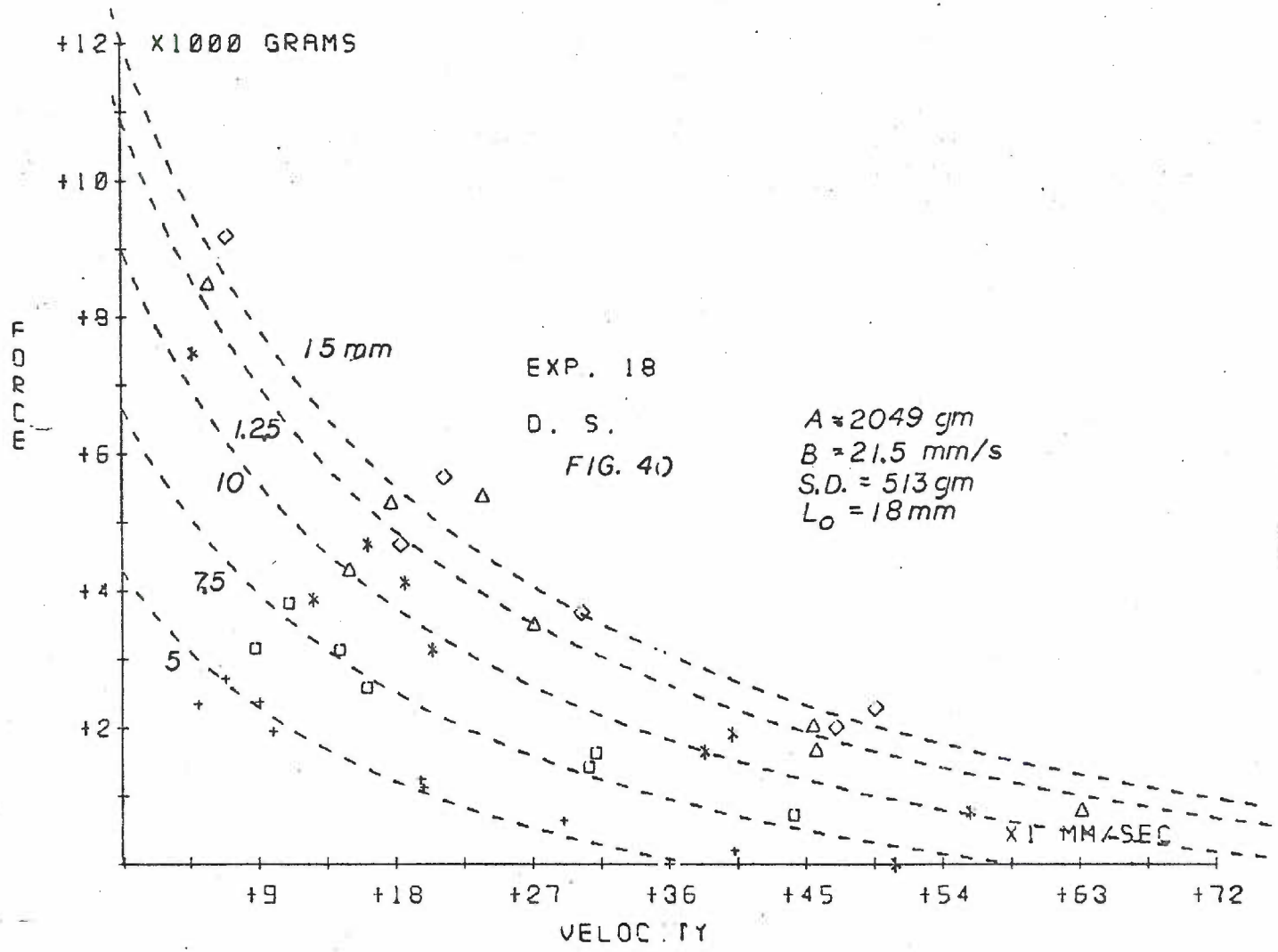
+12
X1000 GRAMS
+10
+8
+6
+4
+2
FORCE
15 mm
1.25
10
7.5
5
EXP. 18
D. S.
FIG. 40
A = 2049 gm
B = 21.5 mm/s
S.D. = 513 gm
L_o = 18 mm
X1 MM/SEC
+9
+18
+27
+36
+45
+54
+63
+72
VELOCITY

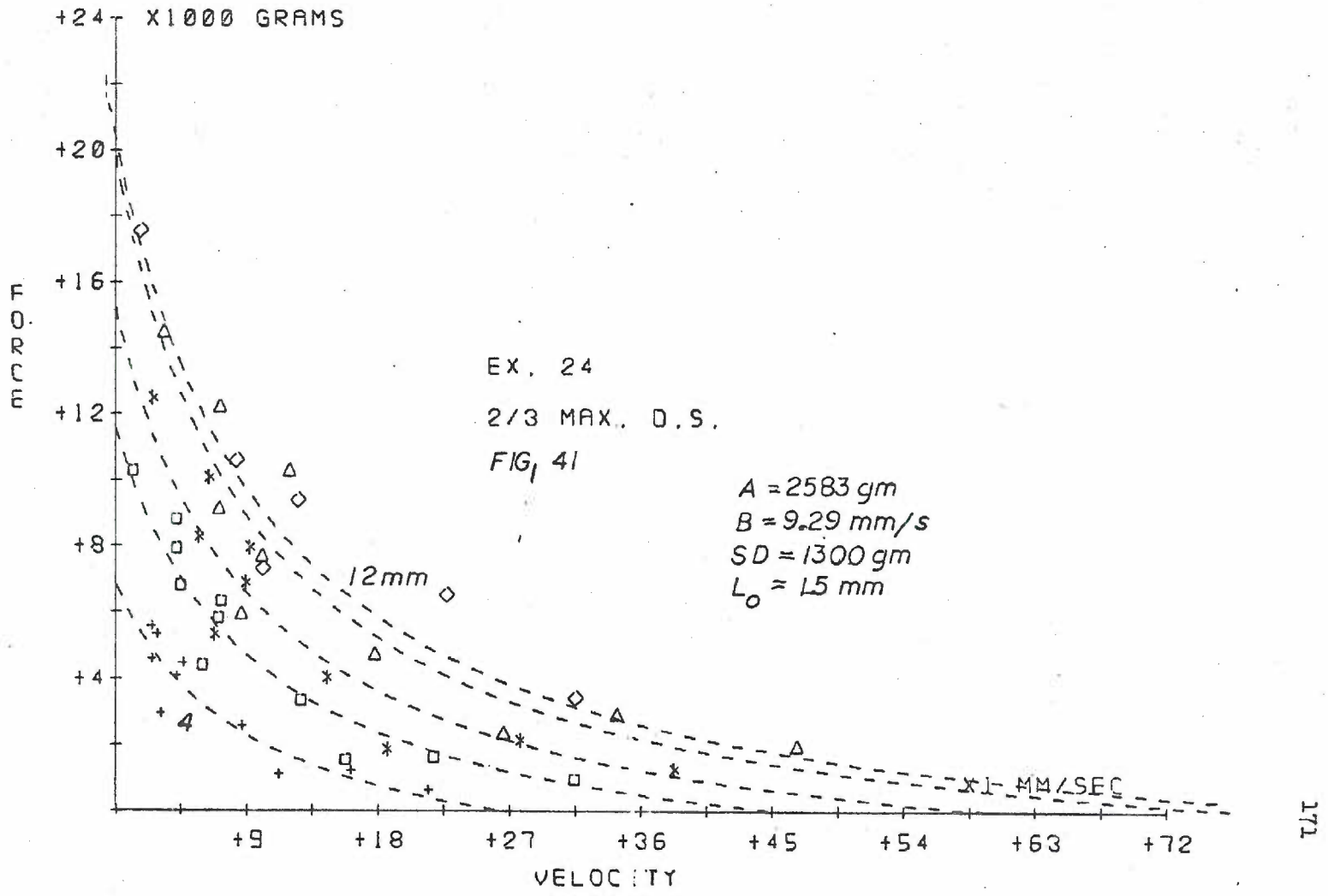
+24
X1000 GRAMS
+20
+16
+12
+8
+4
FORCE
EX. 24
2/3 MAX. O.S.
FIG. 41
A = 2583 gm
B = 9.29 mm/s
SD = 1300 gm
L_o = 1.5 mm
12mm
4
MM/SEC
+9
+18
+27
+36
+45
+54
+63
+72
VELOCITY

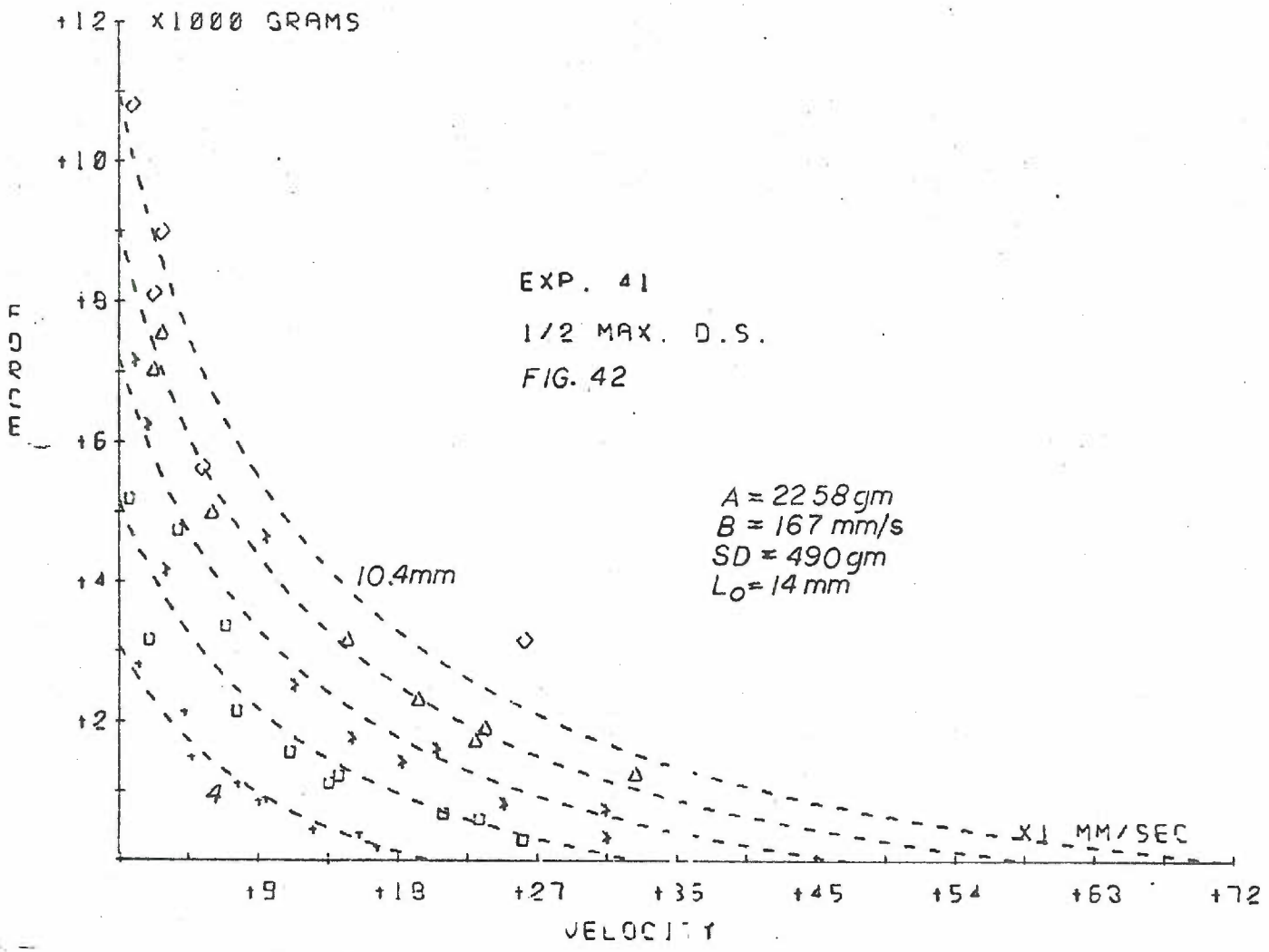
+12
X1000 GRAMS
+10
+8
+6
+4
+2
FORCE
EXP. 41
1/2 MAX. D.S.
FIG. 42
A = 2258 gm
B = 167 mm/s
SD = 490 gm
L_o = 14 mm
10.4mm
4
X1 MM/SEC
+9
+18
+27
+35
+45
+54
+63
+72
VELOCITY

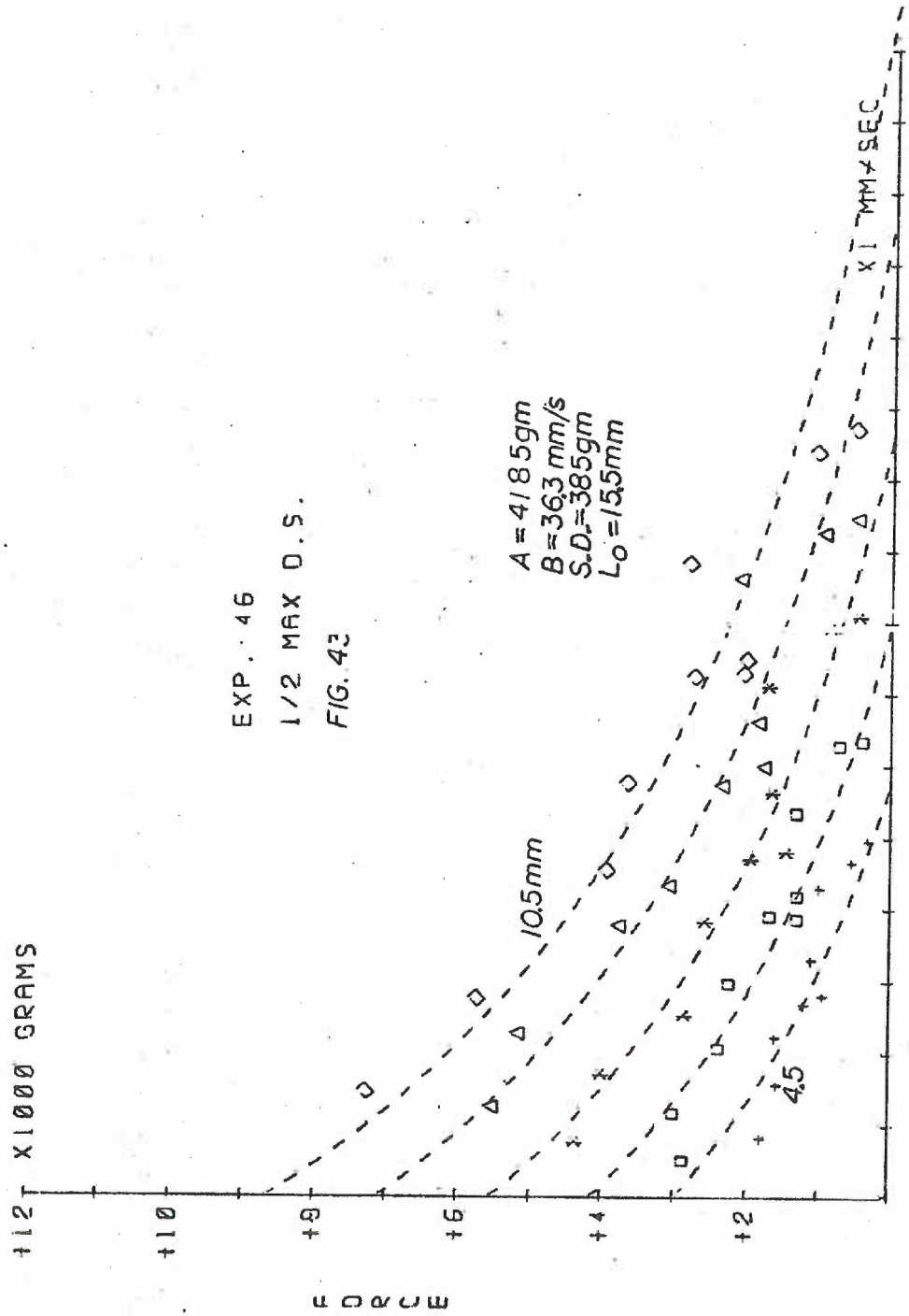
EXP. 46
1/2 MAX D.S.
FIG. 42
A = 4185gm
B = 36.3 mm/s
S.D. = 385gm
L0 = 15.5mm
10.5mm
4.5
FORCE
+12 X1000 GRAMS
+10
+8
+6
+4
+2
+9
+18
+27
+35
+45
+54
+63
+72
VELOCITY
X1 MM/SEC

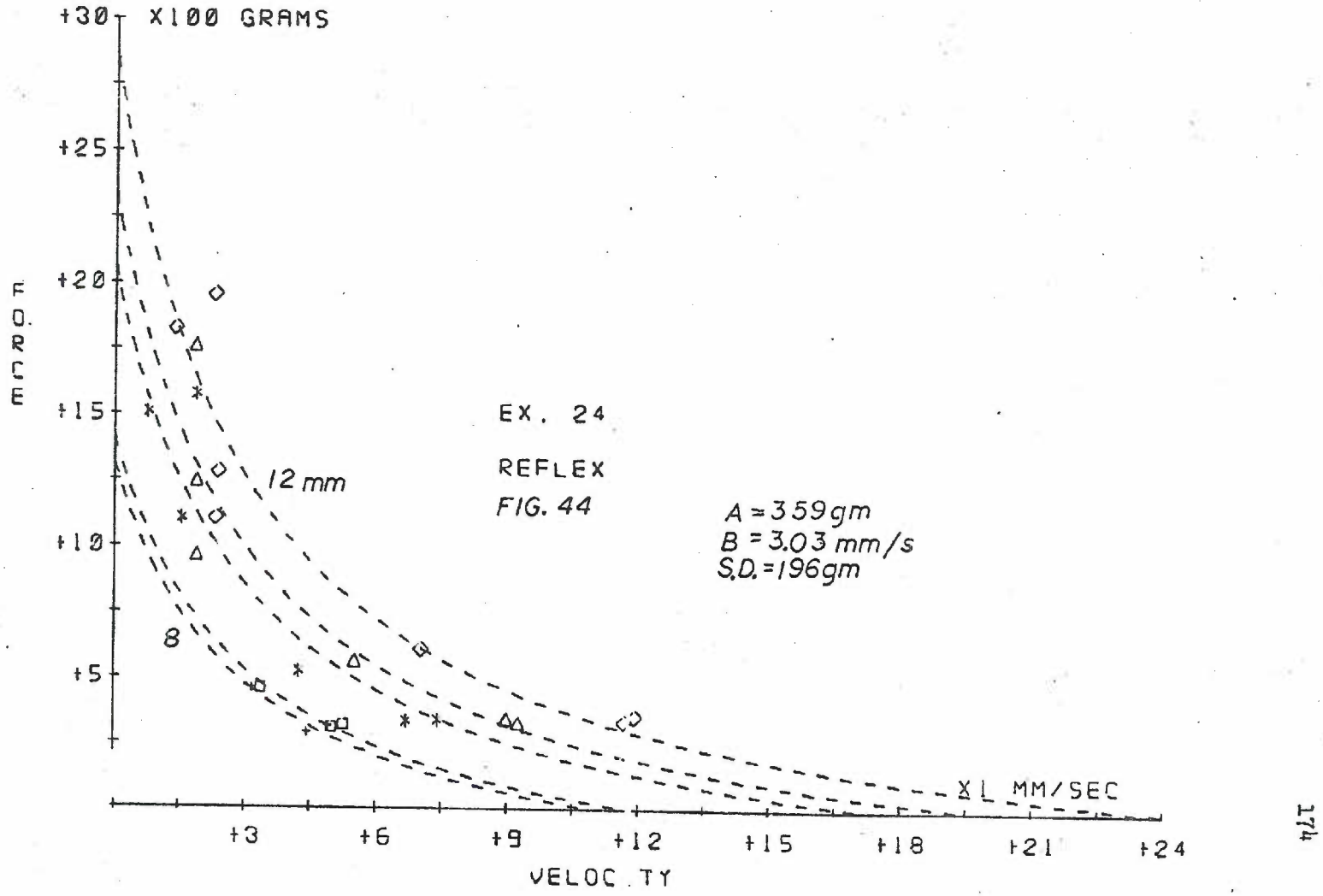
+30
X100 GRAMS
+25
+20
+15
+10
+5
ERROR
12 mm
8
EX. 24
REFLEX
FIG. 44
A = 359gm
B = 3.03 mm/s
S.D. = 196gm
X1 MM/SEC
+3
+6
+9
+12
+15
+18
+21
+24
VELOCITY

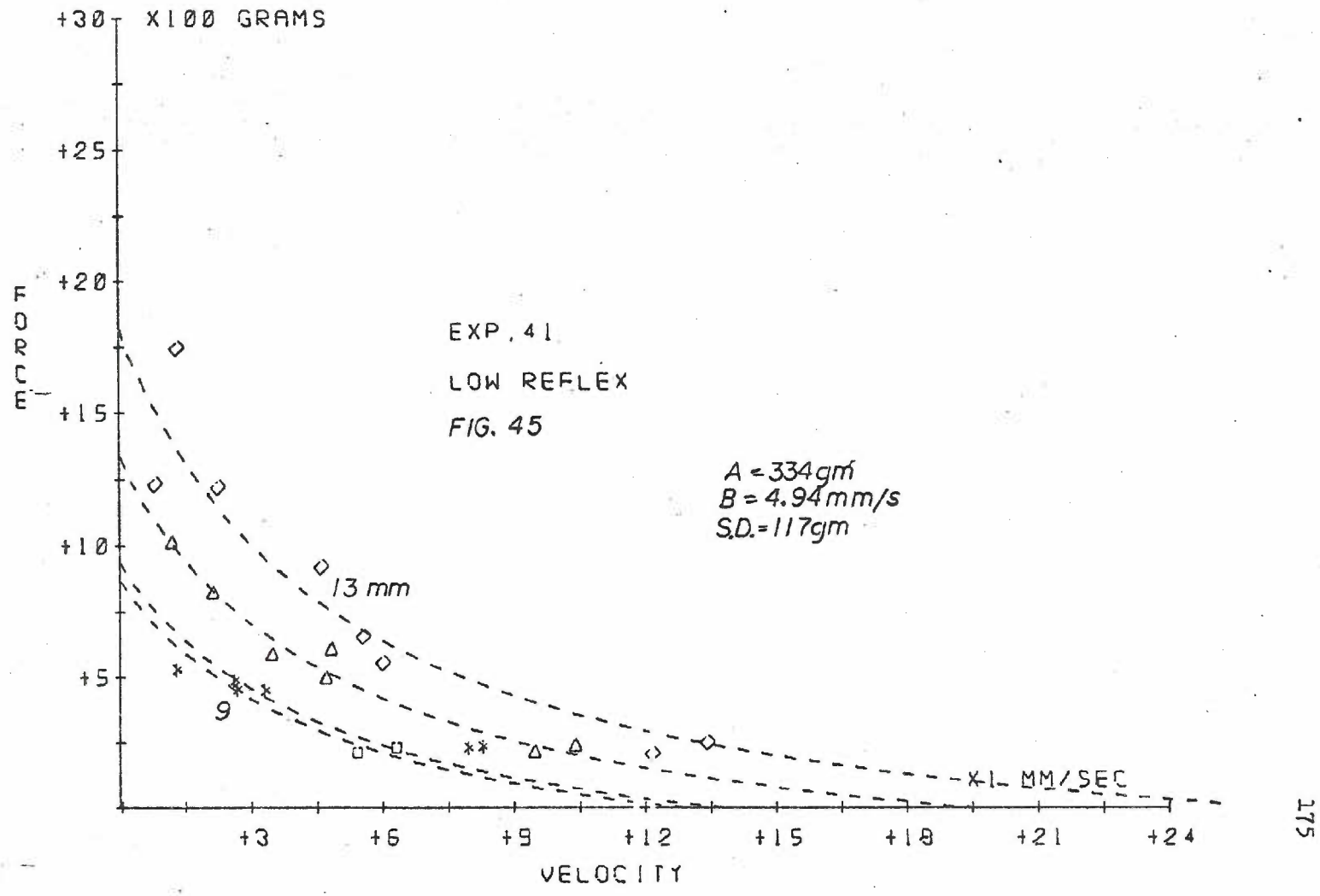
+30
X100 GRAMS
+25
+20
FORCE
+15
+10
+5
EXP. 41
LOW REFLEX
FIG. 45
A = 334gm
B = 4.94mm/s
S.D. = 117gm
13 mm
9
X-1 MM/SEC
+3
+6
+9
+12
+15
+18
+21
+24
VELOCITY

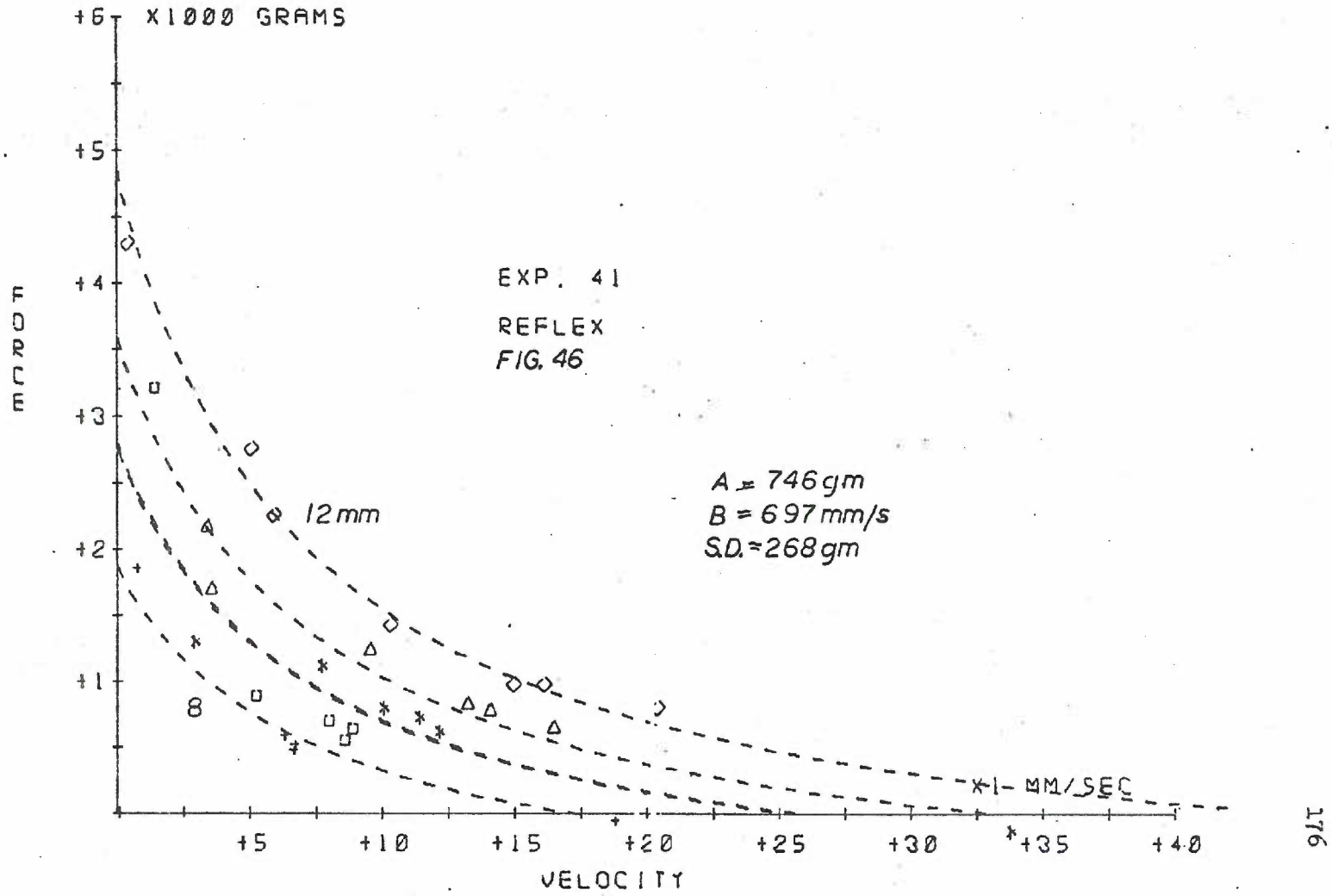
+6 X1000 GRAMS
+5
+4
+3
+2
+1
FORCE
EXP. 41
REFLEX
FIG. 46
A = 746gm
B = 697mm/s
S.D. = 268gm
12mm
8
1 MM/SEC
+5
+10
+15
+20
+25
+30
+35
+40
VELOCITY

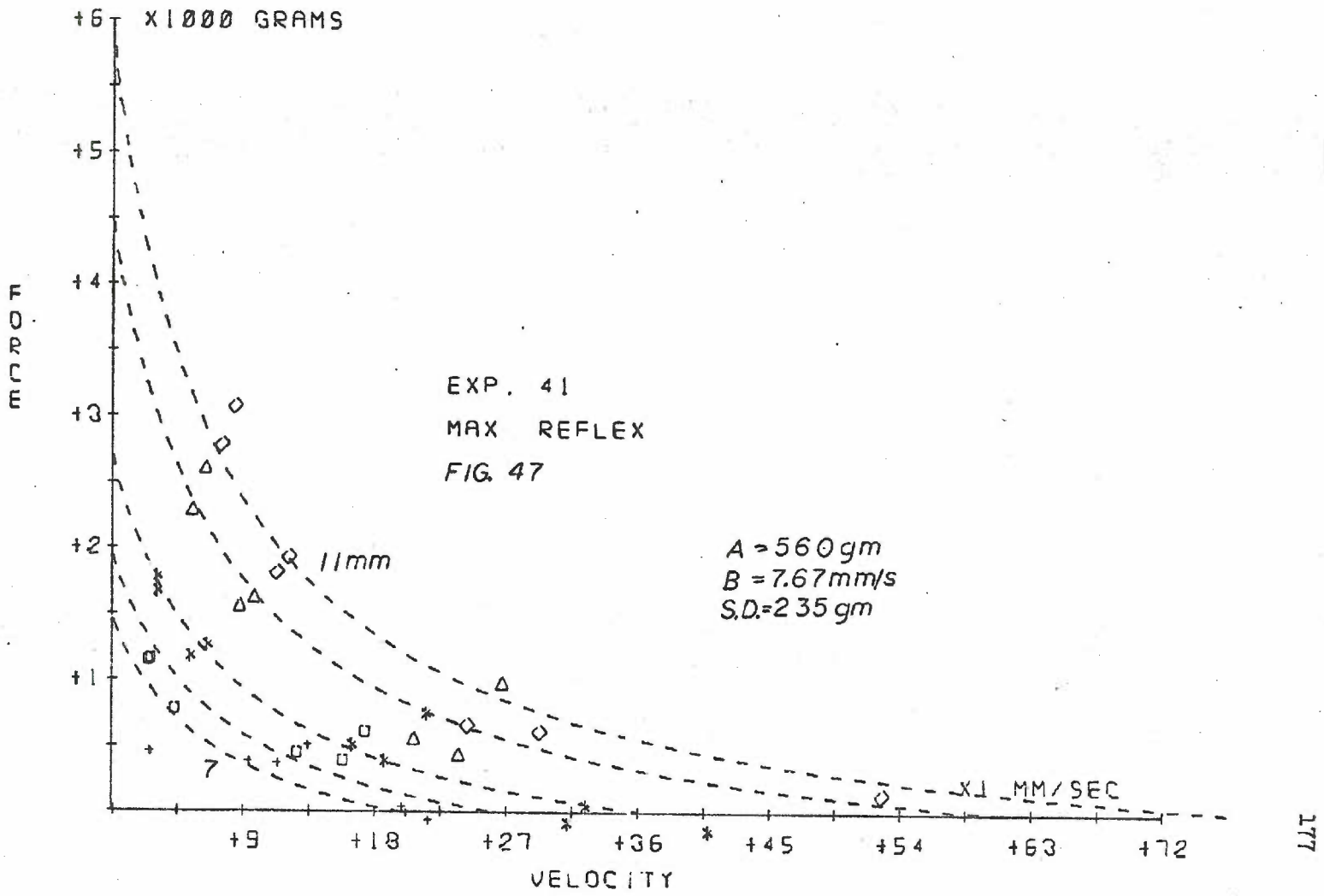
+6
X1000 GRAMS
+5
+4
+3
+2
+1
FORCE
EXP. 41
MAX REFLEX
FIG. 47
A = 560 gm
B = 7.67 mm/s
S.D. = 235 gm
11mm
7
X1 MM/SEC
+9
+18
+27
+36
+45
+54
+63
+72
VELOCITY

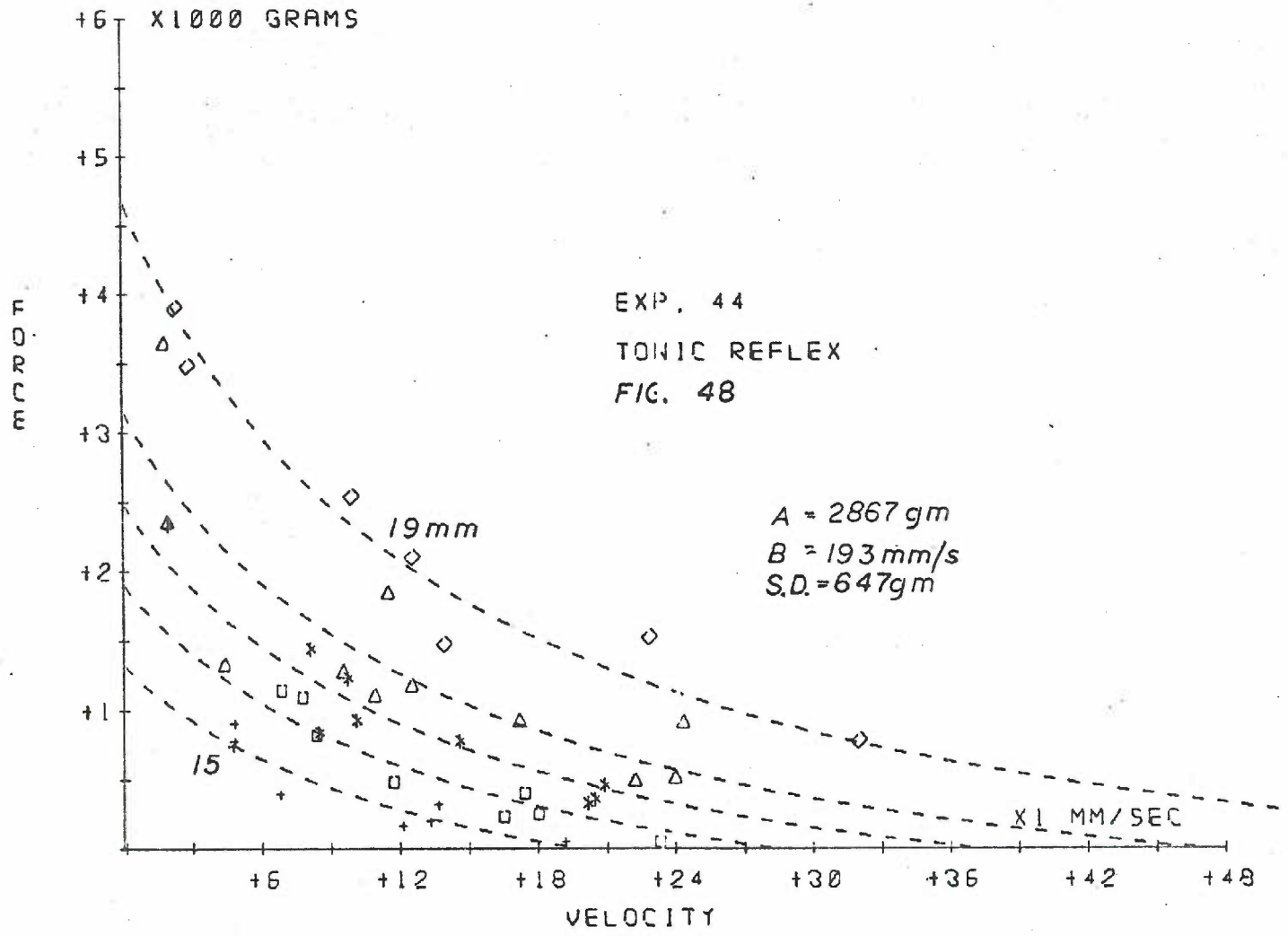
+6
X1000 GRAMS
+5
+4
+3
+2
+1
FORCE
EXP. 44
TONIC REFLEX
FIG. 48
A = 2867 gm
B = 193 mm/s
S.D. = 647 gm
19 mm
15
X1 MM/SEC
+6
+12
+18
+24
+30
+36
+42
+48
VELOCITY

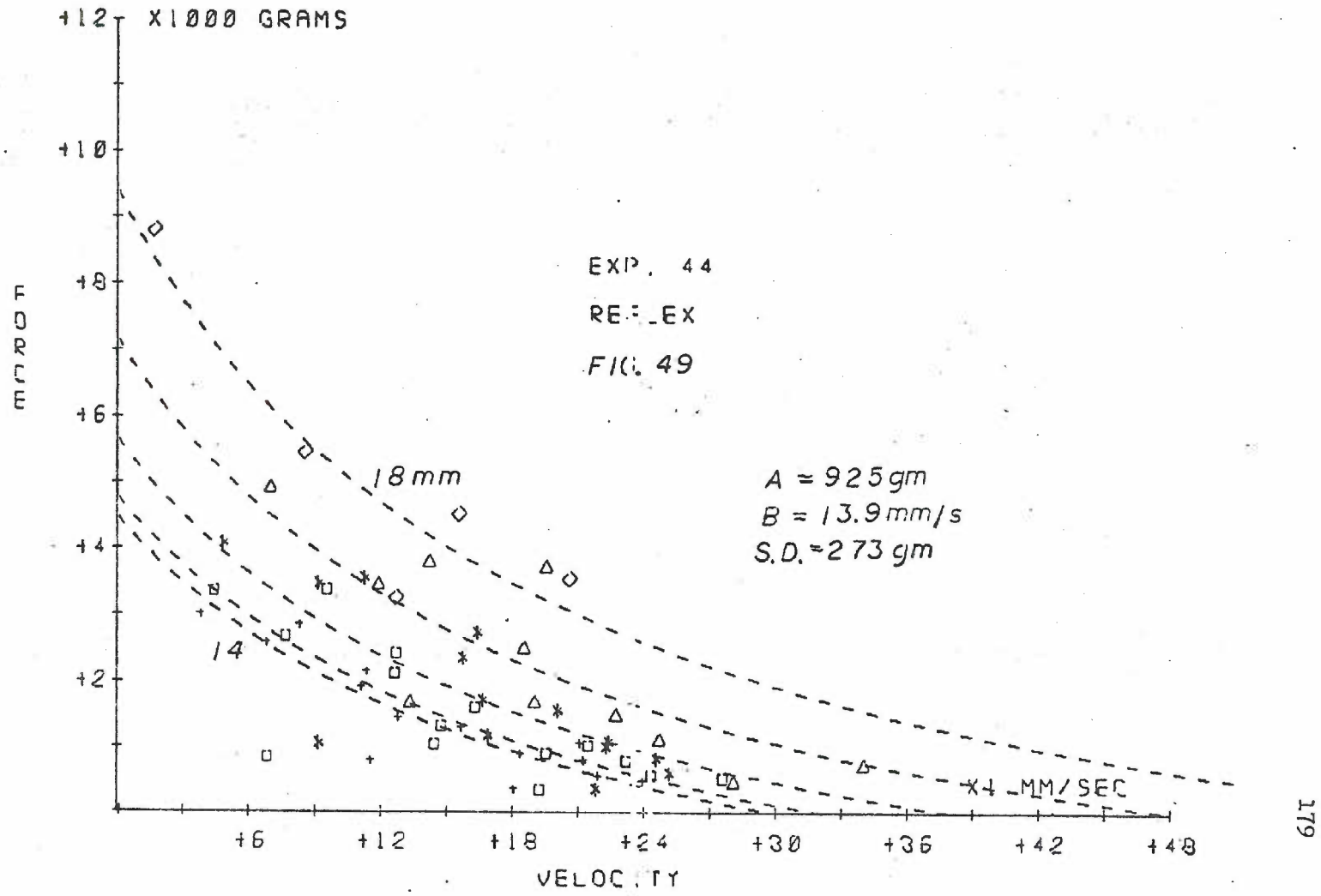
X1000 GRAMS
+12
+10
+8
+6
+4
+2
ERROR
EXP. 44
RE: EX
FIG. 49
A = 925 gm
B = 13.9 mm/s
S.D. = 273 gm
18 mm
14
+4 MM/SEC
+6
+12
+18
+24
+30
+36
+42
+48
VELOCITY

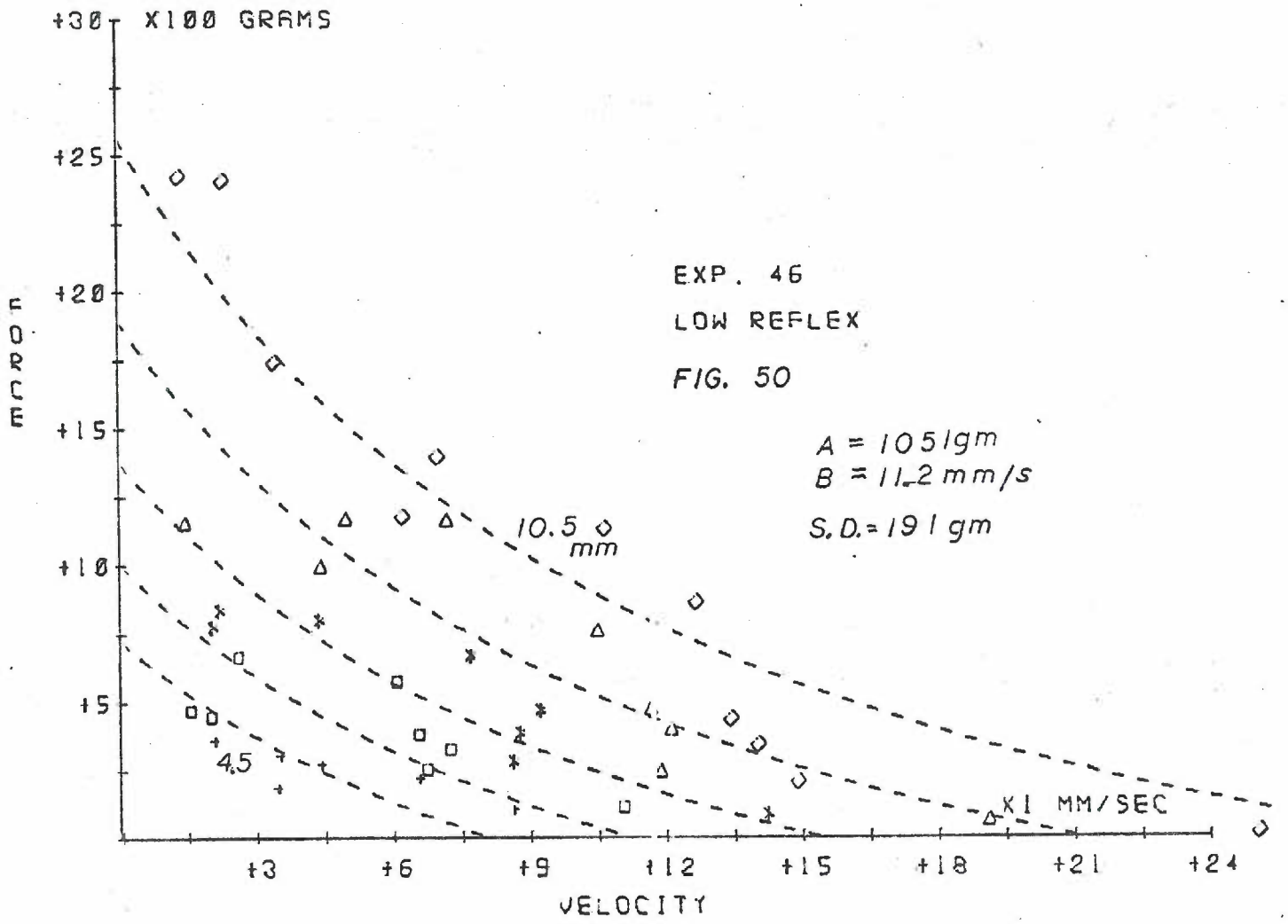
+30
X100 GRAMS
+25
+20
+15
+10
+5
FORCE
EXP. 46
LOW REFLEX
FIG. 50
A = 10.5 gm
B = 11.2 mm/s
S.D. = 1.9 gm
10.5 mm
4.5
X1 MM/SEC
+3
+6
+9
+12
+15
+18
+21
+24
VELOCITY

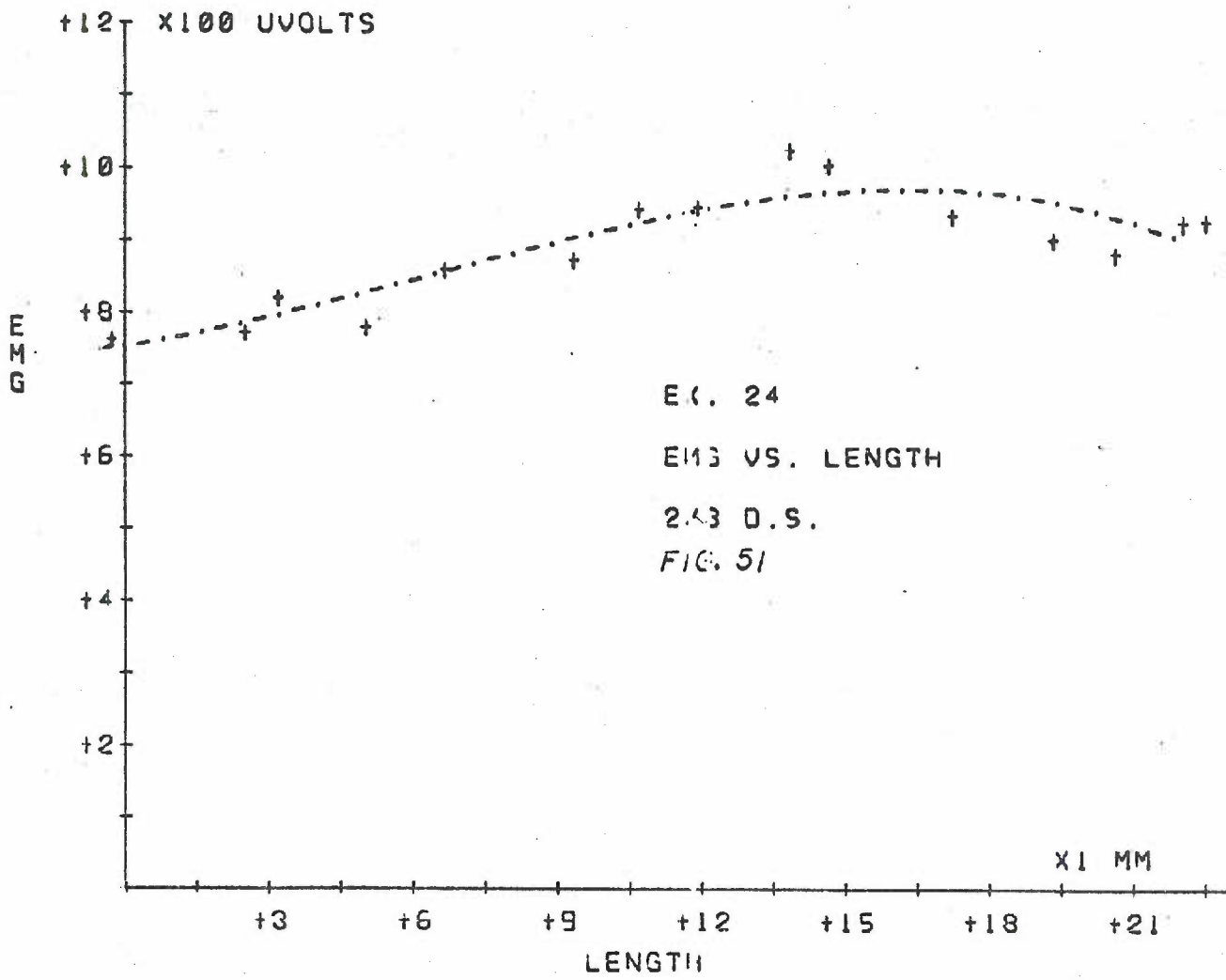

E(. 24

EMG VS. LENGTH

2.43 D.S.

FIG. 51

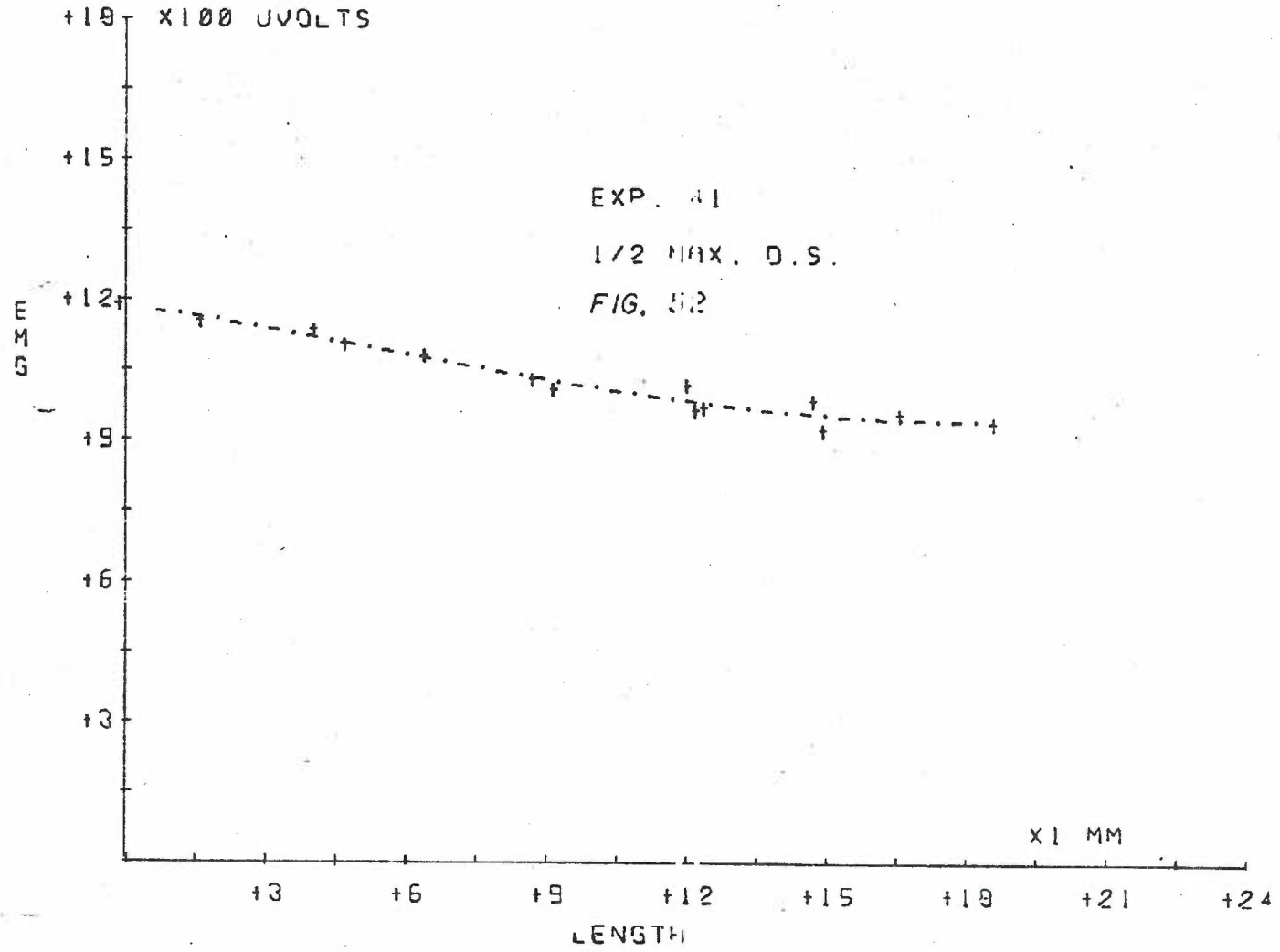
+18
X100 UVOLTS
+15
EXP. 41
1/2 MAX. D.S.
FIG. 52
+12
E
M
S
+9
+6
+3
X1 MM
+3
+6
+9
+12
+15
+18
+21
+24
LENGTH

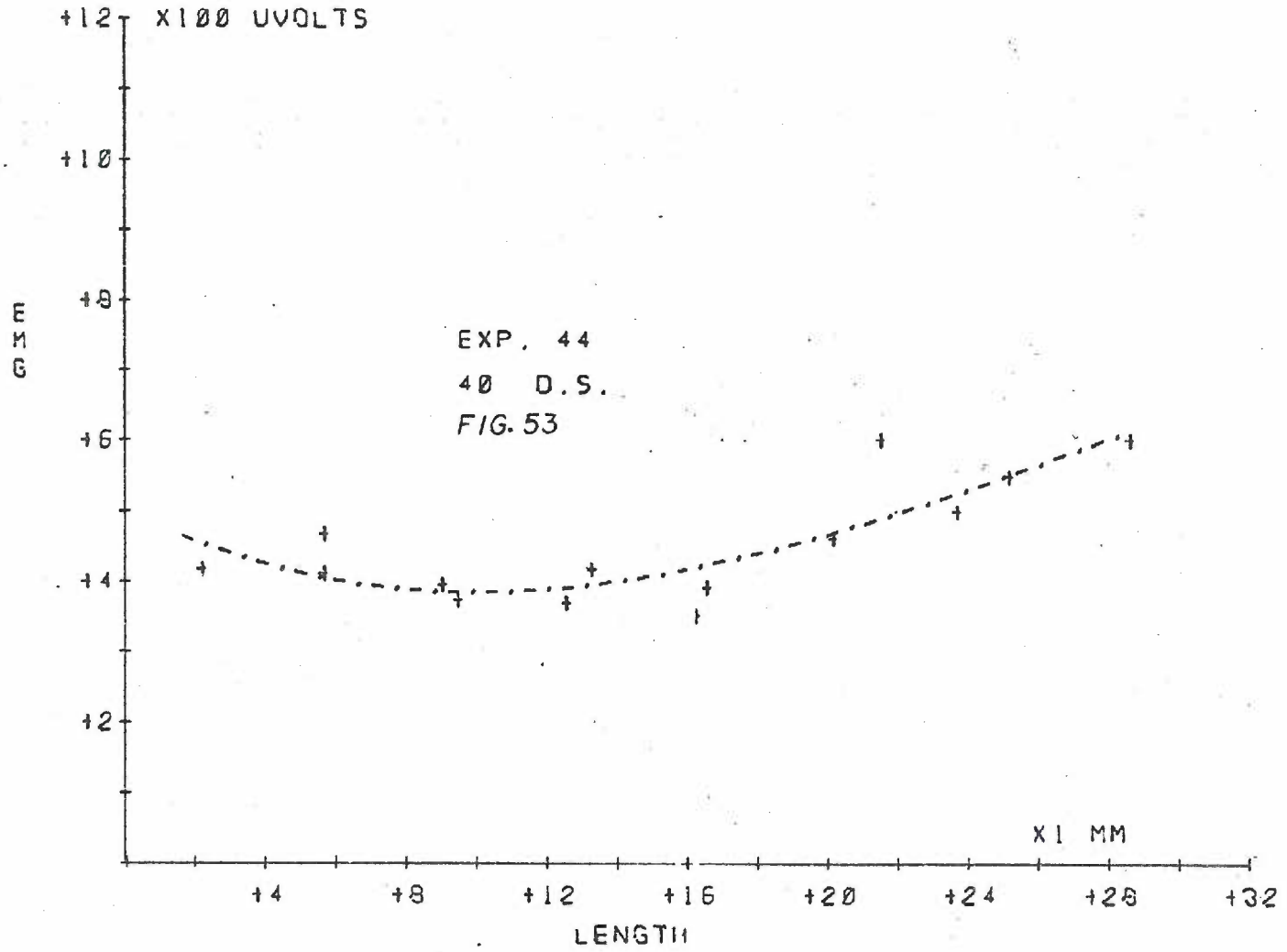
+12
X100 UVOLTS
+10
+8
EMG
+6
+4
+2
EXP. 44
40 D.S.
FIG. 53
X1 MM
+4
+8
+12
+16
+20
+24
+28
+32
LENGTH

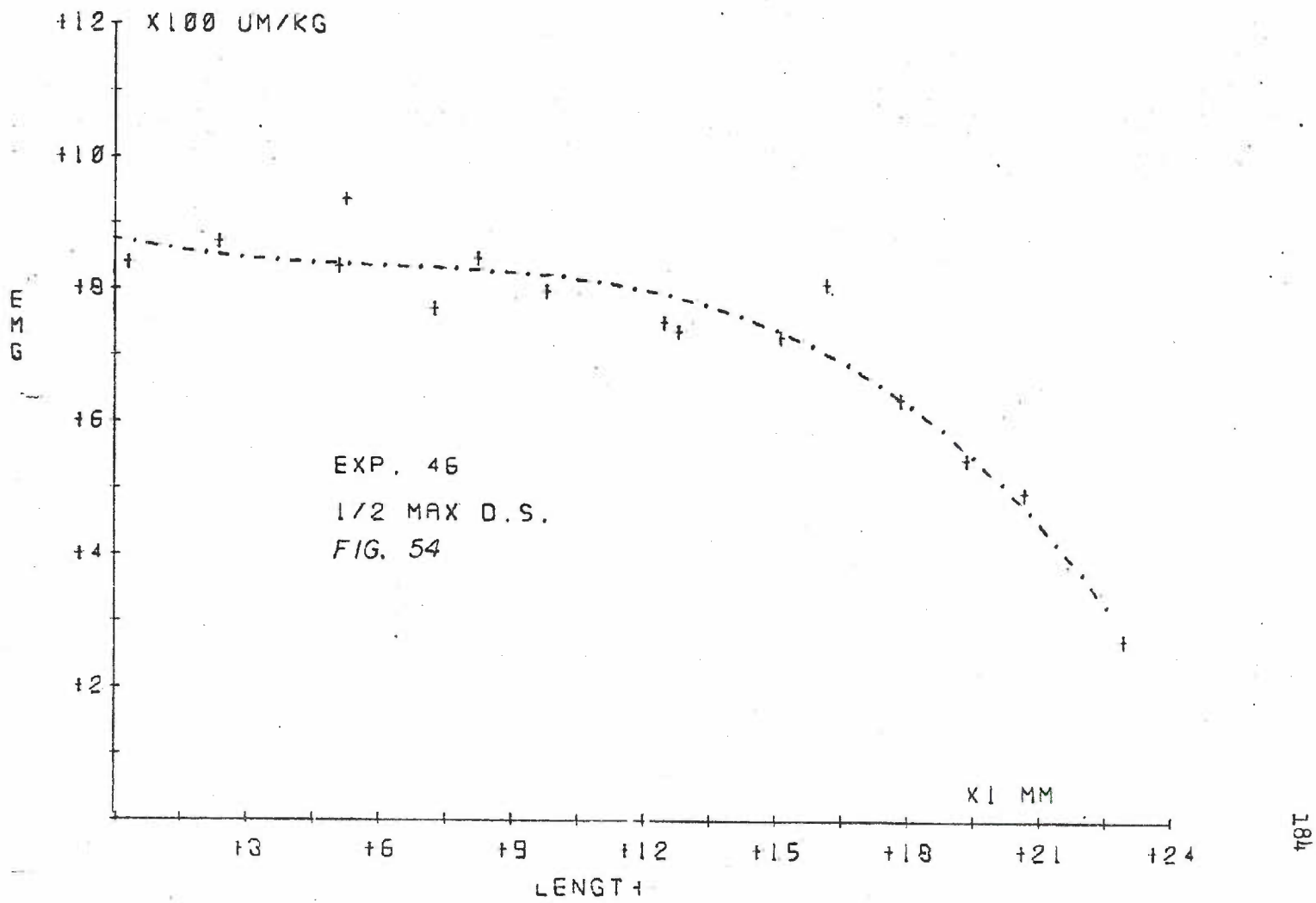
+12
X100 UM/KG
+10
+8
EMG
+6
+4
+2
EXP. 46
1/2 MAX D.S.
FIG. 54
X1 MM
+3
+6
+9
+12
+15
+18
+21
+24
LENGTH

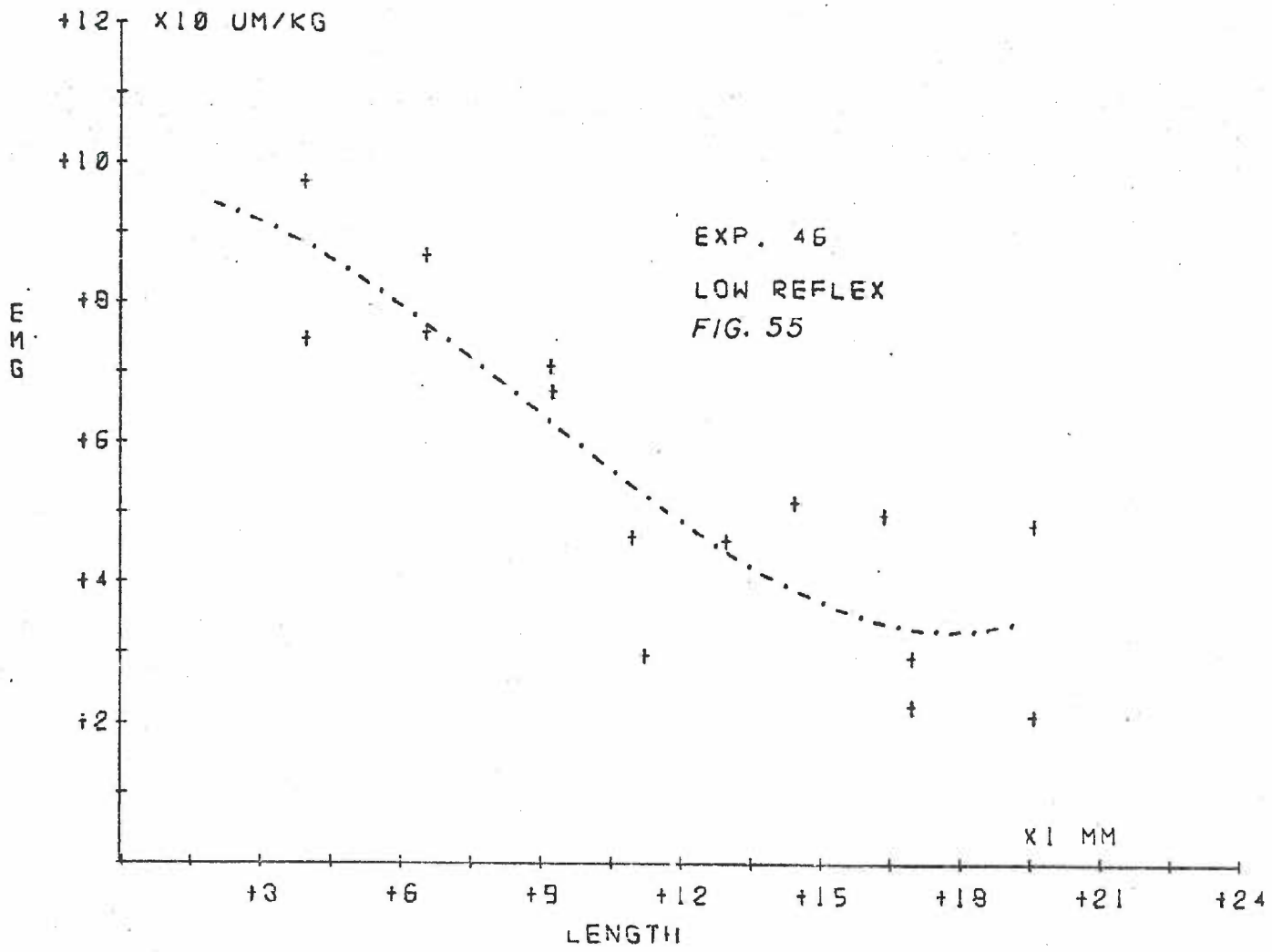
+12
X10 UM/KG
+10
+8
+6
+4
+2
EMG
EXP. 46
LOW REFLEX
FIG. 55
X1 MM
+3
+6
+9
+12
+15
+18
+21
+24
LENGTH